Timber Beams Notched at the Support

Riberholt, Hilmer; Enquist, Bertil; Gustafsson, Per-Johan; Jensen, Ralph Bo

1992

[Link to publication](#)

Total number of authors:
4

h=95−567 mm

b=45−160 mm

Cross section

TIMBER BEAMS NOTCHED AT THE SUPPORT

HILMER RIBERHOLT, BERTIL ENQUIST,
PER JOHAN GUSTAFSSON AND RALPH BO JENSEN

TIMBER BEAMS NOTCHED AT THE SUPPORT

HILMER RIBERHOLT, BERTIL ENQUIST,
PER JOHAN GUSTAFSSON AND RALPH BO JENSEN

Preface

This report concerns wooden beams with a notch cut at a supported end.

It is a result of ressources pooled from many contributors. Grants have been given from Building Research Council, Sweden and the Danish Technical Research Council. Further, many researchers have contributed. From the Div. of Struct. Mech., Lund Inst. of Technology: Bertil Enquist, Per Johan Gustafsson and Hans Petersson, who have dealt with the measurements of the wood properties, specially fracture mechanical ones. From the Dept. of Struct. Eng., Tech. University of Denmark: Ralph Bo Jensen and Hilmer Riberholt, who have measured some wood properties and carried out the tests with the notched beams. The word processing has been carried out by Inge Sørensen and the drawings by Esther Martens and Bo Zadig.

Since two departsments have contributed the report is published from both.

H. Riberholt
October 1991.

CONTENTS

2

Summary

The report deals with wooden beams with a notch cut at the supported end. This results in stress concentrations leading to a severe reduction of the shear force capacity.

There is given a description of the test methods used to measure partly the shear capacities of the notched beams and their mechanical behaviour. Because of the stress singularities the fracture energies of the wood for mode I and II have been determined. The report present all material properties which have been judged necessary to calculate the shear capacity of a notched beam with a theory based on fracture mechanical concepts such as the fracture energies. The report can thus be employed to verify or calibrate theoretical models.

Further, there is presented comparisons between measured and theoretical estimations of the shear capacities of notched beams. It is shown that the analytical model proposed by P.J. Gustafsson overestimated the shear capacity and so does a finite element method based on non–linear fracture mechanics. Meanwhile, the two models give a reasonable agreement between measured and calculated shear capacities.

Resume

Rapporten omhandler træbjælker med en udskæring ved en understøtning. Denne forårsager spændingskoncentrationer, der medfører en væsentlig reduktion af bjælkens forskydningsstyrke.

Der er givet en beskrivelse af forsøgsmetoder anvendt til at måle dels materialeegenskaberne, dels forskydningsstyrken af træbjælkerne ved udskæringerne samt deres mekaniske opførsel. På grund af spændingssingulariteterne er træets brudenergi i mode I og II bestemt. Rapporten præsenterer alle materialeegenskaber, som det er skønnet nødvendigt at måle for at beregne forskydningsstyrken af bjælker med udskæringer med modeller baseret på brudmekaniske begreber som fx. brudenergier. Rapporten kan således benyttes til at eftervise eller kalibrere teoretiske modeller.

Endvidere er der foretaget sammenligninger mellem målte og teoretisk bestemte forskydningsstyrker af bjælker med udskæringer. Det er vist, at den analytiske model foreslået af P.J. Gustafsson overestimerer forskydningsstyrken ligesom en finite element metode baseret på ikke–lineær brudmekanik. De to modeller giver imidlertid en rimelig overensstemmelse mellem målte og beregnede forskydningsstyrker.

3

Sammanfattning

Denna rapport behandlar träbjälkar med urtag vid upplag. Urtag ger spänningskoncentrationer, som leder till betydande reduktion av tvärkraftkapaciteten.

Det ges en beskrivning av provningsmetoderna för mätningarna av dels materialegenskaper, dels tvärkraftskapacitet och brottbeteende hos Träbjälkarna med urtag. Med tanke på aktuell spänningssingularitet har träts brottenergier i modus I och i modus II bestämts. Rapporten redovisar alla materialegenskaper som har bedömts nödvändiga att bestämma för att kunna beräkna tvärkraftskapaciteten med modeller baserad på brottmekaniska begrepp som t.ex. brottenergi. Rapporten kan således användas för att verificera och kalibrera teoretiska modeller.

Vidare presenteras en jämförelse mellan uppmätta och beräknade tvärkraftskapaciteter. Det visas att den analytiska modellen föreslagen av P.J. Gustafsson och även en finit elementmodell baserad på icke–linjär brottmekanik överskattar tvärkraftskapaciteten. De två modellerna ger dock rimlig överenstämmelse mellan uppmätta och beräknade tvärkraftskapaciteter

Nykelord: Trä, träkonstruktioner, limträ, bjälkar med urtag, brottmekanik, brottenergi.

1. INTRODUCTION AND BACKGROUND.

This report deals with wooden beams, where a notch is cut at the supported end. This results in stress concentrations which must be dealt with by means of fracture mechanical concepts.

In previous reports test results have been published, see for example /Larsen & Riberholt, 1972/ and /Gustafsson & Enquist, 1988/. These contain results for notches cut perpendicular to grain and the shear capacity of the beams were reduced severely by the notches. So in this project there has been tested beams with inclined notches, which has a larger shear capacity than the perpendicular notches. Further, the report comprises results for full scale beams of a considerable size.

h=95–567 mm

b=45–160 mm
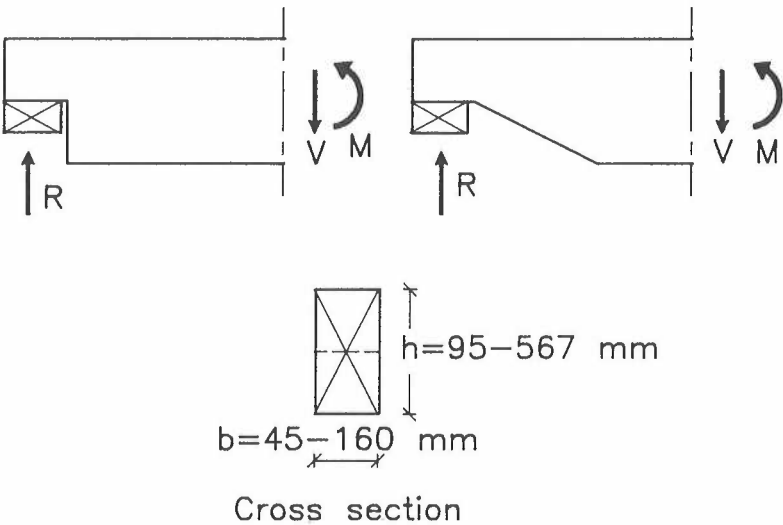
Cross section

Figure 1.1   Front views of beams, perpendicular and inclined notches. Range of cross sectional dimensions.

1.1 Background

The background of this report is a common interest in fracture processes shared by colleagues employed at the Division of Structural Mechanics, abbreviated to BM (Byggnadsmekanik), Lund Inst. of Technology and at the Department of Structural Engineering, abbreviated to ABK (Afdelingen for Bærende Konstruktioner), Tech. University

of Denmark. Together they started the project with economic support from partly Building Research Council, grant no. 890130–2, partly Danish Technical Research Council, grant no. 16–4544.B.

There was a wish to carry out a more comprehensive series of tests comprising notched beams of solid timber and glued laminated timber of sizes and qualities relevant to normal practice.

The tests were coordinated and planned so that all tests with one type of specimens were carried out at only one of the laboratories. So test specimens were transported over Øresund each time a coordination meeting took place.

The cooperation is the reason why this report is published from both institutions. The intention is that the report can be employed by other researchers to verify their theories. It will at least be used by the participants of this project.

1.2 Scope of the project

The scope of the project has been to carry out and report shear tests with beams notched at the support. The beams were of sizes and qualities relevant to practice, and both solid timber and glued laminated timber was tested. Also the strength improving effect of inclined notches was investigated.

There was measured the mechanical properties of the wood assumed to determine the shear capacity of the notched beam. The selected properties are listed in the next section, which also gives an explanation and justification for the choice.

Further, the project had the scope to set up theories describing the fracture process in the wood and predicting the shear capacity of the beams by means of the mechanical properties of the wood. But it has not been included in the project to propose calculation methods for structural timber codes, it is expected that such methods will emerge and the results presented in this report can be utilized for the calibration of the methods.

1.3 Description of basic assumptions in possible theories

The intention of this section is to give an argumentation for the measured material properties.

It was early in the project decided to carry out the stress and strain analyses under the assumption of a plane state. Meanwhile, wood could be described as a cylindrical orthotropic material so the stress and strain in planks cut from a trunk will in reality inevitably deviate from the plane state. Yet, the wood has been assumed to be plane orthotropic with properties in the direction perpendicular to the grain depending on the slope of the annular rings.

The slope or inclination of the annular rings in the cross sections have thus been determined so that the dependency of the inclination on the mechanical properties perpendicular to grain could be investigated in the essential cases.

From experience and tests, see for example /Larsen & Riberholt, 1972/ it is known that knots can counteract splitting of wood. So for such failure modes the lowest capacities is found for wood without knots, that is for almost defectfree wood. Thus, since in the critical case knots will not be present near the notch they will not disturb the stress or strain field here meaning that stress analyses based on homogenious material is a reasonable approximation.

The wood has been assumed to be linear elastic, but in the process zone at the crack tip a non—linear model may be applied. In this zone it has been assumed that the fracture energy required to form a crack is a controlling material property. Wood has so distinct orthotropic properties that it has been assumed, that a crack always propagates in the direction of the grain. It may propagate when subjected either to normal stresses perpendicular to grain, Mode I, or to shear stresses, Mode II. It can of course also propagate when subjected to a combination of these 2 stresses.

In order to perform a static analysis concerning crack propagation in the grain direction it is thus necessary to know the following material properties.

Stiffnesses

E_0 E—modulus in the direction of grain or in the longitudinal direction of the timber member.

E_{90}, α E—modulus perpendicular to grain, where α is the angle between perpendicular stress and the annual rings.

G   Shear modulus, parallel to — perpendicular to grain.

ν Poisson ratio

Strength values

$f_{t,90}$ Tension, perpendicular to grain.

f_v Shear, parallel to − perpendicular to grain.

Fracture energies

$G_{f,t}$ Fracture energy per crack area in tension perpendicular to grain.

$G_{f,v}$ Fracture energy per crack area in shear parallel to − perpendicular to grain.

The tests for the determination of fracture energies have been carried out so that it has not been necessary to assume anything about the stress–deformation relation. The energy has been determined by integration of a force multiplied by a displacement, both measured.

2. BASIC ASSUMPTIONS FOR THE TESTS

All tests have been performed as short term tests with a duration from start to failure of approximately 5 min, except for tests where only a stiffness property was measured. Here the duration was a few minutes. There was aimed at that the specimens were conditioned at a climate of 65% ± 5% relative humidity and $20^{0}C \pm 2^{0}C$ in temperature.

Further, there has been aimed at, that the specimens should be of practical sizes, and that the wood volumes of interest were as free of knots as possible. This means that in all notched beams there should be no knots in the vicinity of the inner corner, and in the small specimens for the determination of the material properties there was no knots in the tested volume.

2.1 Testing scheme

It was decided to test material relevant to practice, so planks, timber and glued laminated timber (glulam) beams were tested in sizes and qualities as they occur in the Nordic countries. All specimens were cut from planed wood.

Figure 2.1.1 shows the tested cross sectional dimensions and the orientation of the annular rings.

The socalled "half timber" is cut from the trunk so that the result is two timber members, which means that the height h is approximately twice the width b. The planks have been cut from larger trunks and they have been selected so that the annual rings were either standing or round as marked in figure 2.1.1 with S or R. In the glulam laminations the annual rings were typical lying, so compared with the solid timber members they were oriented differently with regard to the stress components perpendicular to the grain.

In table 2.1.1 there is an account of the parameters varied in the test series. In general the sizes, the geometric design of the notch and the static eccentricity of the applied reaction have been varied.

The geometry has been varied by cutting the notch more or less inclining with the longitudinal direction and thereby the strength improving effect of the inclination has been investigated. There has been selected some very flat inclinations, which for solid

9

timber are flatter than the threshold value 1:3 for which the timber codes typical assume the same shear capacity of the cross section as for an unnotched beam.
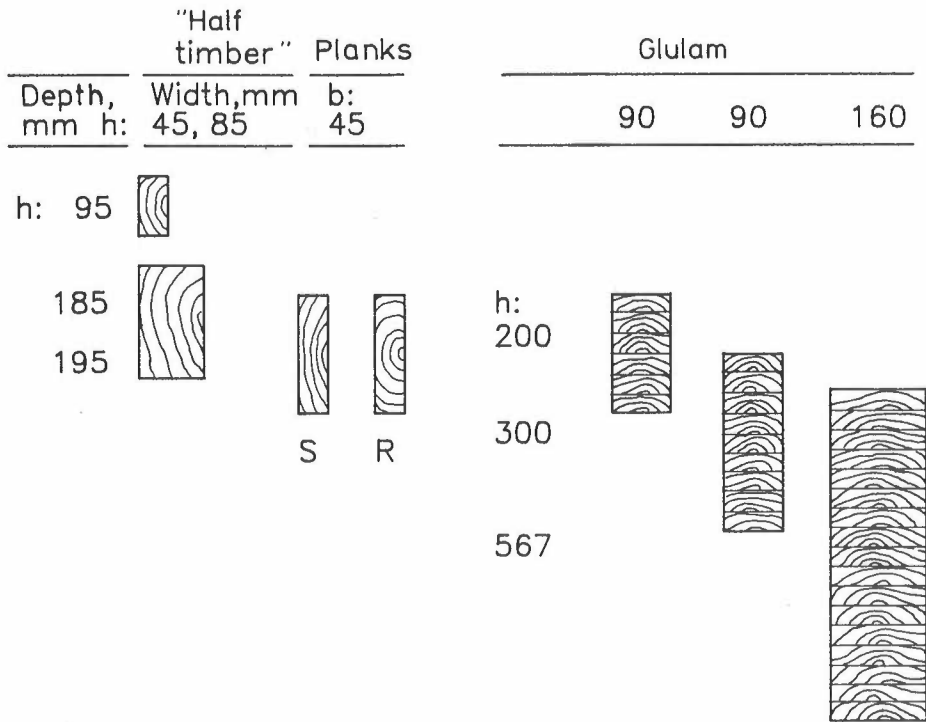
Figure 2.1.1 Overview of tested cross sections of timber and glulam.

The relative heights have been chosen so that also values smaller than those, recognized in the structural timber codes, have been tested. Again in order to investigate what is behind this threshold.

The smallest eccentricity of the reaction was determined by requiring that the contact compression stress was reasonably below the compression strength perpendicular to the grain. In a few cases the contact compression stress reached values up to 4–5 MPa which are close to the strength values when considering the limited loading length or area. So it cannot be excluded that high compression stresses perpendicular to grain just outside the notch corner has influenced (reduced) the shear capacity of the notched cross section. The larger eccentricities were determined simply as twice the smaller ones.
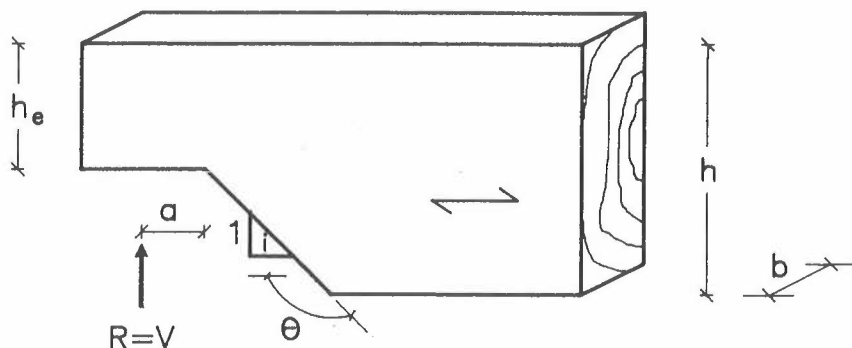
Figure 2.1.2 Geometry and statics of the notched end of the beam specimen.

Table 2.1.1   Parameters varied in the test series.

Size		Sheared area or volume	
	b	Cross sectional width	See
	h	Cross sectional height	figure 2.1.1
Geometry	α	Relative effective height, h_e/h From 0.25 to 0.875 for solid timber and from 0.5 to 0.833 for glulam	
	i/θ	Inclination 1:i or angle θ. From $\theta = 90^0$ to $\theta = 169^0$ (1:5) for solid timber and to 173^0 (1:8) for glulam.	
Statics	β	Relative eccentricity of the reaction. $\beta = a/h$ From 0.16 to 0.66 for solid timber and from 0.12 to 0.30 for glulam.	

The specific parameter values are given in chapter 4 in context with the description of the tested notched specimens.

2.2 Material, selection and conditioning

Species

It was decided to employ European Whitewood (picea abies) from the Nordic countries. This species is prevailing for the production of glued laminated timber and it is also frequently used for solid structural timber.

For the glulam and the solid timber of planed thickness 45 mm the growth places have been in middle Sweden, whereas it for the timber 85 x 185 mm was Sjælland (Zealand) in Denmark.

Qualities
The qualities of the timber were the normal ones used for glulam and structural timber. The boards for glulam complied with the grading rules for T30, which for example require that the narrow—face knots shall be less than half the thickness b and the wide—face knots less than a quarter of the cross sectional height h , both relative to the cross—sectional size of the board. For the solid timber the similar requirements were $4/5 \cdot b$ and $1/2 \cdot h$.

The range of the mean densities for the different timber dimensions and types of test specimens were 410 kg/m^3 ± 30 kg/m^3 (dry weight/wet volume).

Selection
The solid timber and the boards for the glulam were specially selected. They were graded according to the previously mentioned rules. Further, timber with extreme density either high or low was sorted out. The intention was to have a reasonable homogeneous material.

All the solid timber pieces were weighed in the laboratory and based on the density divided into 3 groups. The 6 replicants of each specimen type could thus be randomly selected with 2 from each density group.

The intention with the density grading and weighing was to have a reasonable narrow and controlled density variation. In this way density variations should not influence too much the mean values over the 6 specimens in each type and thereby making density corrections superfluous when comparing. But still there was a controlled and limited density variation so that a correlation between density and other mechanical properties could be performed.

Climatic conditioning
All wood were dried in kilns before delivery to the laboratory. Here it was kept in a climate chamber at 65% ± 5% relative humidity and a temperature of 20^{0}C ± 2^{0}C for at least 10 weeks. The range of the mean moisture content for the different types of test specimens was 14% ± 1,5%. This is a little high when compared with the climate and it could indicate that the moisture content of the wood was not fully in balance with

the climate, which normally would result in a moisture content of 12%. − 14%

2.3 Cutting pattern for the test specimens

From the delivered beams of solid timber and glulam there was cut a pair of notched beam specimens and some small specimens in between. The small specimens were employed for the determination of some of the material properties. Typical it was possible to cut several of such paired specimens from each plank or beam.

The notched specimens were oriented as shown in figure 2.3.1. The material properties measured by the small specimens were thus applicable to both notched specimens so in this way the number of specimens for the material properties were halved.
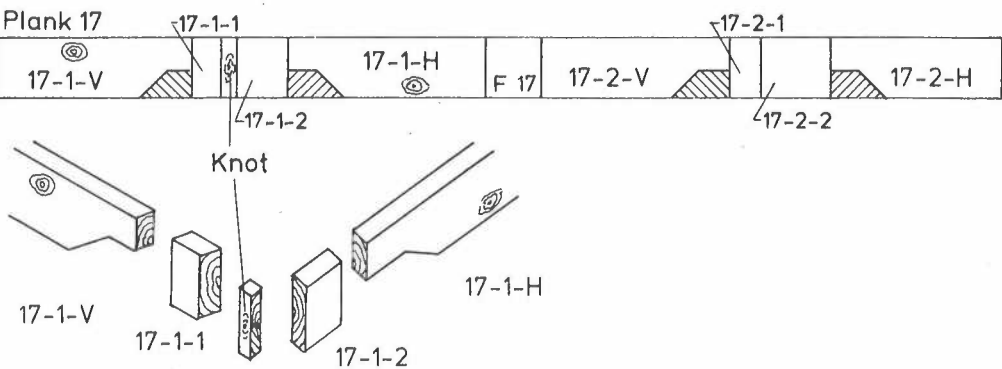
Figure 2.3.1   Cutting pattern for test specimens. End−notched beams, 17−1−V and 17−1−H, and matching test specimens for measurement of material properties, 17−1−1 and 17−1−2. Numbers consistently written on the sapwood side, meaning that the different specimens always can be related to each other.

The numbers were consistently written on the sapwood side, so that a test specimen always can be traced to its original position in the plank.

The following identification was used:

13

End–notched beams: Plank number – pair number – $\begin{cases} \text{Left} & \text{(V)} \\ \text{Right} & \text{(H)} \end{cases}$

Test specimens for material properties: Plank number – pair number – specimen number (1 or 2)

Test specimens for moisture content: "F" – plank number

One of the two test specimens for measurements of material properties was used at BM for measuring:

E_{90}	Modulus of elasticity perpendicular to the grain
$G_{f,t}$	Fracture energy, mode I
$f_{t,90}$	Tensile strength perpendicular to the grain
$G_{f,v}$	Fracture energy, mode II
f_v	Shear strength

The other test specimens were used at ABK for measuring E_{90} and $f_{t,90}$.

The modulus of elasticity in the grain direction, E_0, and the shear modulus, G, were measured on the whole plank before it was cut.

In some cases the notch lamella changed between two beams in the glulam beam. This resulted in different material properties in the notch areas of two neighboring specimens. Thus, in this case it has been necessary to cut out a pair of test specimens for each beam, see figure 2.3.2.
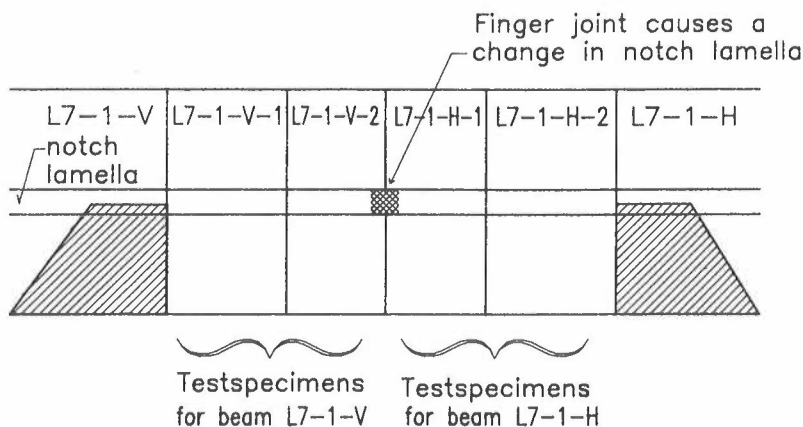
Figure 2.3.2   Test specimens in the case where the notch lamella changes between two neighbour beams. A pair of test specimens is required for each beam.

To avoid influences from knots, the test specimens were aimed to be free from knots, see figure 2.3.1. For the end—notched beams there should be no knots within a cross—sectional height from the notch, as a possible knot in this area could catch and stabilize a propagating crack. For the small in between specimens knots were cut away if there was any.

2.4 General about the determination of material properties.

Because of the large variability in the material properties of wood it would be advantageous to determine all the properties by measurements of specimens as close as possible to the notch. But this was difficult to obtain of two reasons. The first is that knots and other growth defects sometimes prevented the cutting of small specimens close to the notch, instead these were cut 1 m away may be. The second reason is that the testing method required a certain length of the specimen, and this made it impossible to measure close to all notches. This was the case for the determination of the E—modulus in the grain direction and the G—modulus.

It has thus in several cases been necessary to rely on that the material property measured over a short length is representative for a larger length of the beam.

By employing the pair of neighbouring notched beams the number of the material property tests were reduced, but it was still overwhelming.

So the moisture content was measured electric based on conductivity with a meter, which was calibrated specificly for each wood parcel by means of the weighing and dry

15

ing method.

Further, some material properties were only measured for a fraction of the specimens. Still it was for a considerable number so that it was possible to establish a multiple regression equation by which the property could be estimated for the other specimens by means of some material properties, such as density, moisture content and so on. In the next chapter this is described in details, but a few examples will be given here.

Because of the measuring methods the modulus of elasticity E_0 in the direction of the grain (the longitudinal direction) and the shear modulus G was measured over a small gauge length (approx. 1 m) and at a certain position, respectively. It has been assumed that these locally measured stiffness properties are applicable to the whole structural timber member.

For the glulam members the modulus of elasticity E_0 was not measured directly. Instead it was measured in flatwise bending tests with specimens cut from the laminations containing the notch point. The density and moisture content of these specimens were measured and a linear regression equation E_0 (density, moist) was determined. Based on the density and moisture content of the whole glulam specimen E_0 was calculated from this regression equation.

Further, the wood density was in some cases determined as the density of the whole notched beam specimen, whereas it in other cases was measured from small specimens cut from the beam.

3. MEASUREMENTS OF MATERIAL PROPERTIES

Test type

By deciding the test type for measuring a material parameter there was aimed at tests which gave a strain field and/or stress field of the same type as that occuring at the notches in the timber members. In this way it was sought to come as close as possible to the state in the wood around the notch point of the beams. For example the shear modulus G was measured in a short span bending test by means of strain gages and knowledge of the stress distribution from a FEM–analysis.

Size and shape of specimens

The size and shape of the specimens will influence the result, not only because of the size effect originating in the brittle failure (weakest link) but also because of that wood is cylindrical orthotropic. Since it has been decided to analyze the timber specimens in a plane state it will be of importance to test the whole width of the cross section in order to measure the relevant "mean value" over the cross section. Futher, by employing specimens cut from the whole thickness one will measure the correct response in the sense that it is a plane state response. Figure 3.1 shows an example, where one will measure different E–moduli perpendicular to the grain for a small necked–down specimen and a full–width specimen.
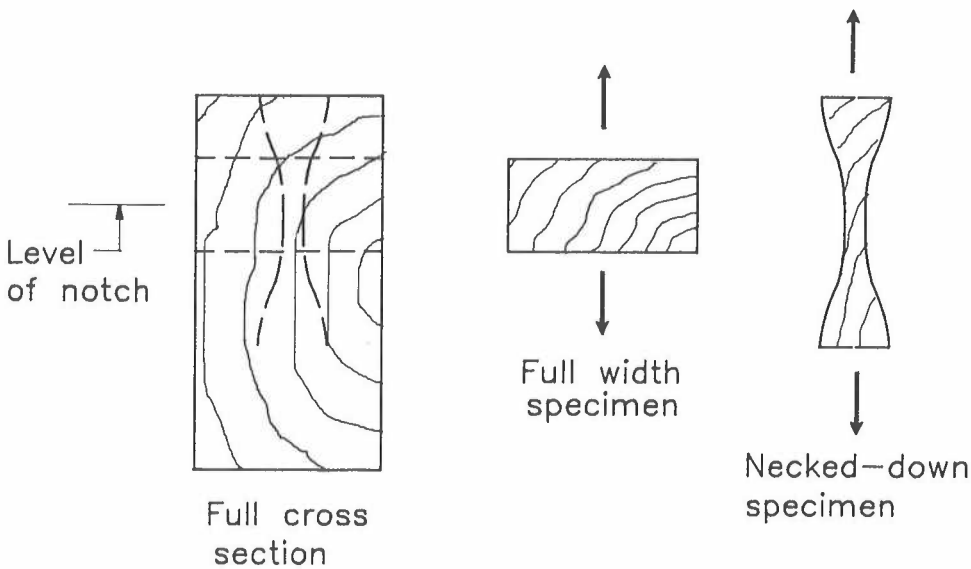
Figure 3.1   Full width specimen and necked–down specimen from the same cross section.

17

For the necked down specimen the elongation will originate in a combination of an axial strain in the principal directions (radial and tangential) and a shear strain. The strain field in the full width specimen will differ because the shear strain tendency in some regions will be counteracted by the stiffness of other regions in the cross section.

This difference in strain and stress distribution between the two specimens could also result in different values of the tensile strength perpendicular to the grain, when it is determined as the failure force divided by the cross sectional area.

Testing scheme considering determination of material parameters by regression
Considering the overwhelming effort to determine by tests all material parameters for all notched specimen it was decided to reduce the number of material parameter tests specially those requiring a lot of labour or ressources. Table 3.1 gives an outline of the material parameters which either were measured for all specimens or for a fraction.

Table 3.1 Fraction of specimens in which material parameters have been measured. Doubtfull measurements have been disregarded.

Measured in:	Structural timber		Glulam	
	All specimens	Specified fraction %	All specimens	Specified fraction %
Moisture content	x		x	
Density	x		x	
Density of notch lami.	Not relevant		x	
E_0	x			0
$E_{0,notch\ lami}$	Not relevant		x	
E_{90} BM[1]		84		0
E_{90} ABK[2]		84		87
G		43		23
$f_{t,90}$ BM[1]		87		0
$f_{t,90}$ ABK[2]		99		87
f_v		86		94
G_{ft}		90		88
G_{fv}		72		71

1) BM: Measured at Dept. Struct. Mech., Lund
2) ABK: Measured at Dept. Struct. Eng., Lyngby

In the following sections each test type has been described in details.

Results

The results are presented in Annex 1. Annex 2 contains the mean and standard deviation for each type of notched beam specimen. Further, some mean values are given in the following sections together with the results of correlation and regression analyses.

3.1 Density and moisture content of the wood

Density

The densities were measured on 2 types of specimens, partly the whole notched beam, and partly small wood blocks cut from the full length timber beam. See figure 2.3.1.

The density of the specimen was measured by weighing the "wet" specimen and determination of its volume by measuring the length of the sides. This wet density ρ_{wet} was transformed to a dry density from the following formula.

$$\rho_{dry} = \rho_{0,\omega} = \frac{dry\ mass}{wet\ volume} = \rho_{wet}/(1 + \omega) \tag{3.1.1}$$

where ω is the moisture content of the timber member which was in the range of 12% to 15%. Based on an average moisture deformation perpendicular to the grain of app. 2% per change in percent–point of moisture the exact dry density can be calculated.

Moisture content

In general the moisture content was measured by means of an electrical moisture meter, which measured the electrical resistance between 2 probes driven into the wood. The brand: Gann, Hydromette HT 85 equipped with isolated needles (probes).

The moisture meter was calibrated for each timber parcel of a certain dimension. This was done for a certain number of specimens cut out of the planks. Table 3.1.1 gives the results of the calibration, which was based on the formula (3.1.2)

$$\omega_{correct} = \omega_{elec.} + \omega_{add} \tag{3.1.2}$$

where $\omega_{correct}$ moisture content measured by weighing and drying according to ISO 3130.

       $\omega_{elec.}$ moisture content measured electrical

ω_{add} constant additive term.

Table 3.1.1   Results from calibration of electrical moisture meter

Timber: Dimension	Nationality	Number of specimens	Mean values ω_{correct} %	ω_{elec} %	ω_{add}	Max single deviation %
45 x 95	S	14	12.8	11.7	1.1	0.9
45 x 195	S	7	13.4	11.8	1.6	0.8
85 x 185	DK	13	14.2	12.4	1.8	0.9
33 x 90	S	14	11.9	11.8	0.1	1.2
33 x 160	S	7	12.7	12.5	0.2	0.5

From table 3.1.1 it can be seen that the maximum deviation between the estimation from (3.1.2) and the correct measured moisture content is about 1%–point.

Results

The measured density and moisture content for each specimen is given in annex 1 and annex 2 for each specimen type. In table 3.1.2 there is stated the mean values and standard deviations for each timber dimension.

Table 3.1.2   Mean values and standard deviations for each timber dimension

Cross section		Timber: 45 x 95	45 x 195	85 x 185	Glulam 90 x 300 90 x 200	160 x 567
ρ_{dry} st. dev	kg/m³	429 27	388 32	388 25	442 16	418 9
$\bar{\rho}_{\text{dry}}$ Notch lam st. dev					441 35	386 33
$\bar{\omega}$ st. dev	%	12.8 0.5	14.0 0.3	15.1 1.1	12.0 0.6	12.8 0.5
Small specimens from compression tests, see subsection 3.4.4:		46 tests	17 tests	8 tests		
$\bar{\rho}_{\text{dry}}$ [kg/m³] st.dev.		416 28	378 36	360 37		
$\bar{\omega}$ [%] st.dev.		12.6 0.6	14.3 0.3	14.7 0.3		

It appears from table 3.1.2 that the standard deviations are reasonable small and homogenious, meaning that the variation between test specimens is rather limited.

3.2 Modulus of elasticity in the direction of grain, the longitudinal direction.

Test method – solid timber

The modulus of elasticity in the grain direction, E_0, was measured by placing the whole plank in a 4–point–bending arrangement. A deflection difference u_{bridge} was measured in the middle section where the curvature was constant, leading to the determination of E_0.
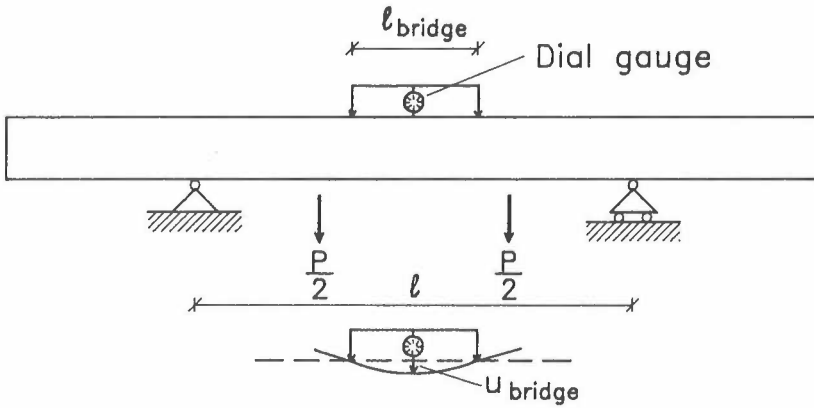
Figure 3.2.1   Measurement of E_0. E_0 can be determined from the measured deflection, u_{bridge}, over the middle length with constant curvature.

The plank was laid on two trestles and symmetrically loaded at two points. Thus, in the middle section, the bending moment and the curvature were constant.

A measuring bridge was placed in the middle section, and the deflection, u_{bridge}, over the length of the bridge, ℓ_{bridge}, was measured.

The deflection u_{bridge}, is related to the curvature κ by the equation $u_{bridge} = \kappa \cdot \ell_{bridge}^2/8$, and using that $\kappa = M/EI$, the following formula is obtained:

$$E_0 = \frac{1}{8} \frac{M}{I} \frac{\ell_{bridge}^2}{u_{bridge}} \qquad (3.2.1)$$

21

Because of accuracy of the employed dial gauge, the deflection u_{bridge} should be of a considerable size, at least $1/2$ mm and preferable 1 mm. But for very stiff planks, this could be difficult to obtain. As it can be seen from equation (3.2.1), the deflection, u_{bridge} can be increased by increasing the bending moment, i.e. the span. However, the bending moment should be kept under a certain level (50% of the bending moment capacity). As an alternative the deflection could be increased by increasing the measuring length, ℓ_{bridge}.

Measurements in pilot tests showed, that if the modulus of elasticity was measured over different lengths, even for a small shift, results differed 5–10%, indicating a variation along the plank. Especially knots and irregular grain affected the modulus of elasticity.

In general it is estimated that the E–modulus is measured with an accuracy of up to 10%.

The final arrangement for measuring E–modulus in the grain direction for solid timber planks is shown in figure 3.2.2.

The load was applied manually by putting lead weights on the pan. A load distributing arrangement or a yoke was used to apply the 2 forces at the third points approximately. For the larger planks it was more convenient to apply the load through a hydraulic jack.
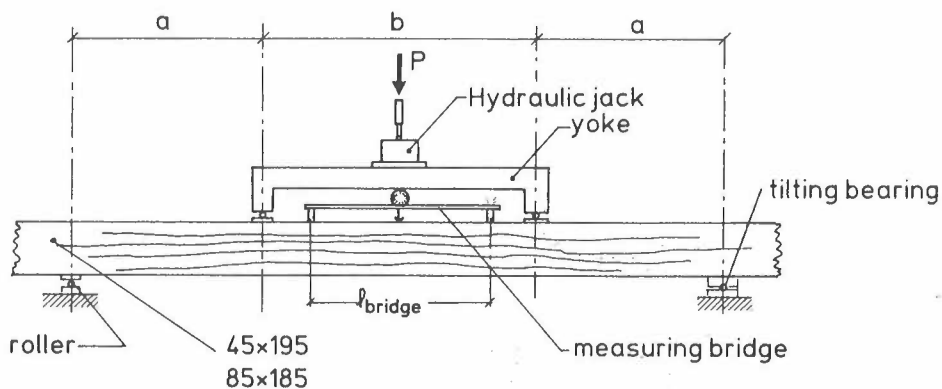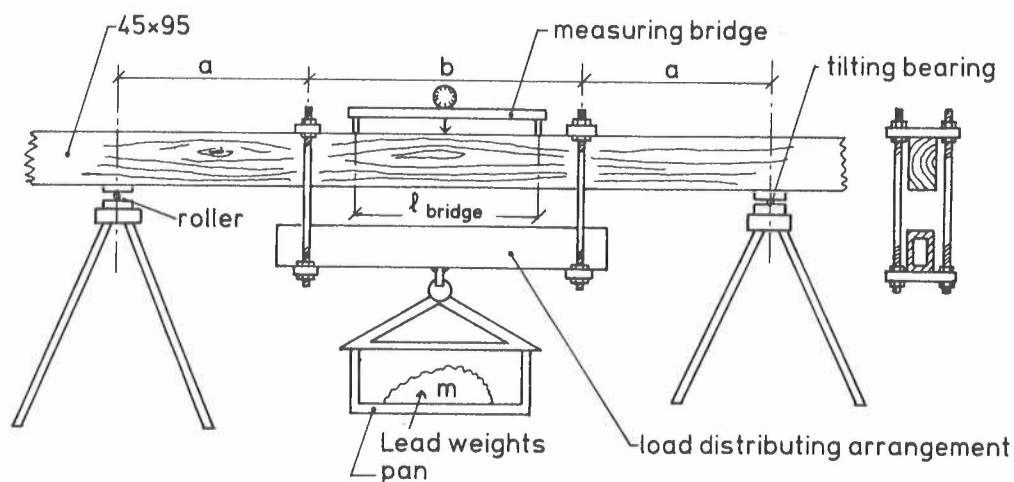
Dimension	Load m (kg)	Load P(kN)	a (m)	b (m)	ℓ_{bridge} (m)	Expected[1] u_{bridge} (mm)
45 x 95	191.7	—	0.75	1.00	0.60	0.8
45 x 195	—	7.8	0.85	1.00	0.80	0.7
85 x 185	—	12.8	0.95	1.00	0.80	0.8

[1]Based on expected E–modulus, $E_0 = 13$ GPa

Figure 3.2.2   Measurement of E–modulus in the grain direction for solid timber planks.

Test method – glued laminated timber

For the glued laminated beams the E–modulus for the notch lamination was of primary interest. The E–modulus for the whole beam was estimated from the correlation with the density and moisture content of the wood. This correlation was determined from bending tests with the notch lamination.

The same test principles as for timber were employed for the laminations – only the parameters were changed. The arrangement for measuring E–modulus in the grain direction for the notch lamination is shown in figure 3.2.3.

In this case, however, the bending moment is not constant in the total measuring area and a shear contribution to the deflection must be added. Because of the short lengths it was necessary to employ a bridge length larger than the moment span, 24 cm. Otherwise the deflection u_{bridge} was too small to be measured accurately with the dial gauge.

Dimension	Load P (kN)	Expected[1] u_{bridge} (mm)
33 x 100	5	3.5
33 x 175	7	2.8
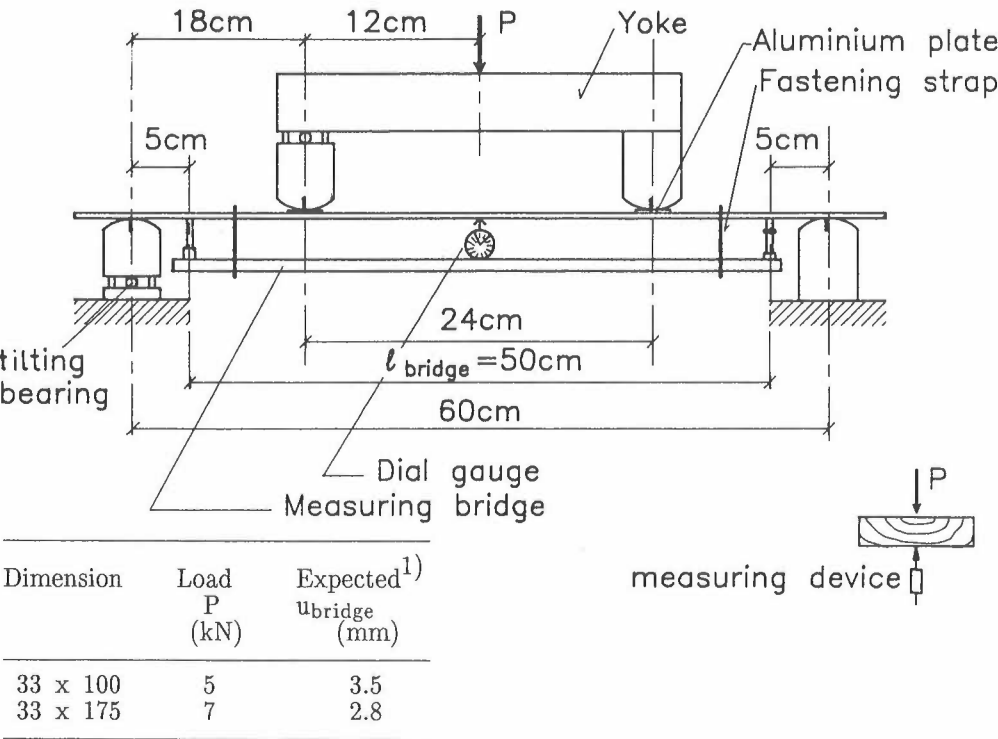
[1]Based on expected G–modulus: G = 750 MPa
Based on expected E–modulus: E = 13 GPa

Figure 3.2.3   Measurement of E–modulus in the grain direction of laminations in glued laminated timber.

It can be shown, that the E-modulus can be calculated from formula (3.2.2), when the arrangement in figure 3.2.3 is employed.

$$E_O = \frac{2.629 \cdot 10^{-3} \cdot P/I}{u_{bridge} - 0.078 \cdot P/G \cdot A} \qquad (3.2.2)$$

where   P = applied load
         I = moment of inertia
         G = shear modulus (to be estimated)
         A = cross-sectional area
         u_{bridge} = measured displacement

There was tested two different notch lamination dimensions, 33 x 100 mm² and 33 x 175 mm², corresponding to the beam dimensions, 90 x 200 mm²/90 x 300 mm² and 160 x 567 mm².

As it can be seen in figure 3.2.3, the relative accuracy of the measured deflection u_{bridge} is good when a dial gauge with an accuracy of 1/100 mm is used.

The determination of the moment of inertia, $I = \frac{1}{12}bh^3$, however, is encumbered with considerable inaccuracies because of the sawn surfaces.

As the dimensions only can be measured within an accuracy of not less than 0.5 mm, the moment of inertia is determined within an accuracy of 10%. Moreover, the cross-
-sectional dimensions are likely too vary along the length of the lamination. The cross-
-sectional dimensions were measured at the middle, giving a reasonable average value.

Test results
The results are given in table 3.2.1, showing the mean values and standard deviations for each group of dimensions. Further, the individual values for each notched specimen are given in annex 1.

Table 3.2.1   Measured E–modulus for solid timber beams and notch lamella in glued laminated beams. The E–modulus for the glued laminated beams is estimated from the density relation. Mean values and standard deviations.

Dimensions	Number of tests	E–modulus measured on beam		E–modulus measured on notch lamination		Estimated E–modulus for beam	
		E_0(GPa)	Standard deviation	notch E_0(GPa)	standard deviation	E_0(GPa)	
45 x 95	45	13.9	1.7	–		–	
45 x 195	21	13.1	2.2	–		–	
85 x 185	24	12.0	2.3	–		–	
90 x 200 and 90 x 300	23	–		13.9	2.8	13.8	0.5
160 x 567	8	–		11.3	0.7	13.0	0.3

Comments to test results

It is typical that the E–modulus of the Danish grown 85 x 185 mm timber members is a little lower than the Swedish planks of thickness 45 mm. The wider boards in the glulam have a lower E–modulus because of thicker annual rings.

Correlation and regression analysis

The results of a multiple linear regression analysis between the modulus of elasticity E_0 and the free parameters the density ρ and the moisture content ω of the timber members are given in table 3.2.2. The employed regression equation was:

$$\text{Mat.param} = \text{Intercept} + k_\omega \cdot \omega + k_\rho \cdot \rho \tag{3.2.3}$$

where the material parameter was E_0 of either the structural timber members or the laminations.

Table 3.2.2   Parameters in the regression equation for the modulus of elasticity E_0 in the grain direction and with the free parameters moisture content ω and the density ρ.

		Number of tests	Coeff. of correl.	Intercept GPa	k_ω GPa/%	k_ρ GPa/kg/m³
Structural timber:						
b x h	45 x 95 mm	45	0.68	1.4	−0.515	0.0444
	45 x 195 "	21	0.53	−32.9	1.485	0.0259
	85 x 185 "	24	0.43	25.8	−0.914	Not signifi.
Glulam, notch lami.:						
All dimensions		31	0.48	0.9	−0.124	0.0327
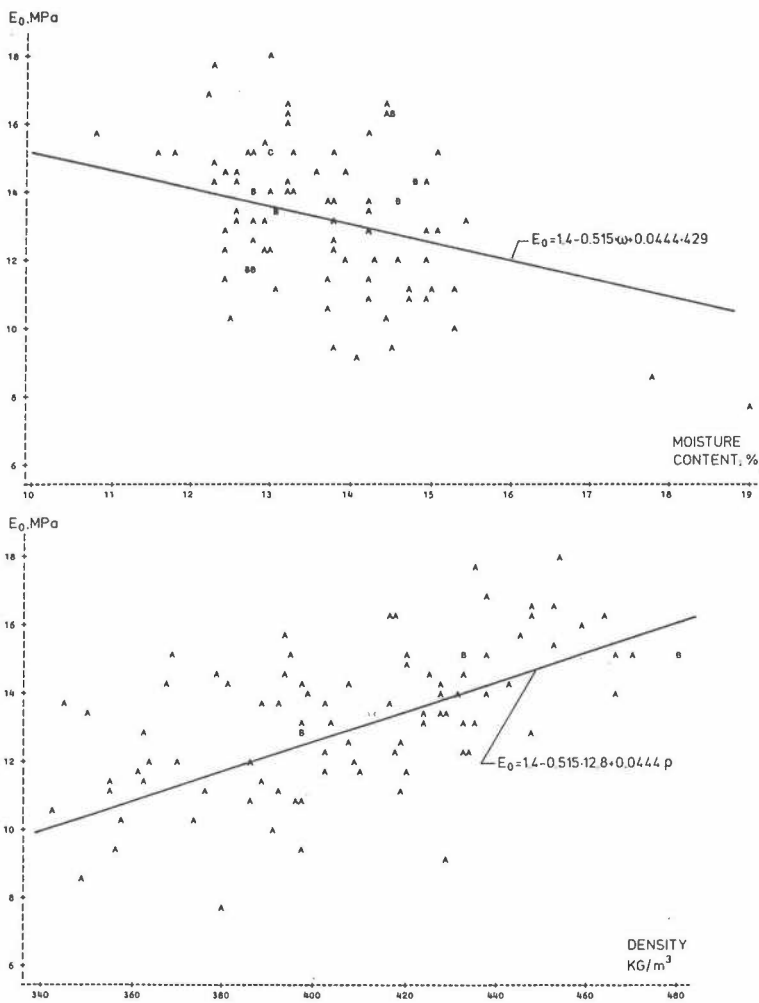
Figure 3.2.4   Graphic illustration of the relation between E—modulus E_0 and (moisture content, density).

27

In almost all the cases the coefficient of correlation is of moderate size. The reason why is that some inevitable growth defects disturbed the measurements and these defects were not considered in the regression equation. For example, for the timber of dimension 85 x 185 mm the density was not found to be significant at the 0.15 level, but it is known from other research, that this cannot be correct.

3.3 Shear modulus G

Two different test methods were employed. At ABK the shear modulus was measured on the planks subjected to shear in a 3– or 4–point–arrangement. In this way there was aimed at having the same stress and strain distribution over the width of the cross section as in the notched beams.

At BM the shear modulus was measured indirectly on a cubiform specimen cut out of the plank and with a side length of 45 mm in the width direction. The stiffness properties for four directions, $v = 0^0$, 45^0, 90^0 and 135^0, in relation to the material principal axis, were compared and from this the shear modulus was determined.

The two methods will be discribed seperately in the following.

3.3.1 Shear modulus G from planks subjected to shear

The plank was supported at the ends and loaded with a concentrated force at the middle of the span resulting in a constant shear force, equal to the half of the applied load. However, for the solid timber planks of 45 x 95 mm^2 , a 4–point–arrangement was employed. In this case the shear force was also equal to half of the applied load.

The shear strain, γ , was measured in the shear span by means of strain gages positioned at the middle of the cross section on both sides, where the normal stresses are expected to be zero. The position was selected so, that there were no knots in the vicinity. The shear stress, τ , is calculated from the shear force, and the shear modulus, G, can then be found from the wellknown equation:

$$\tau = G \cdot \gamma \qquad (3.3.1.1)$$

The arrangement is shown in figure 3.3.1.1.

Figure 3.3.1.1   Arrangement for measurement of the shear modulus G. The shear
strain γ is measured by means of strain gages.
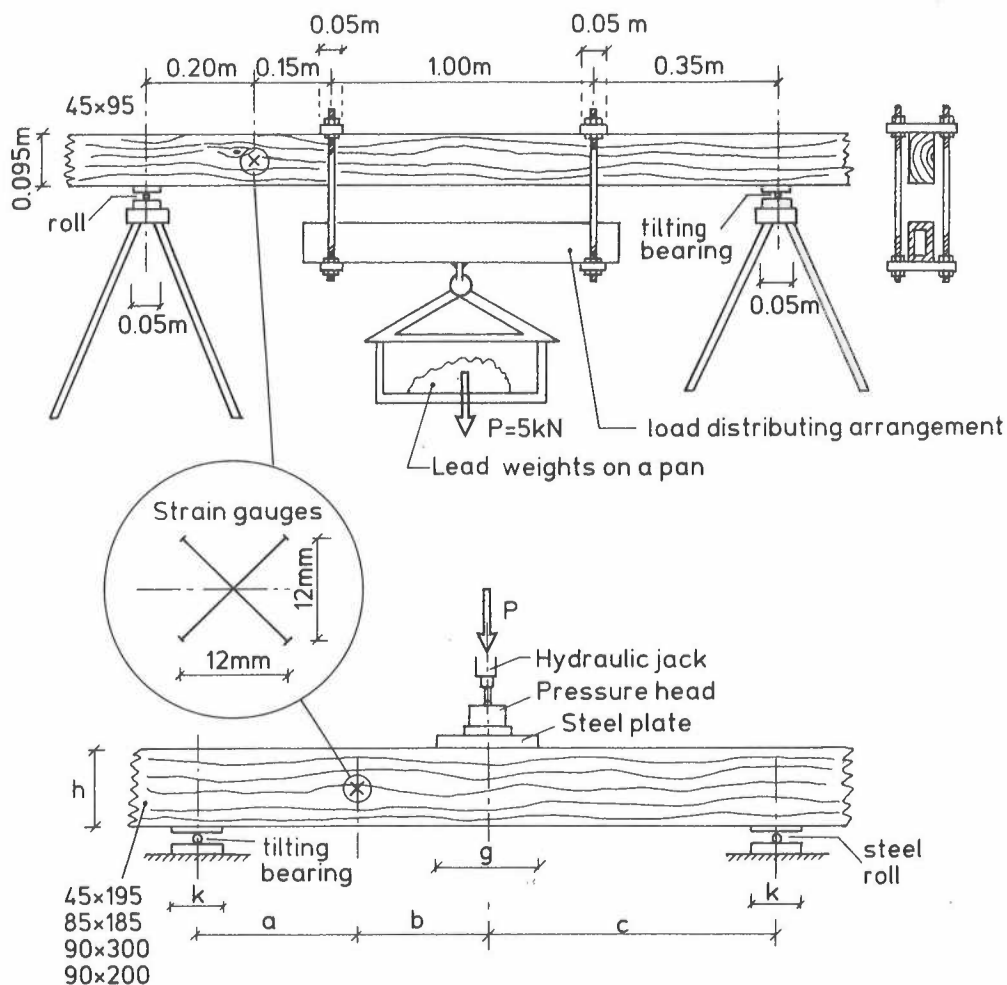
Dimension	Load P (kN)	a (m)	b (m)	c (m)	g (m)	k (m)	h (m)
45 x 195	10	0.40	0.40	0.80	0.25	0.08	0.195
85 x 185	20	0.40	0.40	0.80	0.25	0.08	0.185
90 x 300	40	0.44	0.44	0.88	0.25	0.15	0.300
90 x 200	40	0.29	0.29	0.58	0.25	0.15	0.200

The shear stress distribution over the cross section of a beam subjected to shear can approximately be found from Grashof's equation:

$$\tau(z) = \frac{3}{2} \frac{V}{b \cdot h}(1 - (\frac{2 \cdot z}{h})^2)$$

$$\tau_{max} = \frac{3}{2} \frac{V}{b \cdot h}$$
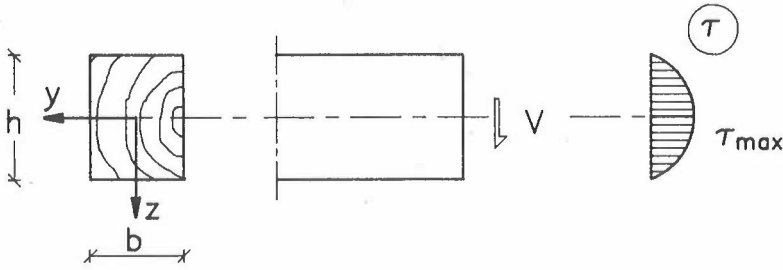
(3.3.1.2)

Figure 3.3.1.2 Shear stress distribution under ideal conditions.

To determine the exact plane stress distribution and to investigate the influence of the boundary conditions on the measurements, a series of Finite Element–Analysis were carried out.

The employed Finite Element model for planks of 45 x 95 mm² is shown in figure 3.3.1.3. There was employed a triangular plane element with a complete cubical displacement field. The measured orthotropic elastic constants for the actual test beams were used in the FEM–analysis. These were in the range $E_0 \sim 11 - 16$ GPa, $E_{90} \sim 150 - 250$ MPa and Poisson's ratio ~ 0.5. The shear modulus G was estimated to be in the range of $G \sim 630 - 850$ MPa.
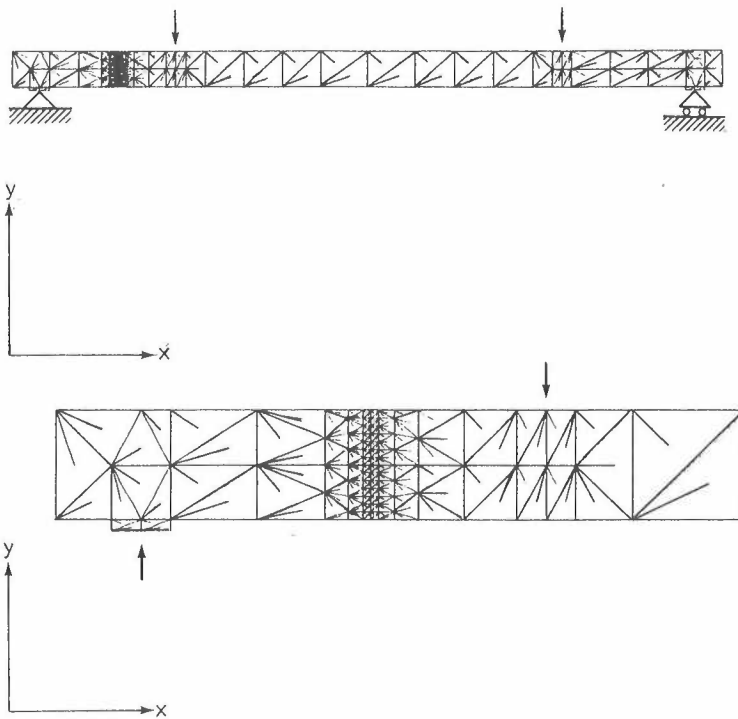
Figure 3.3.1.3   Finite Element model for the stress analysis employed by the de-
termination of the shear modulus , G, for planks of 45 x 95 mm².

Some deviations from the Grashof shear stress distribution were found, especially for
the glued laminated beams.

The deformed Finite Element model for glued laminated planks of 90 x 200 mm² , is
shown in figure 3.3.1.4, which also shows the FEM shear stress distribution compared
with the Grashof distribution.
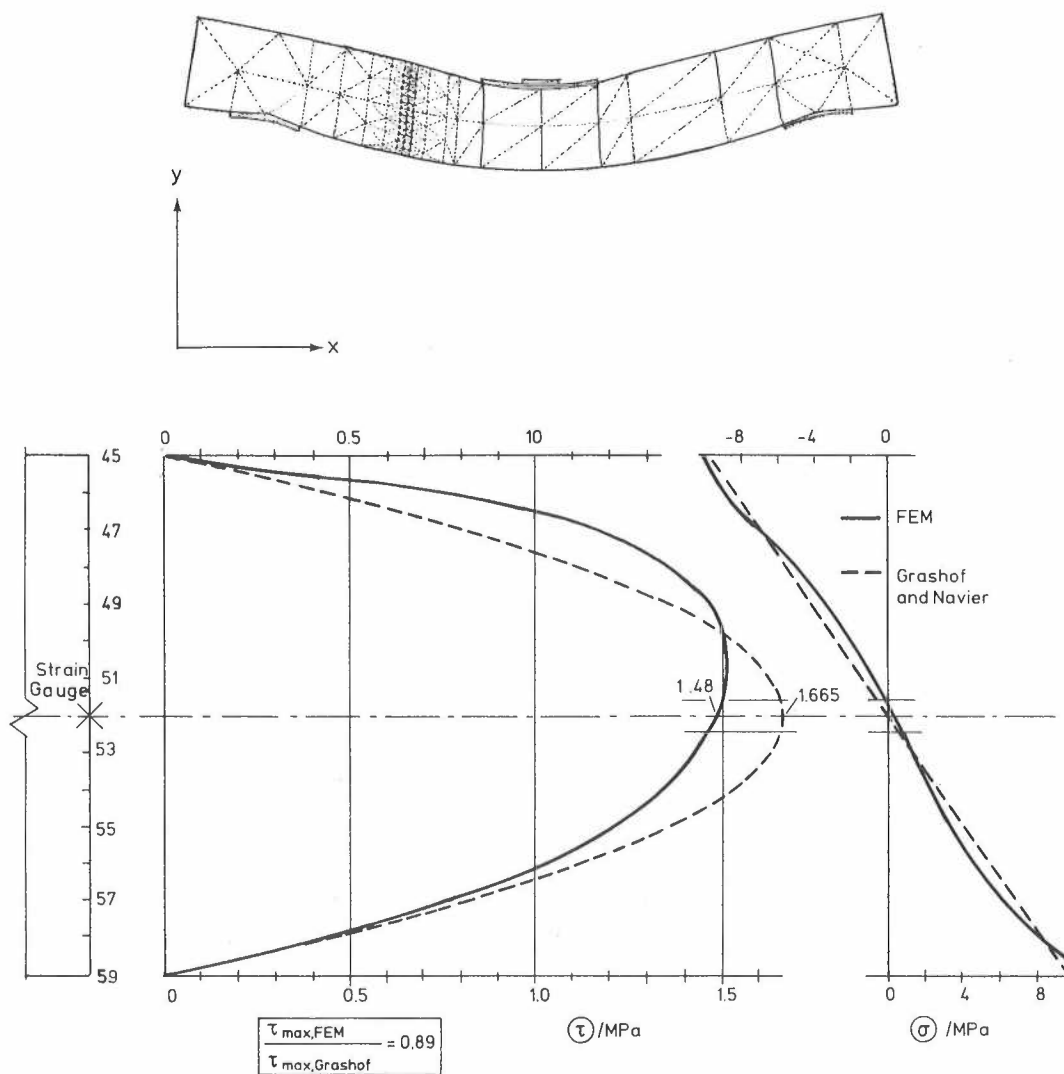
Figure 3.3.1.4   Results from a FEM–analysis of a 90 x 200 mm² beam.

It can be seen from figure 3.3.1.4 that the maximum shear stress in the FEM analysis is in this case only 89% of the maximum value from Grashof's formula.   The correction factors found for the other dimensions are shown in table 3.3.1.1.

32

Table 3.3.1.1 Correction factor for equation (3.3.1.3) based on shear stress in the strain gauge area determined by in FEM–analysis.

Dimension	Correctionfactor k_1 $(\tau_{\text{max,FEM}}/\tau_{\text{max,Grashof}})$
45 x 95	1.02
45 x 195	0.99
85 x 185	0.99
90 x 300	0.94
90 x 200	0.89

Thus the shear stress in the strain gauge area can be found from equation (3.3.1.3)

$$\tau_{\text{cor.}} = k_1 \cdot \frac{3}{2} \cdot \frac{V}{b \cdot h} \qquad (3.3.1.3)$$

The shear strain was, as mentioned, found from strain gage measurements. The strain in two orthogonal directions, ϵ_{45^0} and ϵ_{135^0}, as shown in figure 3.3.1.5, were measured. Further, it was assumed that the stress and strain in the grain direction was zero because the gages were placed at the middle of the depth of the cross section.
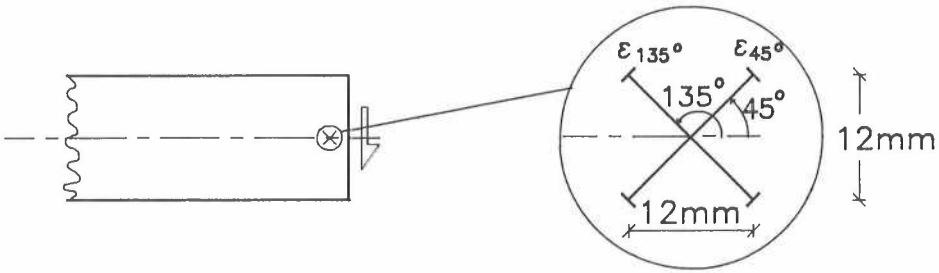
Figure 3.3.1.5 Measurement of strains in two orthogonal directions,ϵ_{45^0} and ϵ_{135^0}.

It can be shown, that the shear strain γ is found from

$$\gamma = \epsilon_{135^0} - \epsilon_{45^0} \qquad (3.3.1.4)$$

Thus, the shear modulus $G = \tau_{\text{cor.}}/\gamma$ is found from

$$G = k_1 \cdot \frac{3}{2} \frac{\Delta V}{b \cdot h \cdot (\Delta \epsilon_{135^0} - \Delta \epsilon_{45^0})} \tag{3.3.1.5}$$

where k_1 = correction factor from table 3.3.1.1

ΔV = increment in shear force equal to half the applied load.

b,h = width and depth of cross section

$\Delta \epsilon_{135^0}, \Delta \epsilon_{45^0}$ = increment in measured strains

According to the accuracy of the datalogger employed, the strain gage properties and the measuring conditions in general, the accuracy of the strain gage measurement was $\Delta \epsilon = 0.038$ ‰.

In table 3.3.1.2 the actual accuracy on the measured strains for the different dimensions are shown. The table shows that the strains are determined within an accuracy of less than 6%.

Table 3.3.1.2   Accuracy of strain gage measurements.

Dimension	$\tau_{cor.}$ eq.(3.3.1.3) (MPa)	$\hat{\gamma}$ [1] ‰	$\hat{\epsilon}$ [2] (‰)	$\frac{\hat{\Delta \epsilon}}{\epsilon}$ (%)
45 x 95	0.90	1.3	0.65	5.8
45 x 195	1.69	2.4	1.2	3.2
85 x 185	1.89	2.7	1.35	2.8
90 x 300	2.09	3.0	1.5	2.5
90 x 200	2.96	4.2	2.1	1.8

[1]   Based on the assumption that   G = 700 MPa

[2] $\hat{\epsilon} = |\epsilon_{45^0}| \simeq |\epsilon_{135^0}| \simeq \frac{1}{2} \cdot \hat{\gamma}$

Test results

The results are given in table 3.3.1.3, showing the mean values and standard deviations for each group of dimensions. Further, the individual values for each notched specimen are given in annex 1.

Table 3.3.1.3   Measured shear modulus for solid timber beams and glued lamina-
                ted beams. The shear modulus was determined by measuring the
                shear strain in a plank subjected to shear. Mean values and stan-
                dard deviations.

Dimensions	Number of tests	Mean G MPa	Standard deviation MPa
Timber beams			
45 x 95	9	787	139
45 x 195	3	730	149
85 x 185	4	678	124
Glulam:			
90 x 200 and			
90 x 300	12	733	155

The shear modulus was not measured for the 160 x 567 mm² glued laminated beams.

Correlation and regression analysis

In table 3.3.1.4 there is stated the results of an analysis of G(density, moisture). Equa-
tion (3.3.1.3) has been employed for the determination of G.

Table 3.3.1.4   Parameters in the regression equation for the shear modulus G
                with the free variables moisture content ω and density ρ

	Coeff. of correl.	Intercept MPa	k_ω MPa/%	k_ρ MPa/kg/m³
Structural timber:				
b x h: 45 x 95 mm	0.71	−2808	246	1.02
45 x 195	Only 3 measurements			
b = 45 & h = 95 or 195 mm	0.58	−714	40	2.25
85 x 185 mm	0.81	−4232	207	4.81
Glulam:				
b = 90 & h = 200 or 300 mm	0.37	1913	23.8	−3.33[1]
b = 90 & h = 200 or 300 mm	0.34	−174	11.3	0.78[2]

[1] Density of the whole beam.
[2] Density of the notch lamination.

It is surprising to see that the shear modulus is estimated to be positively correlated
with the moisture content. One reason to this could be that the range of the measured
moisture contents is limited and thus not suitable for a regression analysis.

Further, it is remarkable that the coefficient of correlation is very low for the glulam,
both for the density of the whole beam and for that of the notch lamination.

Test method

In order to verify the shear modulus from beam tests in section 3.3.1, a few tests of shear modulus were carried out on small cubes cut from the beams. In this alternative manner only four specimens were tested. For these specimens not only G, but also E_{90}, E_0 and ν were determined. The cube test, in a previous study used for testing E_{90}, E_0, G and ν see /Gustavsson and Enquist, 1988/, is in this study used through-out only for testing E_{90} in compression, see section 3.4.3.

Each specimen was uniaxially loaded in compression in four different directions, see figure 3.3.2.1. The E–modulus in the grain direction, x–direction, and perpendicular to the grain, y–direction, were determined by loading and strain measurements in the x– and y–direction, respectively. The Poissons ratio was determined by loading in the x–direction and strain measurements in the y–direction. After this the corners of the specimen were sawn away. In this way a new smaller specimen was obtained and the load direction and also the direction of strain measurements were thus rotated 45°.
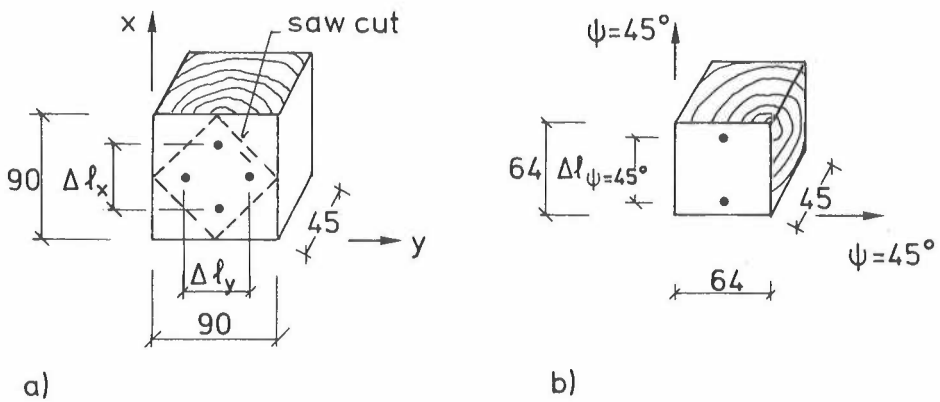
Figure 3.3.2.1   Geometry of small test specimen used for determining the shear modulus
a) Determination of E_x, E_y and ν_{xy}
b) Determination of $E_{\psi=45}$

36

On the loaded surfaces of the specimen plates covered with square shaped pieces of rubber were placed, see figure 3.3.2.2. The rubber faced the steelplates of the testing machine. Three layer of plastic film with grease between each layer was placed between the fibre board and the specimen. This arrangement was to allow for lateral expansion. Moreover, together with the centric application of load the actual setup should give fairly uniform stresses and strains within the specimen.

The gauge length was in all cases 40 mm and the tests were carried out with a constant rate of piston movement, 1 mm/min. Deformation was recorded as the mean value from two gauges, one placed at the front of the specimen and one at the back. The test was stopped and the specimen unloaded at a load corresponding to approximately 20% of the short term failure load.
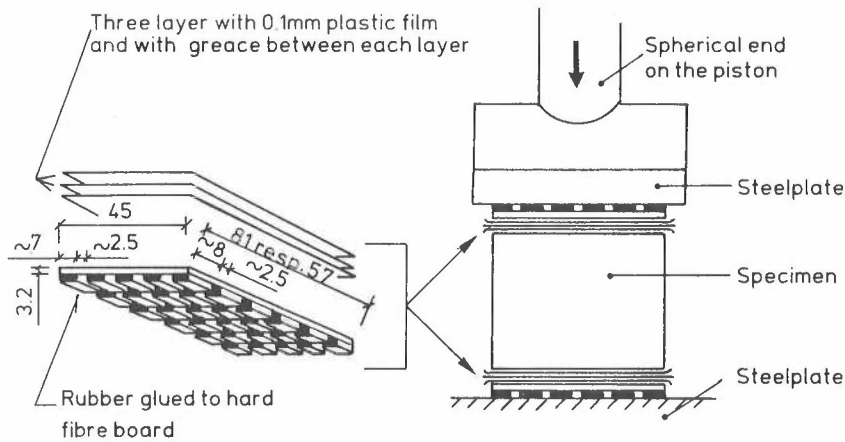
Figure 3.3.2.2 Support of small specimen in compression

Test results

Knowing $E_y = E_{90}$, $E_x = E_0$ and ν from the initial tests of the cube, G is obtained from:

$$G = \left[\frac{4}{\Delta\sigma_{45}} \Delta\epsilon_{45} - \frac{1}{E_x}(1-2\nu) - \frac{1}{E_y} \right]^{-1}$$

where $\Delta\epsilon_{45}$ is the recorded change in strain for the direction of load $\psi = 45^{\circ}$, produced by an increase in load corresponding to the increase $\Delta\sigma_{45}$ in stress. In the present

37

tests the choice $\Delta\sigma_{45} = 0.48$ MPa was made, this increase starting from a load corresponding approximately to $\sigma_{45} = 0.04$ MPa.

The test results indicated by "cube compression" are given in Table 3.3.2.1. In this table the corresponding results for E_0 and G as obtained in the tests of the whole beams, see sections 3.2 and 3.3.1, are also given. Moreover, E_{90} as obtained by two tensile test methods, see section 3.4, are also given.

Table 3.3.2.1   Results from tests of four small specimens, E–modulus, Poissons ratio and shear modulus. For comparison the values measured by ABK on whole beams or full width specimens have also been given.

Specimen	E_0 [MPa]		E_{90} [MPa]			ν_{xy}	G [MPa]	
	Cube comp.	Whole beam	Cube comp.	Small tens.	Full width		Cube comp.	Whole beam
30–2–1	27726	14700	321	188	223	0.93	432	704
17–1–1	10131	13500	154	136	276	0.66	2253	808
15–1–1	15196	16700	152	212		0.44	418	1102
11–2–1	10899	12500	159	188	197	0.71	486	653

Specimen denoted 17–1–1 should be neglected because it had some small knots that became visible when the specimen was cut to the smaller size, figure 3.3.2.1.1.b).

3.3.3 Comments to the two test methods for the G–modulus

In the beam tests with the planks there has been aimed at to measure the stress–strain relation for a state, which is as close as possible to the state in the notched beams. Further, the shear modulus was measured directly from 2 strain gage measurements. On the other hand the cylindrical orthotropic and the inhomogeneous properties of the wood means that the measurements were not carried out on a specimen with a homogeneous stress–strain field at the strain gages and with exactly zero strains in the grain direction.

For the cube tests can be argued that the stress distribution is inhomogeneous. The reason why is that wood can be perceived as a fibre reinforced material, and when the fibres are inclined with the surfaces the boundary condition at a free surface is that they shall be stress free, see figure 3.3.3.1. But inside the material they shall carry their share of the stresses. So in a boundary layer at the surface the axial stress in the

fibres will decrease to zero meaning that large shear stresses occure in the matrix material. The size of this boundary layer is not known. But if it has a relatively large size compared with the size of the test specimens then the stresses and strains over the measuring length will be larger than assumed. This will lead to smaller values of the G–modulus.

In this relation, it can be seen from table 3.3.1.4 and 3.3.2.1 that the G–moduli from cube tests are smaller than those from beam tests.
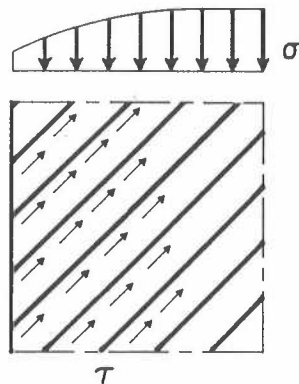
Figure 3.3.3.1   Stresses at a free surface of a fibre reinforced material with inclined fibres.

Further, when comparing the E–modulus E_0 it must be remembered, that E_0 measured from beam tests represents a mean value over the gauge–length, whereas the cube––test results in an E–modulus measured locally. For the G–modulus the beam test results in a G–value which is influenced from the properties over the whole cross section, whereas the cube tests reflect the properties in a smaller part.

It has been decided to employ the G–modulus measured by beam tests in the further analyses in this report, partly because very few cube tests were carried out.

3.4 E–modulus and tensile strength perpendicular to grain.

3.4.1 Shape and size of test specimens. Possible explanations of differences between measured values.

The shape and size of the test specimens are discussed in this section 3.4. Further, it appears from this section that the strength and stiffness properties perpendicular to grain depend on the shape and size of the test specimens. In the following there is given some possible explanations of this. One is based on that wood can be described as a fibre reinforced material. Another is based on an orthotropic continuum material model and the difference originates in different stress and strain states in the narrow and in the full width specimens allowing more or less shear deformation.

The models have been developed by members of the project team, and have been discussed with the whole team. But no final clarification has been reached.

General about the stress–strain state and the type of test specimens
It was the intention to employ a test specimen, which as far as possible reflected the stress and strain field in the notched beams at the failure zone. This zone is very limited, figure 3.4.1.1 shows the tensile stress distribution along the process zone and inward along the grain. The stress distribution have been calculated by means of the Finite Element Program specially developed for this project.
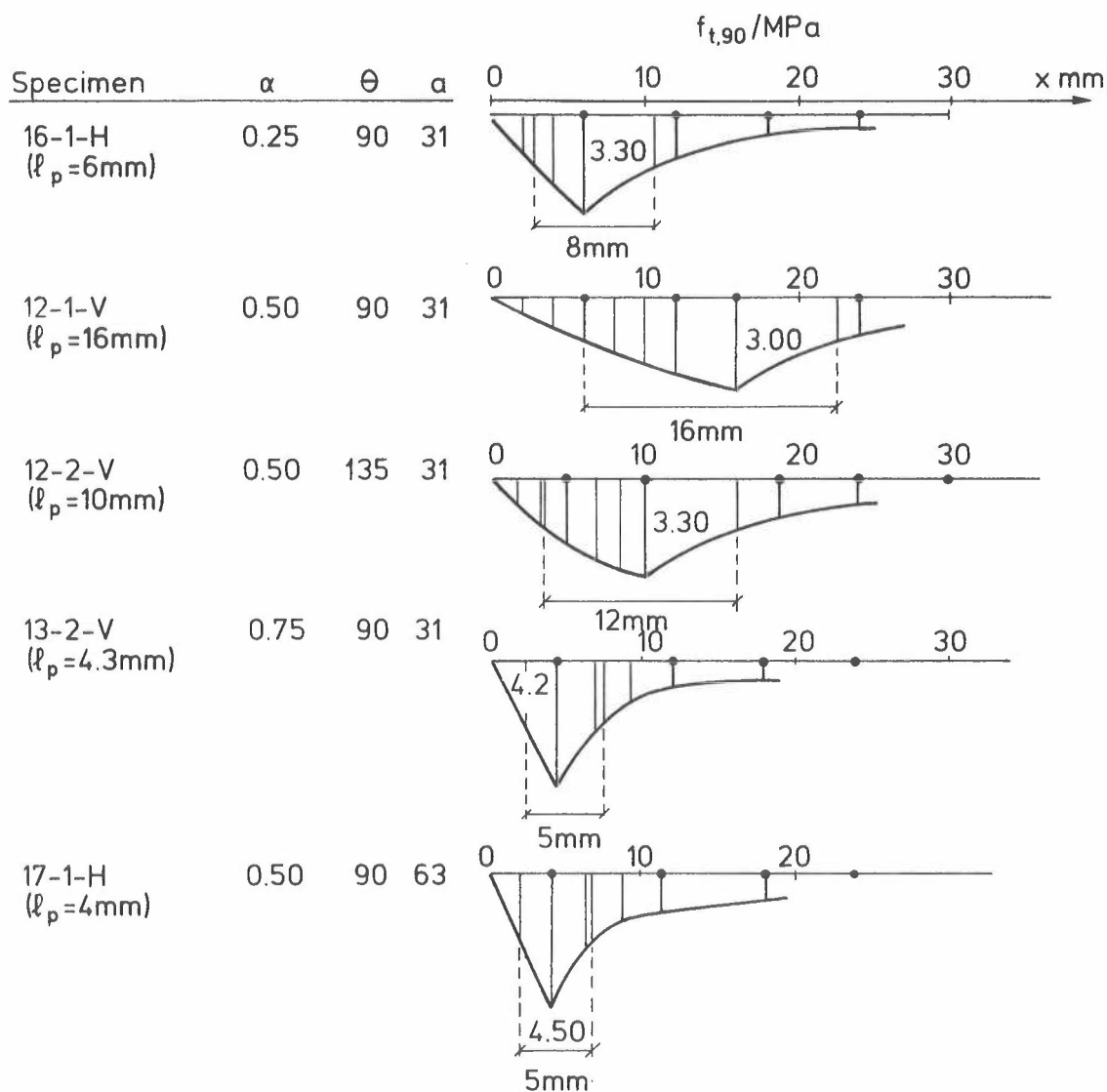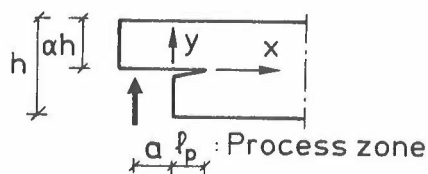
Figure 3.4.1.1   Distribution of tensile stresses perpendicular to grain at failure in some selected specimens. The stress analysis has been carried out by a special FEM–program and the material parameters are given in appendix 1.

In figure 3.4.1.1 there is marked the lengths over which the tensile stresses were above half the maximum value $f_{t,90}$ (the tensile strength perpendicular to grain). The range of these lengths are from 5 to 16 mm.

Because of the size effect in a brittle inhomogeneous material as wood it is of importance to employ test specimens with a length in the grain direction of the same size 10–15 mm.

The dimensions perpendicular to the grain were:

In the depth direction 20–50 mm
In the width direction Either 16 mm or the total width.

The specimens with a width of 16 mm were employed by BM in Lund, whereas the specimens with a width equal to the width of the notched beams were employed by ABK.

There was performed a stress analysis of the employed specimen types. It was carried out by means of the group of programs in PAFEC. A rectangular plane stress element with 8 nodes and the following orthotropic constants were used. These were determined from tests with narrow specimens, width = 16 mm. The following values have been used in the FEM analysis. They were determined before the results had been analyzed so they do not reflect the findings shown in figure 3.4.3.2 where E_R = $E_{v\ mean\ =\ 0}$ > E_T = $E_{v\ mean\ =\ 90}$. They reflect the measured mean values given in table 3.4.2.2.

E–modulus:
  Tangential direction $E_T = 300$ MPa
  Radial direction $E_R = 200$ MPa

Shear modulus $G = 100$ MPa

Poisson ratio $\nu_{R,T} = 0.5$

Figure 3.4.1.2 shows the elements. The shaded part models glued–on steel parts with E = $210 \cdot 10^3$ MPa and $\nu = 0.3$.

42
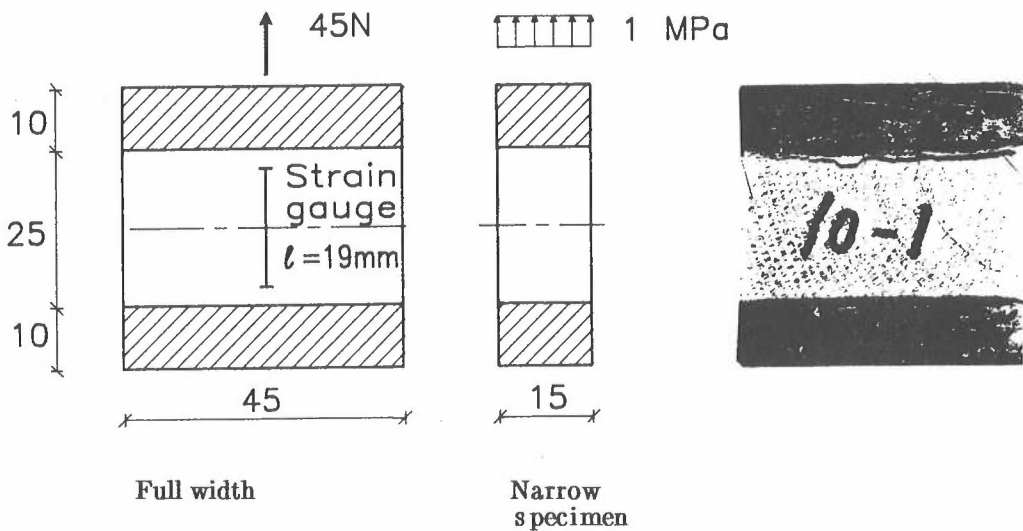
Figure 3.4.1.2   Elements in the plane model of specimens for tension perpendicular to grain, and to the right specimen number 10–1 after failure. Sizes in mm.

The model of the 45 mm wide specimens in case 2 and 3 were loaded with a concentrated force in the middle of the steel part. The force was 45 N resulting in a average stress of 1 MPa. The narrow specimen was subjected to a boundary tensile stress of 1 MPa.

The results of 3 cases are reported here. They are:

Case 2   A model of specimen 10–1

"   3   A 45 mm wide specimen with the orthotropic axis inclined 45°.

"   4   As case 3 but with a width of 15 mm.

For the model of specimen 10–1 each element had allocated homogeneous material properties with the orthotropic T–axis parallel to the average inclination of the tangent of the annular rings in the element.

Figure 3.4.1.3 shows the undeformed and deformed models. Deformations exaggerated. It is remarkable to see the slanting deformation field originating in the material anisotropy, specially the low G–modulus.

43
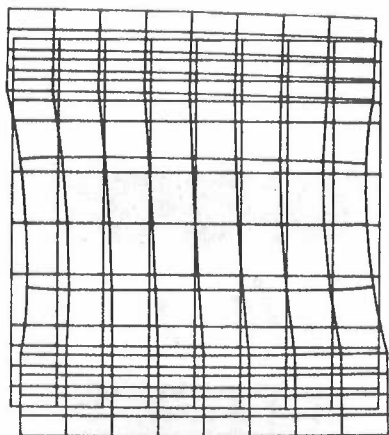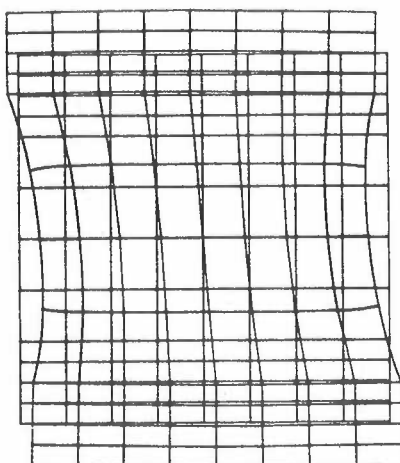
Case 2   Case 3   Case 4

Figure 3.4.1.3 Deformed and undeformed models of the tensile specimen.

From figure 3.4.1.4 it can be seen that there is not a homogeneous stress field in the tensile specimens. At the glue–line between steel parts and wood there is a pronounced stress peak at the sides. In the middle of the wood there is also a ununiform stress distributions.
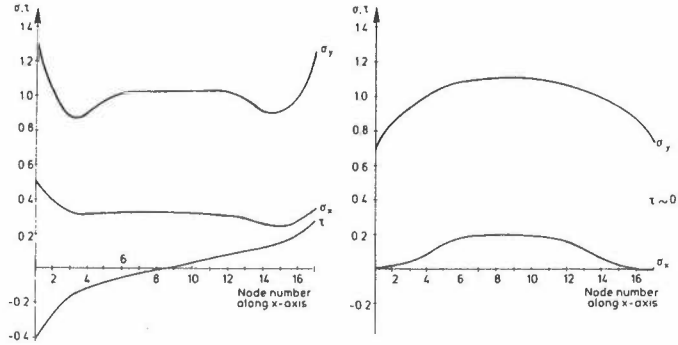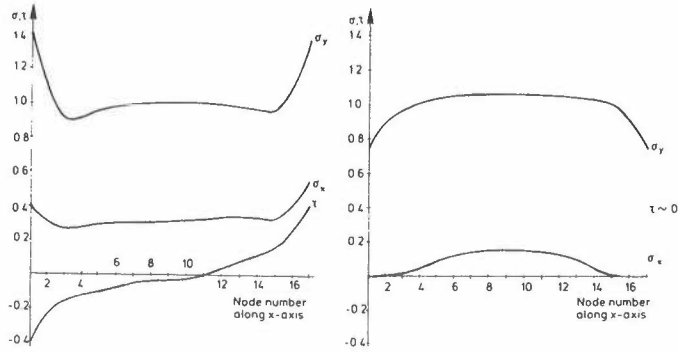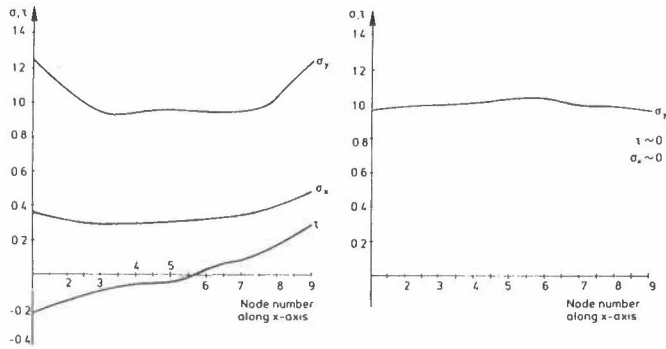
Figure 3.4.1.4   Stresses over the wood from side to side. Left: Stresses at the glue—
—line. Right: Stresses in the middle of the wood. Notice: The x—a-
xis is not a length scale, but gives the node members, so all models
are shown with the "same width" even though they have different
geometric width.

The stress peaks in the corners of the wood part could indicate that there is a tendency to, that the stresses are transferred as scew normal stresses from corner to corner. There will be dealt with this effect in the following.

From the FEM analysis the average strain $\epsilon_{av,y}$ over the gauge length 19 mm employed for the specimens with glued–on steel parts were determined from the displacements. The E–modulus in the tensile direction (the y direction) for case 2 was calculated from

$$E_y = \sigma_y/\epsilon_{av,y} = 1.0/3.476 \cdot 10^{-3} = 288 \text{ MPa} \tag{3.4.1.1}$$

From the well known formula for a continuum the E–modulus can be determined

$$E_y = \frac{E_0}{\cos^4 v + (\frac{E_0}{G} - 2 \, \nu_{90,0})\sin^2 v \, \cos^2 v + \frac{E_0}{E_{90}} \sin^4 \alpha} \tag{3.4.1.2}$$

$$= 288 \text{ MPa}$$

In formula (3.4.1.2) the zero–direction is the tangential direction and the angle $v = 90 - 57^0{,}38$, where $57^0{,}38$ is the average inclination of the annular rings of specimen 10–1 in case 2.

It can thus be concluded that the inhomogeneous stress field does not influence the measurement of the E–modulus in this case. Further, it has been demonstrated for the specimen that the shear deformation in the wood could occur freely, there has been no blocking effect of the deformation field from one part of the specimen to another. This blocking effect will occur when the annular rings are symmetrical in the specimen. But it must be remembered that in both cases a continuum mechanical description has been employed.

A description of wood as a fibre reinforced material

As already mentioned in section 3.3.3 wood can be understood as a fibre reinforced material. The aligned cell walls in the latewood constitutes in a way a stiff and strong band, which statically acts as a fibre. For fibre reinforced materials the fibres at free boundaries will have zero stress at their ends and the axial stress will over a zone increase rapidly to a level compatible with inner part of the material.

In the following there is described a simple material model by which the apparent E–modulus can be calculated. It is assumed that the difference between the apparent E–moduli measured in the narrow and full width specimens originates in that the stress distributions are different. So the two stress states should illustrate the effect on the E–modulus of the above mentioned boundary effect and the effect from the tendency to have only scew normal stresses in the directions of the principal axes of the material.

In both models it has been assumed that the "annular rings" are straight and with a constant inclination α. This appears reasonably for the small specimens.
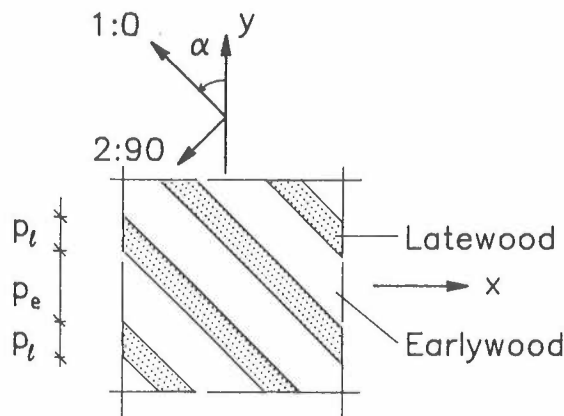
Figure 3.4.1.5   The cell structure and a plane model of the wood in a plane per-
                      pendicular to the grain.

The earlywood and latewood are modelled as a orthotropic continuum and they consti-
tute each a part p_e/p_ℓ of the wood. So the sum $p_e + p_\ell$ is equal to 1.0. The neces-
sary material constants are:

Earlywood:	$E_{e,0}$	$E_{e,90}$	G_e	$\nu_{e,0,90}$ $\nu_{e,90,0}$	$= \nu_e$
Latewood:	$E_{\ell,0}$	$E_{\ell,90}$	G_ℓ	$\nu_{\ell,0,90}$ $\nu_{\ell,90,0}$	$= \nu_\ell$

The Poisson ratios are signified by ν_e and ν_ℓ which both are related to E_0. They

shall be assigned "large values".

The modulus of elasticity for each part of the wood can thus be calculated from formula (3.4.1.2).

The orthotropic constants

$$E_{e,0} \quad E_{e,90} \quad E_{\ell,0} \quad E_{\ell,90}$$

can be found from 2 basic tests with axial stress in the principle directions of the material.

Further it is here, for simplicity, suggested to assess the E–moduli of the earlywood from

$$\begin{aligned} E_{e,0} &= k_0 \; E_{\ell,0} \\ E_{e,90} &= k_{90} \; E_{\ell,90} \end{aligned} \qquad (3.4.1.3)$$

The factors k_0 and k_{90} are judged from the difference in cell sizes, density, alignment of cell walls and so on. There is a limitation on these factors because the apparent E–modulus $\overline{E}$ originating in the average deformation shall be equal to the measured value.

When the stress is applied perpendicular to the annular ring then

$$\begin{aligned} \frac{1}{\overline{E}_{90}} &= \frac{p_e}{E_{e,90}} + \frac{p_\ell}{E_{\ell,90}} \\ E_{\ell,90} &= \overline{E}_{90} \; (p_\ell + p_e/k_{90}) \end{aligned} \qquad (3.4.1.4)$$

When the stress is applied parallel to the annular rings then the strain is equal in both layers so

$$\begin{aligned} \overline{E}_0 \; \epsilon &= E_{e,0} \; p_e \; \epsilon + E_{\ell,0} \; p_\ell \epsilon \\ E_{\ell,0} &= \frac{\overline{E}_0}{k_0 p_\ell + p_e} \end{aligned} \qquad (3.4.1.5)$$

The shear strain for a homogeneous shear stress will be

$$\frac{\tau}{G}(p_e + p_\ell) = \frac{\tau \; p_e}{G_e} + \frac{\tau \; p_\ell}{G_\ell}$$

$$\overline{G} = 1/(\frac{p_e}{G_e} + \frac{p_\ell}{G_\ell}) \tag{3.4.1.6}$$
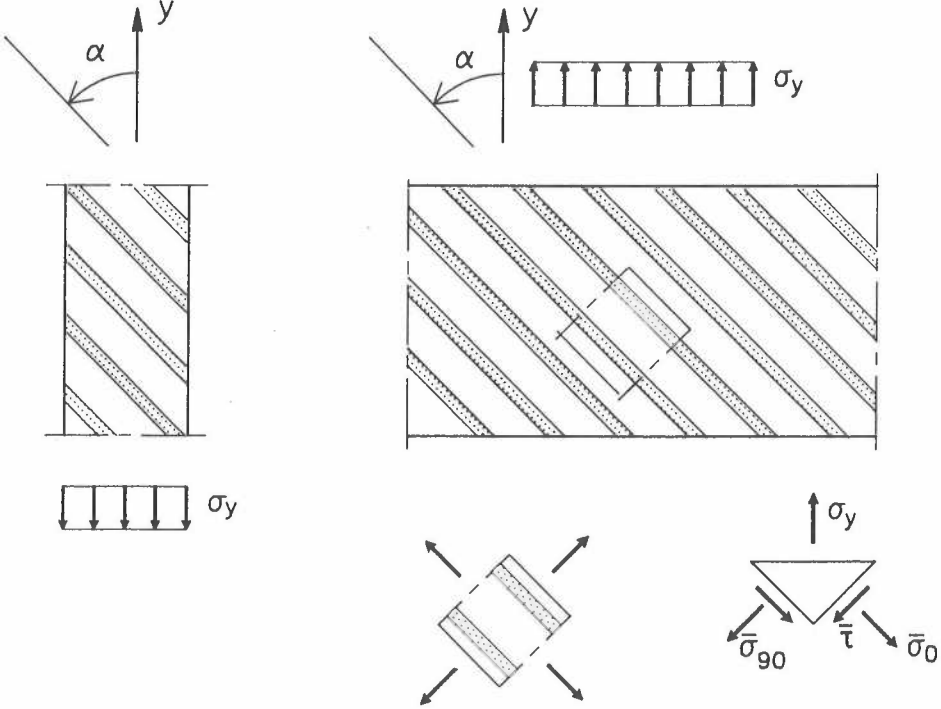
Figure 3.4.1.6   Left a narrow tensile specimen.   Right a wide tensile specimen bonded to steel parts.

The apparent E–modulus of a narrow tensile specimen

In the narrow specimen it is assumed that there will be a homogeneous stress field with the principal stresses $\sigma_1 = \sigma_y$ and $\sigma_2 = 0$, see figure 3.4.1.6. So the elongation in the y–direction can be calculated from a summation of the elongations in the 2 materials

$$\overline{\epsilon} = \frac{\sigma_y}{E_\alpha} = (\frac{p_e}{E_{e,\alpha}} + \frac{p_\ell}{E_{\ell,\alpha}})\sigma_y$$

This gives the apparent E–modulus

$$E_\alpha = 1/(\frac{p_e}{E_{e,\alpha}} + \frac{p_\ell}{E_{\ell,\alpha}}) \tag{3.4.1.7}$$

where the E–moduli for the inclined material bands can be determined from formula (3.4.1.2).

The apparent E–modulus of a wide tensile specimen

In the wide specimen it is assumed that the directions of the principal stresses coincide with the principal axes of the material. This stress state is illustrated in figure 3.4.1.6, to the right. It is obvious that this stress state is only possible in the inner parts of the wide specimen. So the boundary effects are neglected.

Equilibrium of the triangle in figure 3.4.1.6 results in the following equations when the shear stress is zero.

$$\overline{\sigma}_0 = \overline{\sigma}_{90} = \sigma_y \tag{3.4.1.8}$$

The strains in the principle axes are calculated from the equations (3.4.1.9). A geometric transformation results in (3.4.1.10)

$$e_0 \;=\; \frac{\sigma_y}{E_0} - \frac{\nu_{0,90}\ \sigma_y}{E_{90}} = (\frac{1}{E_0} - \frac{\nu}{E_0})\sigma_y$$

$$\tag{3.4.1.9}$$

$$e_{90} = \frac{\sigma_y}{E_{90}} - \frac{\nu_{90,0}\ \sigma_y}{E_0} = (\frac{1}{E_{90}} - \frac{\nu}{E_0})\sigma_y$$

$$e_y = e_0 \cos^2\alpha + e_{90} \sin^2\alpha \tag{3.4.1.10}$$

This strain is per definition equal to σ_y / E_α so

$$E_\alpha = \frac{E_0}{\cos^2\alpha \; + \; \dfrac{E_0}{E_{90}} \sin^2\alpha \; - \; \nu} \tag{3.4.1.11}$$

Comparison between E–moduli measured from narrow and wide specimens

By employing the apparent E–moduli measured from narrow specimens, $\bar{E}_0 = 300$ MPa, $\bar{E}_{90} = 200$ MPa, and the Poisson ratio $\nu_{90,0} = \nu = 0.5, 0.25$ or 0.0 the formuli (3.4.1.7) and (3.4.1.11) result in the E–moduli given in table 3.4.1.1.

Table 3.4.1.1   E–moduli $\bar{E}_{\alpha}$ calculated for narrow and wide tensile specimens with the angle $\alpha = 45^{0}$.

Poisson ratio $\nu_{90,0} = \nu$	Specimen: Narrow	Wide
0.5	201	400
0.25	200	300
0.0	201	240

The constants used for the calculations of the narrow specimen were

Earlywood: $\qquad$ $p_e = 2/3 \quad k_0 = 1/4 \quad k_{90} = 1/3$

$$G_e \sim \frac{\frac{1}{2}(E_{e,0} + E_{e,90})}{2(1 + \nu)} = 51 \text{ MPa}$$

Latewood: $\qquad$ $p_\ell = 1/3$

$$G_\ell \sim \frac{\frac{1}{2}(E_{\ell,0} + E_{\ell,90})}{2(1 + \nu)} = 178 \text{ MPa}$$

Besides this effect there is the boundary effect, which results in a reduction of the axial stresses in the direction of the stiffer latewood cells close to the sides of the specimen.

Orthotropic continuum material model. Different stress and strain states

This explanation is based on that the deformations are substantially less constrained for the narrow specimens resulting in essential lower E–modulus values.

For narrow specimens it is assumed as in the previous model that

$\sigma_y = P/A$
$\sigma_x = 0$
$\tau_{xy} = 0$

where the stresses refer to the coordinate system shown in the figures 3.4.1.5 and 3.4.1.6. This results in an apparent E—modulus, which can be calculated from (3.4.1.2).

For the full width specimens it is assumed that the strain and stress state can be approximated by

$$\sigma_t = P/A$$
$$\epsilon_x = 0$$
$$\tau_{xy} = 0$$

This results in the following apparent E—modulus

$$E_y = \frac{\sigma_y}{\epsilon_y} = \frac{C_{22}}{C_{11}\,C_{22} - C_{12}^2} \qquad (3.4.1.12)$$

where C_{ij} are the compliances given in the rotated coordinate system.

$$\begin{aligned}
C_{11} &= \frac{1}{E_0}\cos^4\alpha + (\frac{1}{G} - 2\frac{\nu_{0,90}}{E_{90}})\sin^2\alpha\cos^2\alpha + \frac{1}{E_{90}}\sin^4\alpha \\
C_{22} &= \frac{1}{E_0}\sin^4\alpha + (\frac{1}{G} - 2\frac{\nu_{90,0}}{E_0})\sin^2\alpha\cos^2\alpha + \frac{1}{E_{90}}\cos^4\alpha \qquad (3.4.1.13)\\
C_{12} &= (\frac{1}{E_0} + \frac{1}{E_{90}} - \frac{1}{G})\sin^2\alpha\cos^2\alpha + \frac{\nu_{0,90}}{E_{90}}(\cos^4\alpha + \sin^4\alpha)
\end{aligned}$$

By using material properties of wood found in the litterature (not all available by this investigation) a ratio between the apparent E—moduli of narrow and full width specimens of say 0.6 could be explained.

3.4.2 Tensile tests with narrow specimens

The specimens were first sawn to the dimensions in figure 3.4.2.1 a) and then milled to there final dimensions, figure 3.4.2.1 b). This means that material taken from the centre part of the width of the beam cross section was tested. The tensile test specimens were all cut from the test beams at such a hight that their mid—section was taken from the same height as the location of the notch tip. Because of this some of the specimens had to be furnished with an extra piece of wood to get sufficient length.
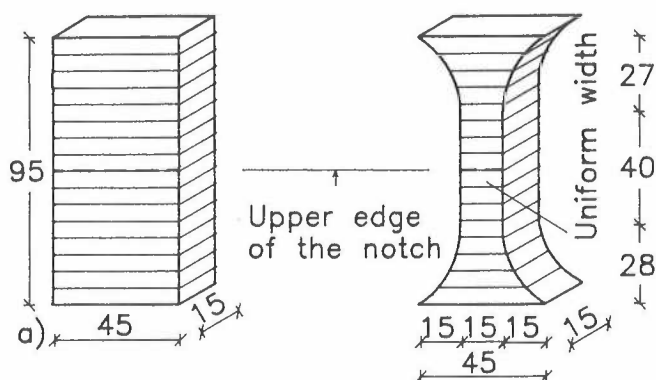
Figure 3.4.2.1   Narrow tension test specimen. a) Geometry after sawing, b) Final geometry.

The gauge length was 40 mm and along this length the specimen had a constant cross section. Tensile force was transferred to the specimen via chains of steel and aluminium profiles glued to the specimen. The rate of the piston was constant, 1 mm/min, and time to failure about three minutes.
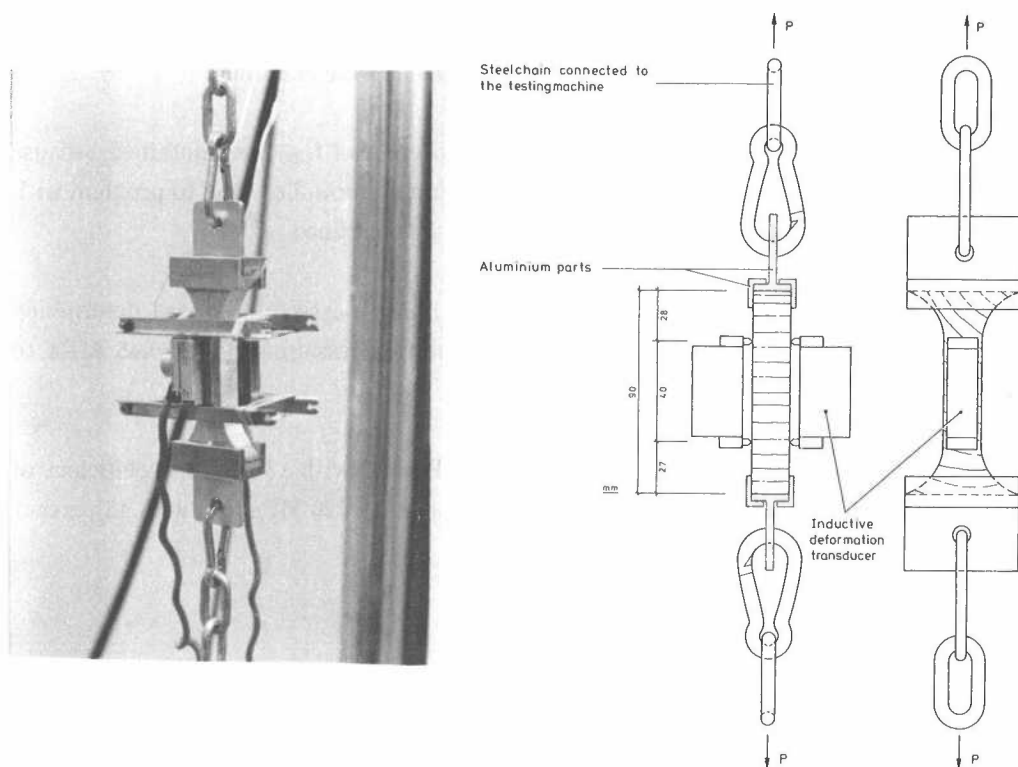
Figure 3.4.2.2 Experimental setup. Tension test.

Test results

Mean values and standard deviations are given in table 3.4.2.1. For individual values, see annex 1. In table 3.4.2.2 test results relevant for illustrating possible effects of location and orientation of test piece are presented.

Table 3.4.2.1   Tensile strength and E–modulus both perpendicular to grain measured by narrow specimens.

	Mean $f_{t,90}$ MPa	St.dev. MPa	Mean E_{90} MPa	St.dev. MPa
Structural timber				
bxh: 45 x 95 mm	3.40	0.53	236	91
45 x 195 mm	3.00	0.48	237	101
All with b = 45 mm	3.31	0.54	236	93
85 x 185 mm	3.50	0.83	143	45

It is remarkable to see the small differences between the mean values, both with respect to different cross sectional dimensions and with respect to location and orientation of the tested volume.
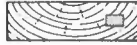
The tensile strength of narrow specimens was only measured for the structural timber beams. For the glulam beams the full width specimens were used only.

71 specimens were tested. For three specimens no value of $f_{t,90}$ was obtained because of failure in the glue between the wood and the aluminiumprofile. Due to problem with a strain gauge for two specimens no value of E_{90} was obtained.

In all tests the performance was approximately linear elastic. E_{90} was determined from change in deformation produced by increase in stress from about 0.45 MPa to about 1.78 MPa.

The tensile strength, $f_{t,90}$, was in average 3.3 MPa and with 18 percent coefficient of variation. The modulus of elasticity, E_{90}, was in average 220 MPa and with 45 percent coefficient of variation.

Table 3.4.2.2   Results from tests of tensile strength E–modulus perpendicular to grain for groups of tested material

Approximate location of tested volume	α (h_e/h)	$f_{t,90}$ average [MPa]	c.o.v. [%]	E_{90} average [MPa]	c.o.v. [%]	Number of tests
	0.5	3.3	15.8	258	35.9	40
	0.75 0.25	3.34	17.0	169	54.9	20
	0.75 0.25	3.8	22.4	127	22.2	4

It appears from table 3.4.2.2 that the E–modulus decreases, as the angle between the annular rings and the stress increases. But there is a discrepancy between the bottom most mean value of 127 MPa and the measured angular dependency shown in figure 3.4.3.2.

Correlation and regression analyses

In table 3.4.2.3 there is stated the results of an analysis of $f_{t,90}$ (density, moisture). Equation (3.2.3) has been employed.

Table 3.4.2.3   Parameters in the regression equation for the tensile strength and E–modulus perpendicular to grain for narrow specimens. Only structural timber.

	Coeff. of correl.	Intercept MPa	k_ω MPa/%	k_ρ MPa/kg/m³
Tensile strength perpendicular to grain:				
bxh: 45 x 95 mm	No significance			
45 x 195 mm	0.64	−0.88	–	0.01008
All with b = 45 mm	0.30	1.30	–	0.00479
85 x 185	0.50	8.02	−0.293	–
E–modulus perpendicular to grain:				
bxh 45 x 95 mm	0.28	808	−67.0	0.678
45 x 195 mm	No significance			
All with b = 45 mm	No significance			
85 x 185	0.95	114	22.7	−0.825

3.4.3 Tensile tests with full width specimens

The specimens were cut from the full cross section with their middle positioned at the level of the notch tip. They were bonded to steel parts by means of Araldit. The dimensions varied with the width of the cross section, but the dimension in the grain direction was always 10 mm.

Dimensions in mm

	a	b	h_s
Struc.	25	45	10
timber:	25	85	30
Glulam	25	90	30
	50	160	60
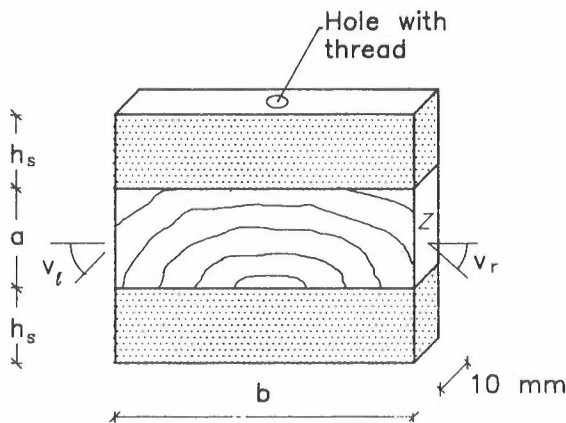
Figure 3.4.3.1   Full width tension test specimen. The wood was bonded to the steel parts. The tensile force was applied by thin threaded rods screwed into the holes.

The force was applied to the specimen by thin (4–6 mm) threaded rods with a length of 150–200 mm. They were flexible and they had almost no bending capacity, so the force was applied at the middle of the tensile specimen.

On both end grain sides of the wooden specimen there was put a deformation transducer in a similar way as shown in figure 3.4.2.2. The gauge length was 19 mm.

The threaded rods were clamped to the testing machine. The piston velocity was 0.5 mm/min resulting in failure in 3 to 5 minutes.

Besides the mechanical properties the inclinations of the annular rings at the positions of failure were measured in both sides of the specimen.

Test results

Mean values and standard deviations are given in table 3.4.3.1. For individual values see annex 1.

Table 3.4.3.1   Tensile strength and E–modulus perpendicular to grain measured by full width specimens.

	Mean $f_{t,90}$ MPa	St.dev. MPa	Estim.$f_{t,90}$ MPa	Mean E_{90} MPa	St.dev. MPa
Structural timber:					
bxh: 45 x 95 mm	3.40	0.53	3.32	392	117
45 x 195 mm	2.91	0.75	3.01	374	119
All with b = 45 mm	3.24	0.77		388	117
85 x 185 mm	2.79	0.76	2.65	410	141
Glulam:					
b=90 h=200&300 mm	3.58	0.68	2.97	576	156
b=160 h=567 mm	1.69	0.15	2.02	568	161

It appears from table 3.4.3.1 that the modulus of elasticity increases when the width b increases. This supports the idea proposed in section 3.4.1, that for wide specimens the applied tensile force will cause a 2–dimensional stress field which results in higher E— moduli than for a uniaxial stress field.

Further, there is a tendency to that the tensile strength increases for increasing density and decreases for decreasing volume of the test specimen. From the regression analyses reported later it appears that there is the following incremental relation

$$\Delta f_{t,90} = 0.0075 \, \Delta\rho \qquad (3.4.3.1)$$

This can further be combined with a brittle failure decription by employing a Weibull theory. The reference volume is chosen to be a = 25 mm, b = 45 mm and t = 10 mm , see figure 3.4.3.1. Since t is 10 mm in all specimens it vanishes so with a reference tensile strength of 3.1 MPa the relation between tensile strength and density plus volume becomes for the employed specimens

$$f_{t,90,\,axb} = \left(\frac{45 \, \cdot \, 25}{a \, \cdot \, b}\right)^{0.2} (3.1 \text{ MPa} + 0.0075\cdot (\rho - 400 \text{ kg/m}^3)) \qquad (3.4.3.2)$$

Formula (3.4.3.2) has been used to calculate the estimated tensile strength values given in table 3.4.3.1. The average values of the 5 measured and the 5 estimated values are equal and the co–variation appears to be good. It must here be remembered that the

patterns of annular rings are quite different in the specimens and the width of the tensile specimens varied between 45 mm and 160 mm.

Correlation and regression analyses

For glulam only a regression analysis between the dependent variables tensile strength and E–modulus and the free variable density has been carried out. The variation of the moisture content was too narrow. For glulam there was employed the density of the notch lamination.

From table 3.4.3.2 it can be seen that the coefficients of correlation are small, specially for the glulam there is no significance. The regression for glulam is useless.

Table 3.4.3.2 Parameters in the regression equation for the tensile strength and E–modulus perpendicular to grain for full width specimens.

	Coeff. of correl.	Intercept MPa	k_ω MPa/%	k_ρ MPa/kg/m³
Tensile strength perpendicular to grain:				
Structural timber:				
bxh 45 x 95 mm	0.55	1.42	−0.0491	0.00597
45 x 195 mm	No significance			
b=45 h=95&195 mm	0.32	0.16	−	0.00736
85 x 185 mm	0.33	2.84	−0.155	0.00589
Glulam:				
b=h h=200&300 mm	0.05	4.08	−	−0.00117
bxh: 160 x 567 mm	0.05	1.56	−	0.00028
Modulus of elasticity perpendicular to grain:				
Structural timber				
bxh 45 x 95 mm	0.30	915	−74.0	0.662
45 x 195 mm	No significance			
b=45 h=95&195 mm	0.17	406	−19.8	0.240
85 x 185 mm	0.37	−400	−	2.07
Glulam:				
b=90 h=200&300 mm	0.07	422	−	0.360
bxh: 160 x 567 mm	0.46	−288	−	2.25

The relative poor correlations in table 3.4.3.2 indicates that another free variable should be incorporation into the analyses. It is obvious to consider the ratio between the density of the earlywood and the latewood but this ratio is difficult to determine. Instead the angles of the annual rings at the failure position in both sides of the specimen were incorporated in the regression analysis. The regression analyses of the tensile strength were based on partly the maximum angle v_{max} , partly the minimum angle

v_{min} and the regression equations were of the following type. This allows a curved variation with the angle.

$$f_{t,90} = \text{Intercept} + k_\rho\, \rho + k_{|v_{max}|}\, |v_{max}| + k_{v^2_{max}}\, v^2_{max} \qquad (3.4.3.3)$$

$$f_{t,90} = \text{Intercept} + k_\rho\, \rho + k_{|v_{min}|}\, |v_{min}| + k_{v^2_{min}}\, v^2_{min} \qquad (3.4.3.4)$$

For the E—modulus the regression analysis was based on a similar relation but with the mean value of the angles in the two sides as free variable. Further there was added a term proportional to the numerical value of the angle difference between the 2 sides.

The regression analyses showed that the maximum angle v_{max} gave the best correlation with the tensile strength, but v_{min} gave an almost equal good correlation. The results are given in table 3.4.3.3.

For the E—modulus the average angle resulted in a weaker correlation, see table 3.4.3.3.

Table 3.4.3.3   Parameters in the regression equation for the tensile strength and the E—modulus perpendicular to grain for full width specimens

	Coeff. of corel.	Intercept MPa	k_ρ MPa/kg/m³	$k_{|v|}$ MPa/deg.	k_{v^2} MPa/deg.²	$k_{|v\,diff|}$ MPa/deg.
Tensile strength perpendicular to grain:						
Structural timber:				$v = v_{max}$		
bxh: 45 x 95 mm	0.59	20.6	0.00814	−0.575	0.00385	
45 x 195 mm	0.39	2.8	0.00470	−0.069	0.00058	
85 x 185 mm	0.54	10.4	0.0032	−0.263	0.00186	
Glulam:				$v = v_{max}$		
b=90 h=200 300 mm	0.54	5.7	0.00006	−0.062	0.00037	
Modulus of elasticity perpendicular to grain:						
Structural timber:						
bxh: 45x95 mm	0.25	218	0.542	−5.33	0.0516	1.38
45 x 195 mm	0.72	7	1.352	−13.70	0.1376	3.05
85 x 185 mm	0.89	1247	−0.458	−36.40	0.334	3.20
Glulam:				$v = v_{mean}$		
b=90 h=200&300 mm	0.22	405	0.316	−1.36	0.0079	4.30

For the glulam with bxh = 160 x 567 mm the number of test results was too little for a reasonable regression analysis.

59

The variation with the annual ring angle is visualized in figure 3.4.3.2 and figure 3.4.3.3 for structural timber and glulam respectively. For the test results from the narrow specimens there is shown a similar relation in table 3.4.2.2, but it gives only the relation between the relative height position α and $f_{t,90}$ and E_{90}. The same type of table is given in table 3.4.3.4 for structural timber.

Table 3.4.3.4   Results from tests of tensile strength and E–modulus perpendicular to grain for structural timber. Mean values and coefficient of variations for the different cross–sectional sizes and locations of the full width specimen given as $\alpha = h_e/h$.

Cross–sec. sizes bxh mm	Location $\alpha = h_e/h$	Number of tests	$f_{t,90}$ Mean MPa	c.o.v. %	E_{90} Mean MPa	c.o.v. %
45 x 95	0.5	22	3.6	20	435	30
	0.25&0.75	20	2.9	20	364	35
45 x 195	Standing annular rings					
	0.5	6	2.9	28	401	13
	0.75	3	2.8	1	334	18
45 x 195	Round annular rings					
	0.5	7	3.3	25	418	44
	0.75	6	2.6	37	339	40
85 x 185	0.5	8	2.6	33	327	31
	0.75	12	2.9	21	457	25
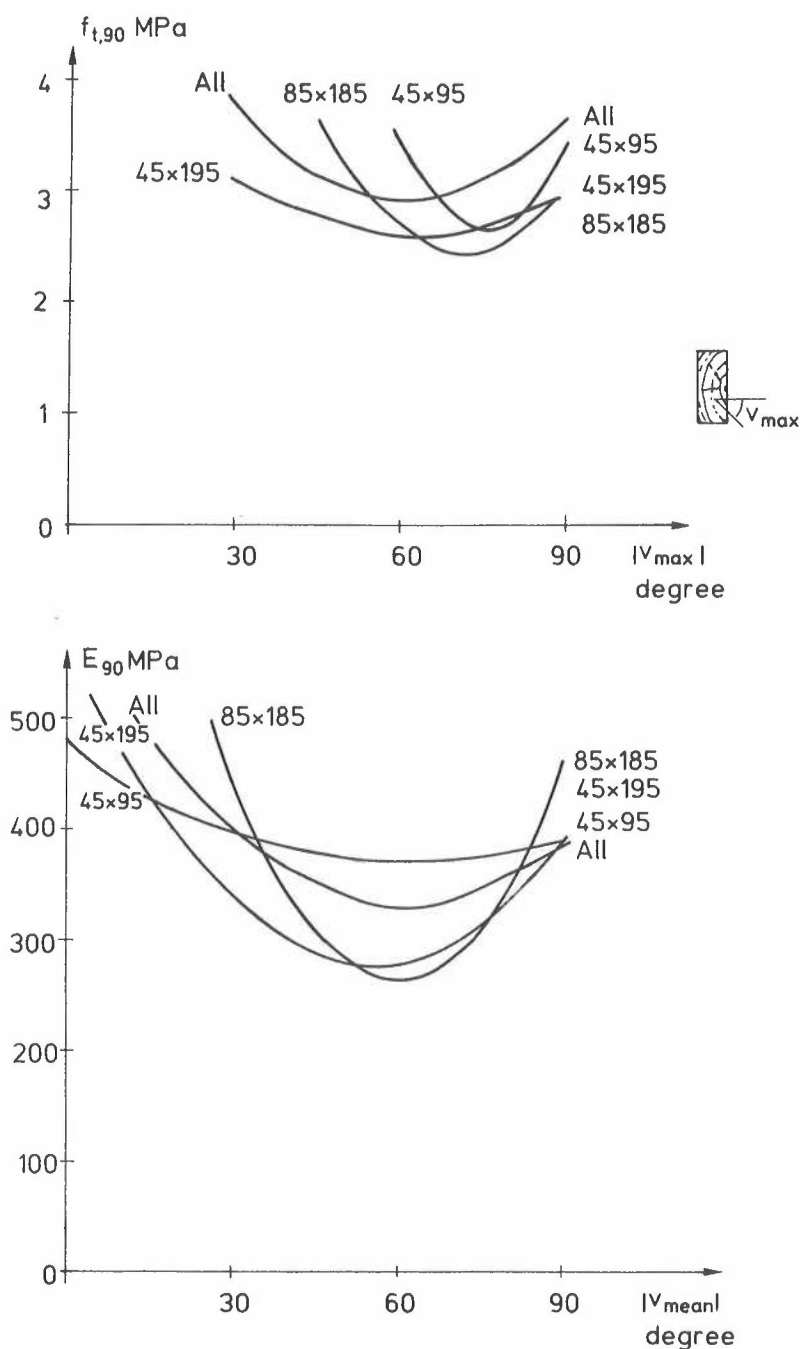
Figure 3.4.3.2   Structural timber. The variation in the tensile strength $f_{t,90}$ and the E—modulus both perpendicular to grain on dependence of the annular ring angle, the maximum angle for $f_{t,90}$ and the mean angle for E_{90}.
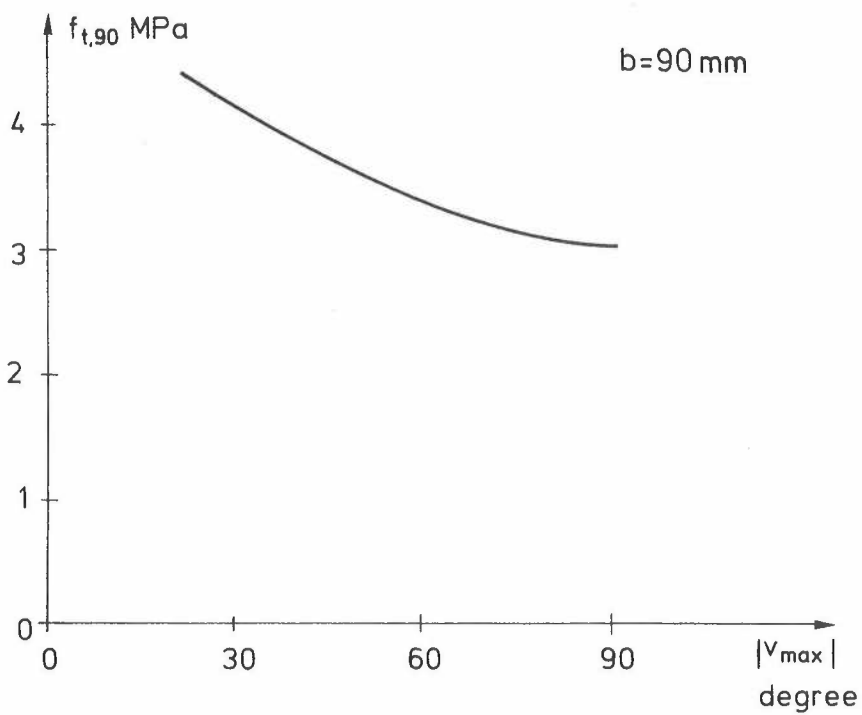
Figure 3.4.3.3   Glulam, width b = 90 mm. The variation in the tensile strength
                      $f_{t,90}$ on dependence of the maximum annular ring angle.

It is remarkable to see that all the curves in figure 3.4.3.2 and 3.4.3.3 are hollow to the same side. Further, for the E–modulus this is theoretical to be expected from the theoretical considerations in clause 3.4.1.

The regression equations given in table 3.4.2.3 have been emploied to estimate $f_{t,90}$ or E_{90} when a value have been missing. This is marked with E (estimated) in annex 1.

Comparison between results from narrow and full width specimens
For the structural timber there has been performed tests with both narrow and full width specimens.

A correlation analysis showed that the tensile strengths measured from narrow and full width specimens were poorly correlated. But the mean values for each timber size are very equal, please compare table 3.4.2.1 and 3.4.3.1. This could indicate that the perpendicular tensile strength varies within a timber member, because the narrow and full width specimens are cut from each of the 2 timber pieces between 2 neighbouring notched beams. This should be remembered by the interpretation of the test results of the notched beams.

For the E–moduli the correlation between the narrow and full width specimens were poor. But here there is a significant difference between the mean values, see table 3.4.3.4. The ratio between the two E–moduli is discussed further in clause 3.4.5.

Table 3.4.3.4   E–modulus. Ratio between the mean value for narrow specimens and full width specimens.

Plank dimension bxh, mm	45 x 95	45 x 195	85 x 185
$E_{90,narrow}/E_{90,full\ width}$	0.60	0.63	0.35

3.4.4 E–modulus in compression perpendicular to grain, density and moisture content by drying.

The E–modulus in compression perpendicular to grain, E_{90}, was tested exactly in the same manner as described in section 3.3.2, but of course in this case only the uniaxial load in compression perpendicular to grain is relevant. Specimen geometry and test setup is shown in figure 3.4.4.1.

After the compression test, the specimen was used to determine density and moisture content of the wood. In this case the moisture content was determined by drying.
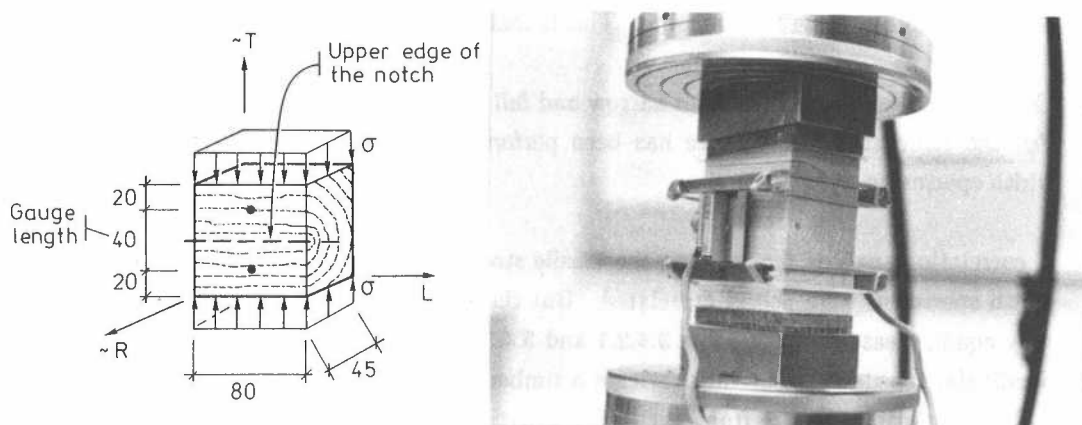
Figure 3.4.4.1 Specimen geometry and test setup. Compression test.

A total of 71 specimens cut from the structural timber were tested. For glulam E_{90} was tested in tension only. Individual test results and mean values are given in Annex 1 and 2, respectively.

In all tests the performance was approximately linear elastic. E_{90} was determined from change in deformation produced by an increase in stress from about 0.28 MPa to about 1.10 MPa.

The average of E_{90} as obtained by the compression tests is 204 MPa and its coefficient of variation is 43 percent. In table 3.4.4.1 average values for certain groups of the tested material are presented in order to illustrate the effect of the location of the test specimen.

The density (dry weight/wet volume) for the same specimens was in average 403 kg/m³ (9 percent c.o.v.) and the moisture content (weight of water/weight of dry specimen) was in average 13.2 percent (7.8 percent c.o.v.). The actual moisture content values were obtained by weighing the specimens before and after drying in an owen with the temperature 105⁰C. The specimens were of clear wood, free from knots and other de-

fects.

Table 3.4.4.1   Results from test of E–modulus in compression perpendicular to grain for narrow specimens.

	E–Modulus, E_{90} Mean	c.o.v.	Density, ρ_{dry} Mean	c.o.v.	Moist, ω Mean	c.o.v.	Number of tests
	MPa	%	kg/m³	%	%	%	
Structural timber							
bxh: 45x95 mm²	213	37.6	416	6.7	12.6	5.0	46
45x195 mm²	212	51.5	378	9.4	14.3	2.2	17
All with b							
= 45 mm	213	41.3	406	8.4	13.1	7.2	63
85x185 mm²	139	45.9	360	10.1	14.7	1.7	8

Table 3.4.4.2   Results from tests of E–modulus in compression perpendicular to grain for groups of tested material and for narrow specimens.

Approximate location of tested volume	α h_e/h	E_{90} average MPa	c.o.v. %	Number of tests
	0.5	209	42.5	35
	0.75 0.25	207	40.5	28
	0.75 0.25	177	41.3	4

3.4.5 Comparison and conclusion

Tension tests have been carried out for structural timber by use of both narrow and full width specimens. Also compression tests have been performed.

A correlation analysis showed that the tensile strengths measured from narrow and full width specimens were poorly correlated. But the mean values for each timber size are very equal, please compare table 3.4.2.1 and 3.4.3.1. This could indicate that the perpendicular tensile strength varies within a timber member, because the narrow and full width specimens are cut from each of the 2 timber pieces between 2 neighbouring notched beams. This should be remembered by the interpretation of the test results of

65

the notched beams.

For the E–moduli the correlation between the narrow and full width specimens were poor. But here there is a significant difference between the mean values, see table 3.4.3.4.

In clause 3.4.1 there is given some theoretical models which can explain this difference. Ratioes between the two measured E–moduli of 0.5 til 0.84 can be explained by the theories and the chosen material properties. A ratio of 0.6 could be typical. The measured ratios for the timber width $b = 45$ mm correspond to this, but for $b = 85$ mm the measured ratio is considerably smaller.

For the E–moduli the correlation between the narrow tension and the wider compression specimen is shown in table 3.4.5.1. It is quite interesting to note the possible influence of fibres oriented in the radial direction.

Table 3.4.5.1   E–modulus. Ratio between the mean values for narrow tension specimens and wider compression specimens.

Location in the "plank"			
$E_{90,narrow\ tension}/E_{90,wider\ compr.}$	$\dfrac{258}{214} = 1.21$	$\dfrac{169}{208} = 0.81$	$\dfrac{127}{177} = 0.7$

So it can be concluded that the apparent E–modulus $\overline{E}$ will depend on the stress state. This means it will depend on the width of the specimen because it is only in a relatively wide specimen that the apparent E–modulus will increase.

Since the stresses perpendicular to the grain in a notch are limited to a very little volume it seems likely that the surrounding material will act as the glued–on steel parts. So the relevant modulus of elasticity should be the one determined from tensile specimens with a width equal to that of the notched beam.

3.5 Fracture energy in tension, $G_{f,t}$. Mode I

Description of test method

The fracture energy for tensile fracture perpendicular to grain, $G_{f,t}$, was determined by three point bending of notched beams, see figure 3.5.1, according to a CIB draft standard , see /Larsen & Gustafsson, 1990/. The fracture energy is here defined as work of fracture divided by the area, bt, of the fracture cross section. The work of fracture is determined as the work carried out by the load, P, and the weight of the beam, mg, when the beam is being brought to complete failure in a stable manner. This can be expressed as

$$G_{f,t} = \frac{1}{b\,t}(\int_0^{\delta_0} P\,d\delta + mg\,\delta_0)$$

where δ is the piston movement and δ_0 its value when the load P has reached zero, see figure 3.5.1.d). The integral, corresponding to the work carried out by the load P, is obtained from the area under the recorded $P - \delta$ curve.

To get required beam length the specimen, 48x45x80 mm^3, was glued between two blocks of wood, 45x80,240 mm^3, figure 3.5.1 a) and b). A notch, 48 mm deep and about 1 mm wide, was then sawn in the middle of the specimen. This gives a remaining cross section area of bxt = 45x32 mm^2. The beam was supported on steel plates with centre distance 480 mm. One support, a steel cylinder, permitted translation and rotation of the beam in its plane and the other support with a steel ball permitted in principle free rotation. A compression force was transferred via a steel ball and a steel plate placed centrically over the notch. A layer of rubber was placed between the different steel prisms and the wood. The rate of the piston was constant, 1 mm/min, and time to failure about 6 to 10 minutes, corresponding to a beam deflection of 6 to 10 mm.

The specimens were all cut from the test beams at such a height that their mid section was taken at the level of the notch tip.

For the beams with a width greater than 45 mm the test specimen was cut at the centre of the cross section.
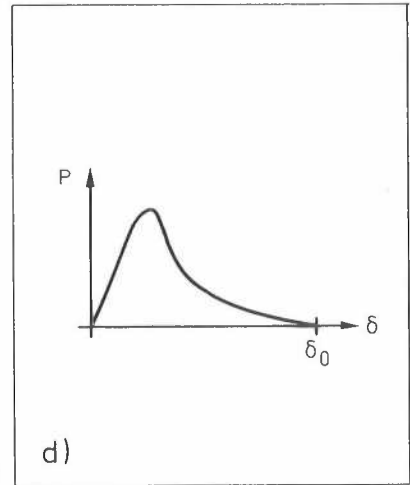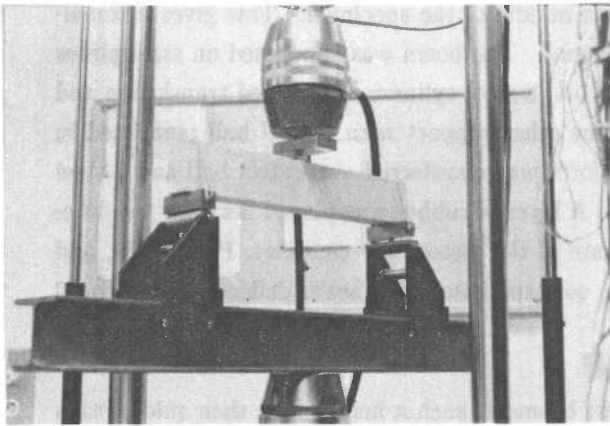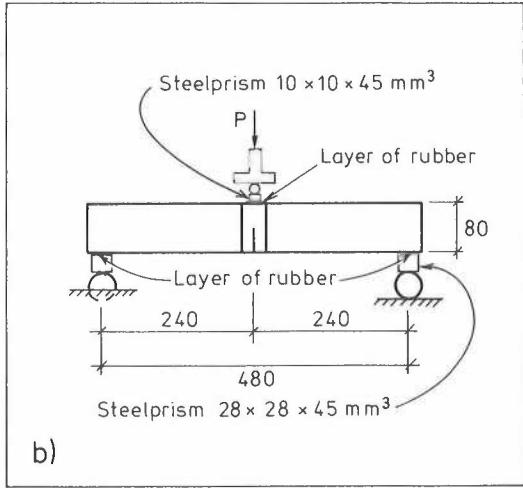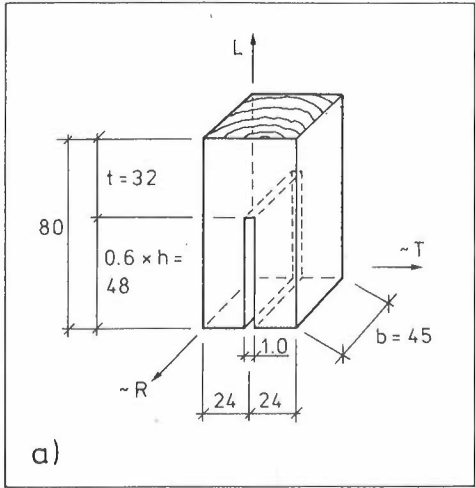
Figure 3.5.1   Fracture energy, mode I, Specimen and test setup
a) Specimen geometry
b) Test setup, geometry
c) Complete test setup
d) A P − δ curve

68

Test results

A total of 102 specimens were tested: 31 made of glulam and 71 of solid spruce. Most of the tests, 87, performed in a stable manner as illustrated by the two examples in figure 3.5.2. Fourteen of the tests were partly unstable, see figure 3.5.3a in the sense that shortly after the maximum load the force dropped 50–100 N without any increase in piston displacement.

One of the specimens was reinforced through the fracture area with a knot, which first became visible after the test. The result of this reinforcement is shown in figure 3.5.3b. This test is not included in the statistical evaluation of the test results.

The mean and standard deviation of $G_{f,t}$ for each group of dimensions are given in table 3.5.1. The individual values are given in annex 1.

Table 3.5.1   Mean and standard deviation of the fracture energy in tension (mode I) $G_{f,t}$

	Mean $G_{f,t}$ Nm/m^2	Standard dev. Nm/m^2
Structural timber:		
bxh: 45 x 95 mm	294	49
45 x 195 mm	255	56
85 x 185 mm	307	35
Glulam:		
b = 90 h = 200&300 mm	304	52
bxh: 167 x 567 mm	304	14

The fracture energy in tension, $G_{f,t}$, was in average (101 specimens) 298 Nm/m^2 (21.1 percent c.o.v.) and the maximum load in average 188 N (19.3 percent c.o.v.)

To illustrate the possible effect of the location of the tested specimen mean results for certain groups of specimens are compiled in table 3.5.2. For the different locations within the glulam cross section the orientation of the annual rings is approximately the same.

Both for the groups of cross–sectional sizes and for the groups of locations it is noticeable to see how uniform the mean values are.
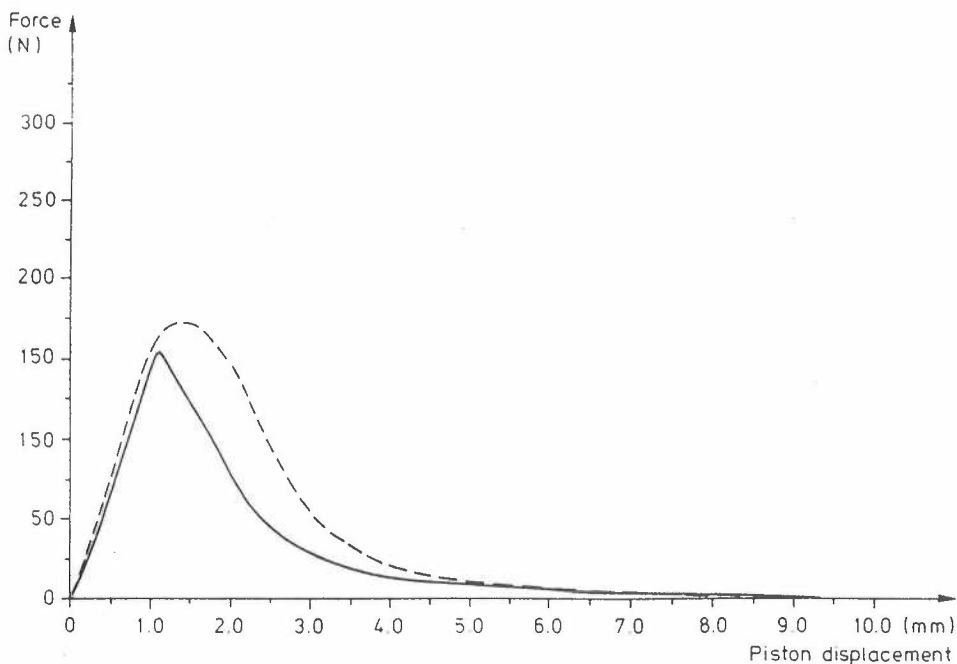
Figure 3.5.2 Examples of stable performance, recorded in most tests.
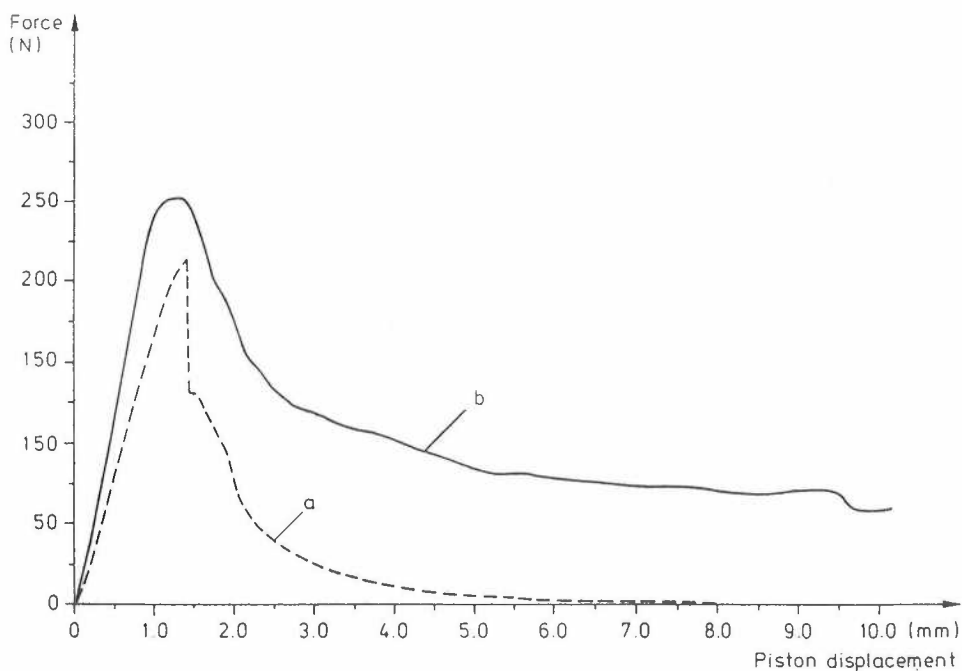
Figure 3.5.3   Results from test of fracture energy in mode I

   a) Partly unstable test performance

   b) Fracture area reinforcement with a knot

Table 3.5.2   Results from tests of fracture energy in tension

Approximate location of tested volume	α (h_e/h)	$G_{f,t}$ average [Nm/m²]	c.o.v. [%]	Number of tests
Structural timber				
	0.5	287	22.6	41
	0.75 0.25	286	15.4	20
	0.75 0.25	316	14.4	4
Glulam	0.5 0.75 0.83	319	22.8	31

Correlation and regression analysis

In table 3.5.3 there is stated the results of an analysis of $G_{f,t}$ (density, moisture). For glulam the density and moisture content is that of the notch lamination. Equation (3.2.3) has been employed.

Table 3.5.3   Parameters in the regression equation for the fracture energy in tension with the free variables moisture content ω and density ρ

	Number of tests	Coeff. of correl.	Intercept Nm/m²	k_ω Nm/m²/%	k_ρ Nm/m²/kg/m³
Structural timber:					
bxh 45 x 95 mm	61	0.21	No significance		
45 x 195 mm	14	0.60	1066	−90.7	1.169
All with b = 45 mm	75	0.36	34	−	0.601
85 x 185 mm	13	0.24	No significance		
Glulam:					
All with b = 90 mm	36	0.46	−74	7.33	0.657 [1]
bxh 160 x 567 mm	7	0.51	517	−17.0	0.008 [1]

1)   Density and moisture content of the notch lamination.

Generally the correlation is poor, mean values could be used just as well.

3.6 Shear strength, f_v, and fracture energy in shear, $G_{f,v}$. Mode II.

The shear strength and fracture energy test was carried out on quite small specimens, cut out of the timber pieces between the test beams as described in chapter 2.3. During the test shear stress—deformation performance of the specimens was recorded both during increase in stress and deformation and during the gradual fracture softening resulting in a decrease in force during further increase in deformation. This means that both shear strength, f_v, and shear fracture energy, $G_{f,v}$, could be determined from the same test result. In addition, from the test result it is possible to evaluate the fracture softening shear stress—slip performance of a shear fracture process region. While peak load, and accordingly f_v, is comparatively easy to determine it is more difficult to achieve a good test performance for evaluation of $G_{f,v}$.

The test setup is shown in figure 3.6.1. It has previously been used for testing wood adhesive bonds /Wernersson, 1990/ and it is designed to give a pure and reasonable uniform shear stress along the fracture section. Pure shear is achieved by antisymmetric loading of a symmetric specimen and uniform stress is achieved by making the tested section short. The small overall dimensions of the specimen and the generous design of the steel parts are to meet significant requirements regarding stiffness and stability, partly decisive for valid results when testing fracture softening.

The details of the specimen design with a narrow sawn notch in the lower part and a smooth milled notch in the upper part are intended to force fracture to start at the centre of the specimen and to allow some inclination of the fracture surface according to possible inclination of grain. The specimen is attached to the steel parts by epoxi resin. The steel ball placed between the steel parts in V—shaped notches and tightened by a spring counteracts bending and torsion of the specimen during testing and previous handling.

Deformation was recorded as the mean value from two clip—gauges, one placed at the front side of the setup, and one at the back side each giving the relative displacement between the two steel parts. By means of closed—loop facilities of the testing machine, all tests were carried out with constant rate of deformation. This rate was 0.0625 mm/min.

Shear strength f_v, was evaluated as peak load divided by the size of the cross—sectional area, nominally 0.90 cm². Shear fracture energy, $G_{f,v}$, was evaluated as area under the recorded load—deformation curve divided by the cross—sectional area.
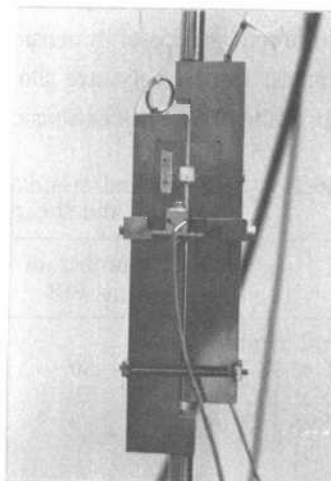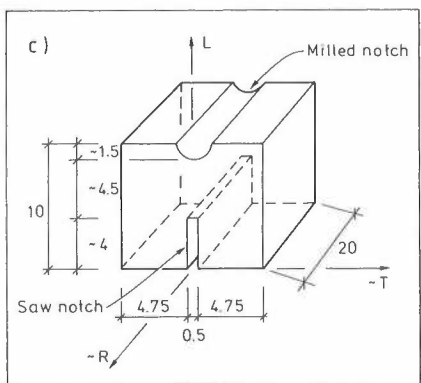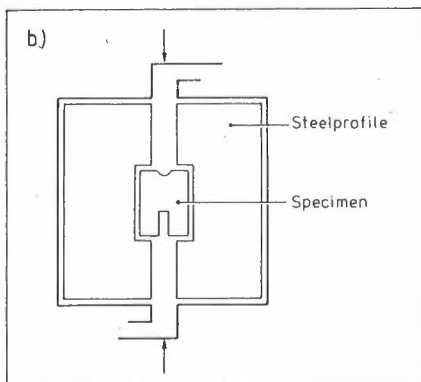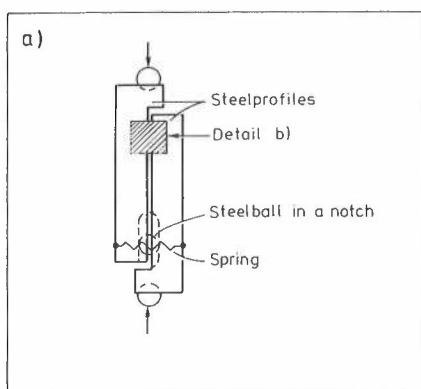
Figure 3.6.1   Experimental setup. Fracture energy, mode II
a) Setup
b) Attachment of the wooden specimen
c) Geometry of the specimen
d) Complete experimental setup

73

Test results

In Figure 3.6.2 two types of force displacement relations are shown. Out of a total of 102 tests (31 of these with specimens of glulam) only 29 were obtained in accordance with Figure 3.6.2a and 52 tests in accordance with Figure 3.6.2b. It was possible to determine shear strength, f_v, for 99 specimens and for these the average of f_v was 8.4 MPa (18.3 percent c.o.v.). The fracture energy, $G_{f,v}$ was determined for 81 specimens and for these the average of $G_{f,v}$ was 965 Nm/m² (23.1 percent c.o.v.). For the 29 stable tests the mean of f_v is 8.9 MPa (14 percent c.o.v.) and the mean of $G_{f,v}$ is 945 Nm/m² (20 percent c.o.v.).

For the different groups of dimensions the mean values of $G_{f,v}$ and f_v for the 81 and 99 specimens, respectively, are shown in table 3.6.1. In table 3.6.2 the corresponding results for some different locations of the tested piece of wood are shown.

Table 3.6.1   Mean and standard deviation of the fracture energy in shear (mode II) $G_{f,v}$ and shear strength f_v

	Number of $G_{t,v}$ test	Mean $G_{f,v}$ Nm/m²	Standard dev. Nm/m²	Mean f_v MPa	St. dev. MPa
Structural timber:					
bxh 45 x 95 mm	50	999	226	8.7	1.3
45 x 195 mm	12	877	201	7.9	0.8
85 x 185 mm	9	1084	304	6.7	0.8
Glulam:					
All with b = 90 mm	28	932	190	8.9	1.8
bxh 167 x 567 mm	3	1077	83	7.4	1.8

Efforts were made to get as many stable and valid tests as possible (in accordance with Figure 3.6.2a) and details of the specimen design, see figure 3.6.1c, were chosen after having tested a number of different alternatives. Better results had probably been attained if the width (T–direction, figure 3.6.1c) of the specimen had been decreased to about the half, i.e. 5 mm.

From the recorded relation between force and displacement a shear stress–slip relation of the fracture zone can be evaluated. Here this evaluation is carried out at the assumptions that all deformations outside the fracture region are elastic and, accordingly, that the post peak stress slip in the fracture region, w, can be evaluated as indicated in figure 3.6.3. In figure 3.6.4 a mean τ–w performance as obtained from the 29 stable tests is shown. In this figure also a straight line simplification of the τ–w curve is shown. The straight line is determined from the mean shear strength, 8.9 MPa, and

the fracture energy, i.e. the area under the τ–w curve, 945 Nm/m². The slip, w_0, corresponding to zero shear stress is for the straight line simplification $(2 \cdot 945 \text{ Nm/m}^2)/(8.9 \text{ MPa}) = 0.21$ mm.
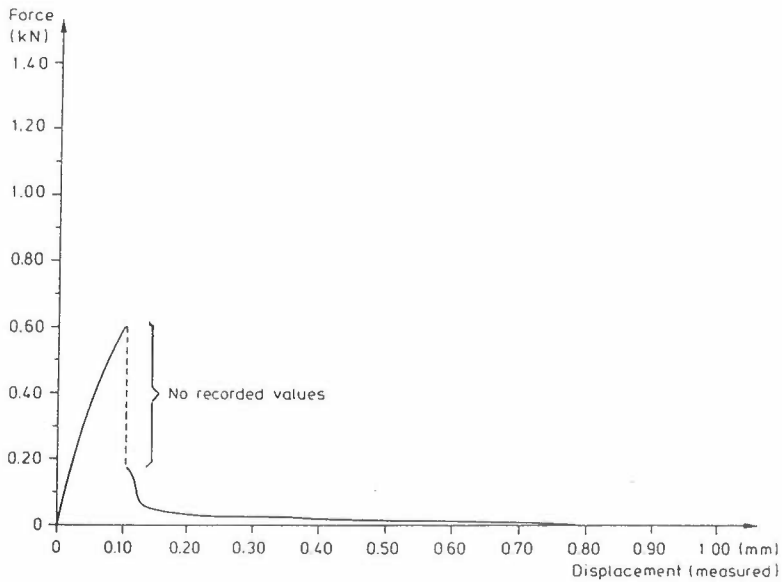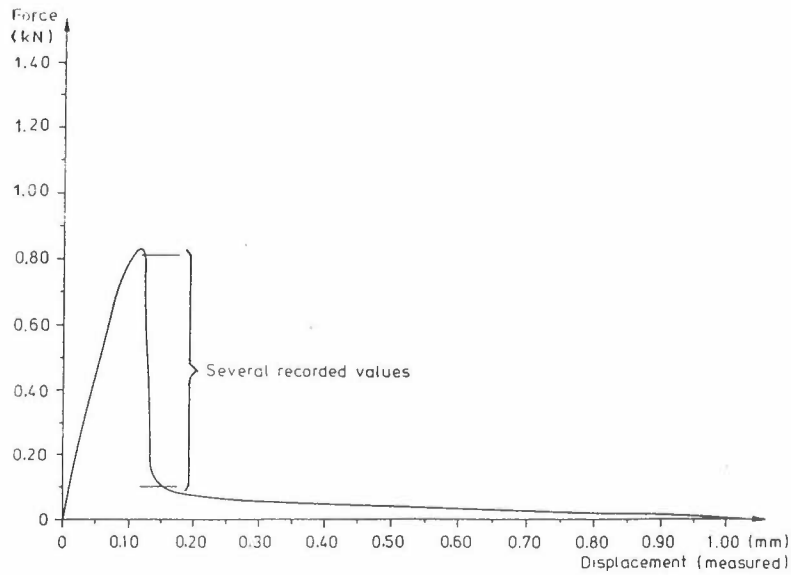
Figure 3.6.2   Principle results from tests of fracture energy, mode II
                 a) Stable test
                 b) Partly unstable test

75

Table 3.6.2   Results from tests of strength and fracture energy in shear.

Approximate location of tested volume	α (h_e/h)	f_v average MPa	c.o.v. %	$G_{f,v}$ average Nm/m²	c.o.v. %	Number of tests f_v	$G_{f,v}$
Structural timber							
	0.5	8.3	16.5	959	22.5	35	32
	0.25 0.75	8.6	13.6	981	26.0	24	19
	0.25 0.75	6.7	11.4	956	15.5	4	2
Glulam							
	0.5 0.75 0.83	8.8	20.9	948	19.9	32	24
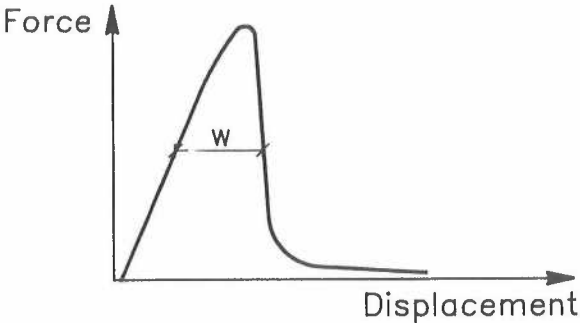
Figure 3.6.3 Evaluation of shear slip, w, from recorded force–displacement curve.

76
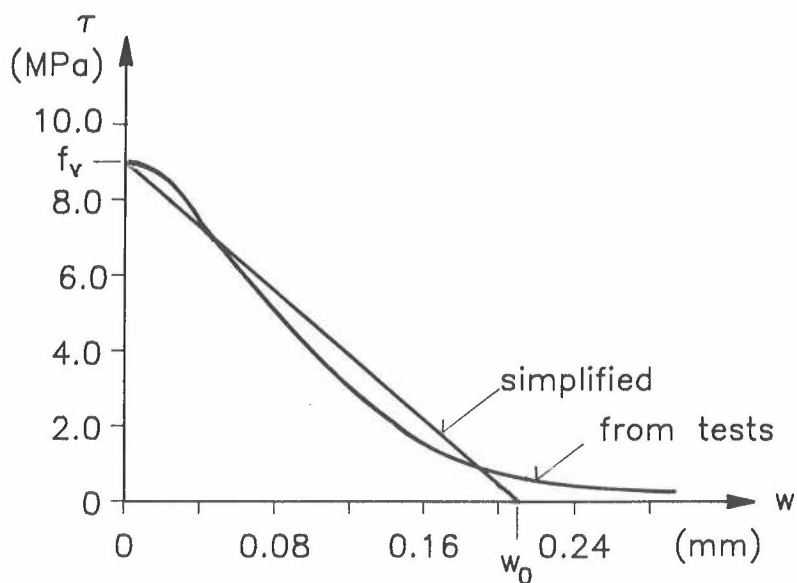
Figure 3.6.4   Mean shear stress–slip performance of fracture zone in wood determined from 29 stable tests of spruce specimens.

Correlation and regression analysis

In table 3.6.3 there is stated the results of an analysis of $G_{f,v}$ (density, moisture). For glulam the density and moisture content is that of the notch lamination. Equation (3.2.3) has been employed.

Table 3.6.3 Parameters in the regression equation for the fracture energy in shear $G_{f,v}$ and the shear strength f_v with the free variables moisture content ω and density ρ.

	Number of tests	Coeff. of correl.	Intercept Nm/m^2	k_ω $Nm/m^2/\%$	k_ρ $Nm/m^2/kg/m^3$	
Fracture energy in shear $G_{f,v}$						
Structural timber:						
bxh 45 x 95 mm	50	0.10	No significance			
45 x 195 mm	12	0.54	2134	−195	3.81	
All with b = 45 mm	62	0.17	No significance			
85 x 185 mm	9	0.93	−1200	172	−1.07	
Glulam:						
All with b = 90 mm	28	0.13	No significance			1)
bxh 160 x 567 mm	3		Too few measurements			1)
Shear strength f_v:						
Structural timber:						
bxh 45 x 95 mm	50	0.46	−1.46	−	0.0239	
45 x 195 mm	12	0.51	2.9	−	0.0126	
All wigh b = 45 mm	62	0.52	−0.7	−	0.0220	
85 x 185 mm	9	0.20	No significance			
Glulam:						
All with b = 90 mm	28	0.28	2.52	−	0.0144	1)
bxh 160 x 567 mm	3	0.84	−11.66	−	0.0486	1)

1) Density and moisture content of the notch lamination.

4. TESTING OF END–NOTCHED BEAM

In table 4.1 there is given an overview of the performed tests with end–notched beams. The number of repetitive tests in each serie is 6 and 4 for structural timber and glulam respectively.

Table 4.1 Overview of the performed tests
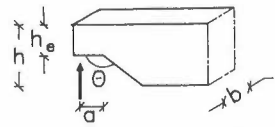
Test serial no.	Cross sec. b x h, mm	Rela.eff.height $\alpha = h_e/h$	Inclination θ,deg	cot θ	Eccentricity a, mm
Structural timber:					
1	45 x 95	0.25	90	∞	31
2	45 x 95	0.50	90	∞	31
3			135	1:1	
4			153	1:2	
5			162	1:3	
6			169	1:5	
7	45 x 95	0.75	90	∞	31
8			135	1:1	
9			162	1:3	
10		0.875	90	∞	
11	45 x 95	0.50	90	∞	63
12			162	1:3	
13		0.75	90	∞	
21S 1)	45 x 195	0.50	90	∞	31
21R 1)					
22S 1)		0.75			
22R 1)					
31	85 x 185	0.50	90	∞	31
32			162	1:3	
33		0.75	90	∞	
34			162	1:3	
Glulam					
1	90 x 300	0.50	90	∞	45
2			135	1:1	
3			153	1:2	
4			169	1:5	
5			173	1:8	
6		0.722	90	∞	
7		0.833			
8	90 x 300	0.50	90	∞	90
9			153	1:2	

cont.

10	90 x 200	0.5	90	∞	35
11		0.75			
12	160 x 567	0.50	90	∞	70
13			153	1:2	

1) Signifies: S   Standing annular rings, see figure 2.1.1.
                          R   Round annular rings

The number of repetitive tests of similar specimens were:
      Structural timber: 6 pieces
      Glulam   4 pieces

4.1 Development of the test method and measuring methods

The test method was developed in the beginning of the testing program of planks with a cross section of 45 x 95 mm. The objectives were primarily to measure the failure load of the notched beam and to measure the beam displacements and some characteristic fracture mechanical strains at the notch.

While the methods for measuring failure load and beam displacement are well developed, the measuring of strains in the notch zone turned out to be more problematic. In the following there is given a review of the development of support conditions and measuring methods.

The load application was controlled manually. The load was increased in steps and kept constant during the reading of the instruments. The time period from the beginning of the test to the final rupture was typical 5 min. to 10 min.

Support conditions

At first the support conditions were as shown in figure 4.1.1. A tilting bearing with an underlayment of teflon, permitting a limited horizontal movement, was used to support the notched end. At the other end a larger freedom of movement was obtained, by using a roller bearing. At the point of force application only a limited horizontal movement was permitted.
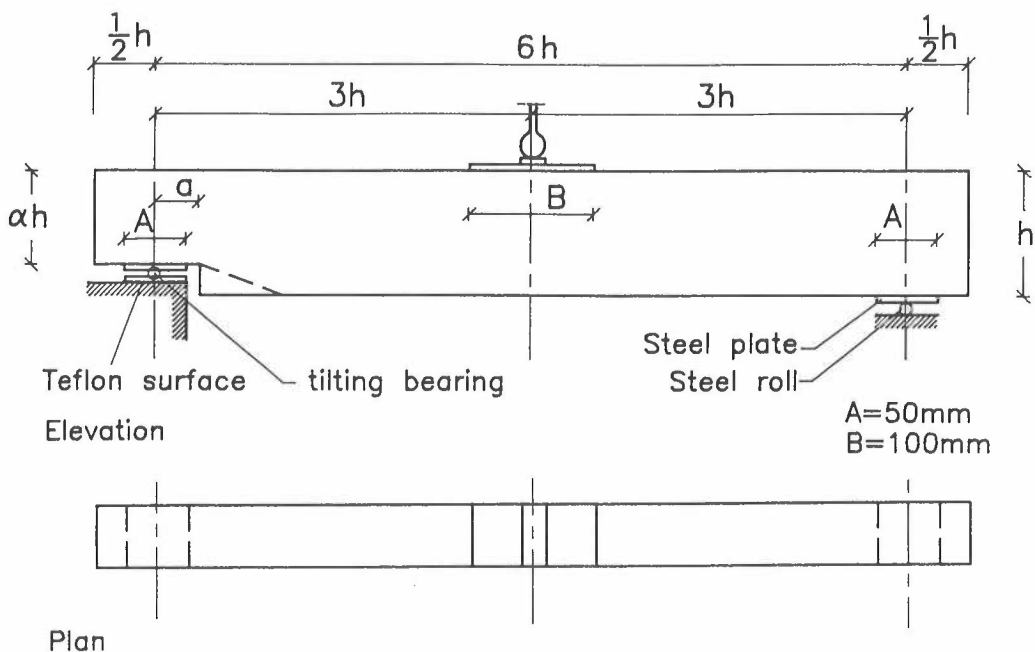
Figure 4.1.1   Support conditions for the first tests.   Early results indicated that torsion was induced. Tests with b x h 45 x 95 mm planks.

These support conditions were soon changed, as early results indicated, that torsion stresses were induced because the planks had twisted during drying. Instead a ball bearing, still with an underlayment of teflon, was used to support the notched end as shown in figure 4.1.2.
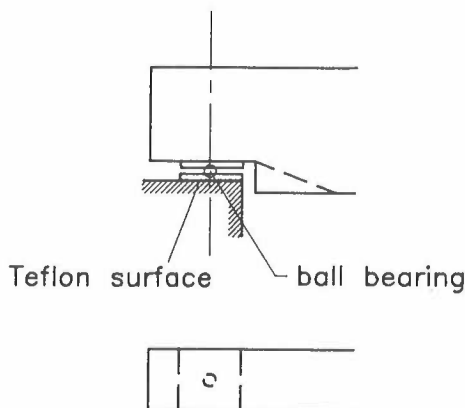
Figure 4.1.2   New support conditions at the notched end intended to eliminate torsion at the notched end by a force application at the geometric middle of the cross section.

81

Measurement of beam displacement

The beam displacement was measured by using displacement transducers (HP, type 7DCT 1000, measuring range 50 mm, accuracy: 0.125 mm). A small piece of wood was nailed underneath the beam, providing measuring points for the transducers, see figure 4.1.3. The beam displacement was measured symmetrical on both sides.
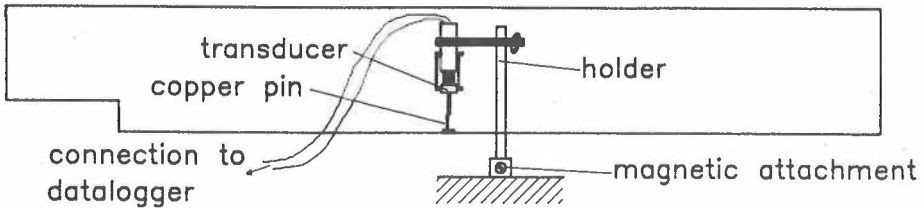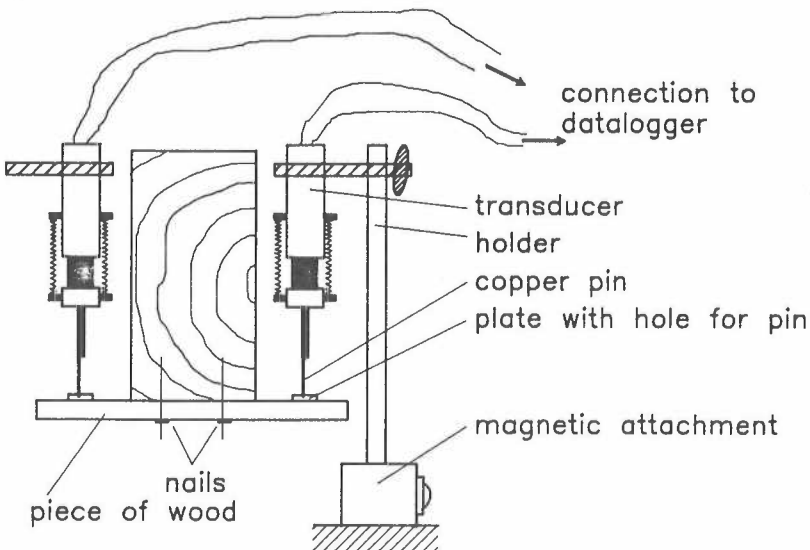
Figure 4.1.3   Measurement of beam displacement by use of displacement transducers.

Measurement of strains in the notch area – transducers

According to the fracture mechanical theory, local strains of a considerable size arise in the notch zone, where the crack will propagate.

Both the vertical opening modes displacements (mode I) and the horizontal sliding mode displacements (mode II) are of interest. According to the physical material parameters the strains at the crack tip are of the magnitude of 100–300 μm, when the crack is

starting to propagate. In order to measure these strains, measuring devices with a high accuracy are required.

At first, displacement transducers with high sensitiveness were used (H.F. Jensen, Type: LDI 8/1, measuring range 2 mm, accuracy: 5 μm).

The transducers were attached to the beam with specially made fittings. Holes were drilled into the beam, and the fittings were screwed on the beam. The transducers were fastened to the fittings by screws. Other screws were screwed on the beam and used as measuring points for the transducers, see figure 4.1.4.
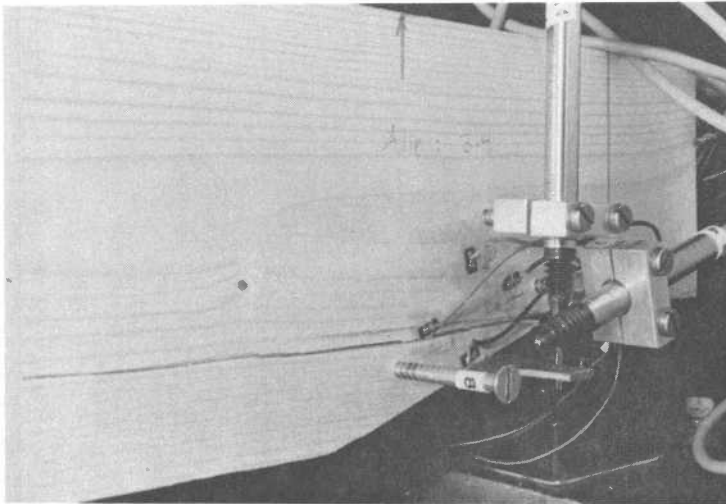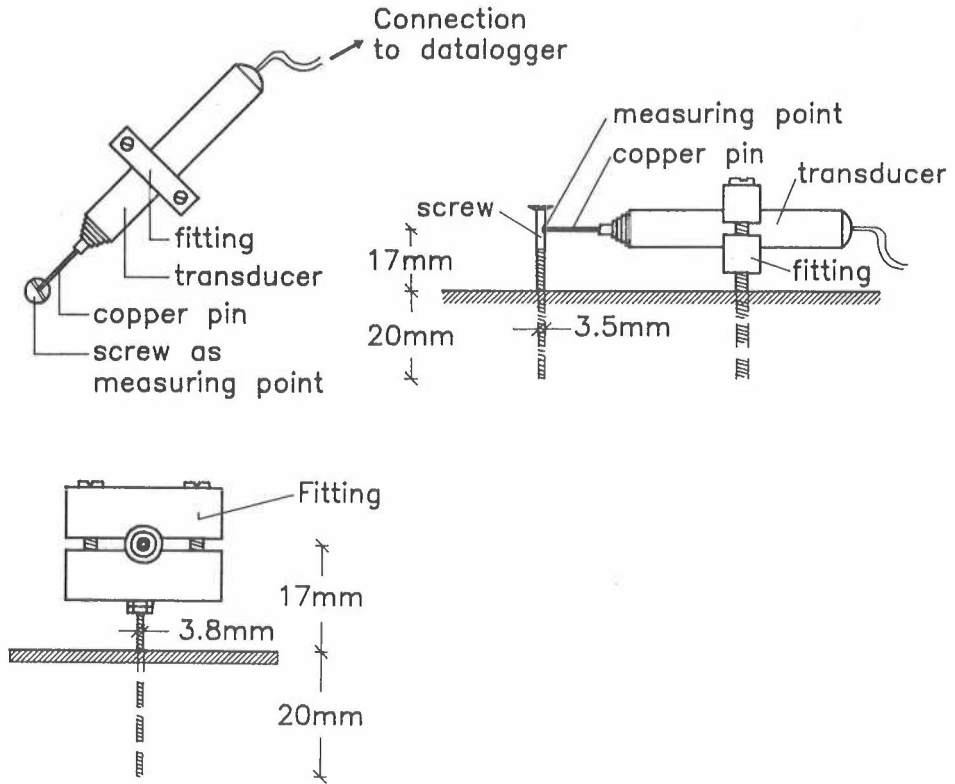
Figure 4.1.4   Displacement transducers used for measuring local strains at the notch. The transducers were attached to the beam by specially made fittings, which were screwed on the beam. Further, strain gages have been bonded to the wood surface for comparison, see picture.

The holes for the screws were drilled to avoid the introduction of local stresses, when the screws were screwed in. The right size of screws and hole diameter were found after a few experiments. If the holes were too small, stresses were introduced. On the other hand, if the holes were too large, the fittings became flexible or loose and the measurements would become inaccurate.

The strains were measured as close to the notches as possible. The position of the transducers is shown in figure 4.1.5. As it was not possible to measure a horizontal displacement with the described equipment, the horizontal displacement was measured indirectly, by placing a transducer diagonally.

For beams with inclined cut—offs, screws could not be used as measuring points, and as an alternative small steel pieces were glued on the cut—off edge, providing the required measuring points, see figure 4.1.5 right and photo in figure 4.1.4.
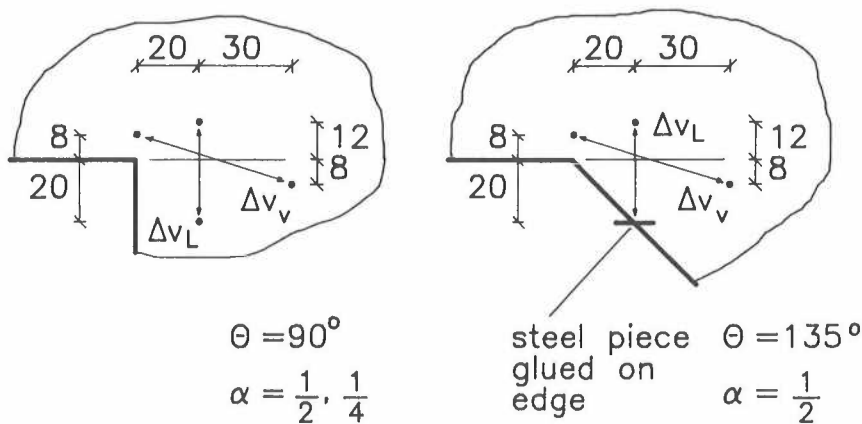
Figure 4.1.5   Examples of positioning of measuring points. ΔV_l is referred to as the vertical displacement and ΔV_v the diagonal displacement (indirect horizontal displacement).

The strains were measured on both sides.

In the first tests the strain measurements appeared unreliable, basicly there were two problems:

1)   Considerable deviations between the measurements on the front and the back.
2)   Irregularities.

Some examples of the two described problems are shown in figure 4.1.6.
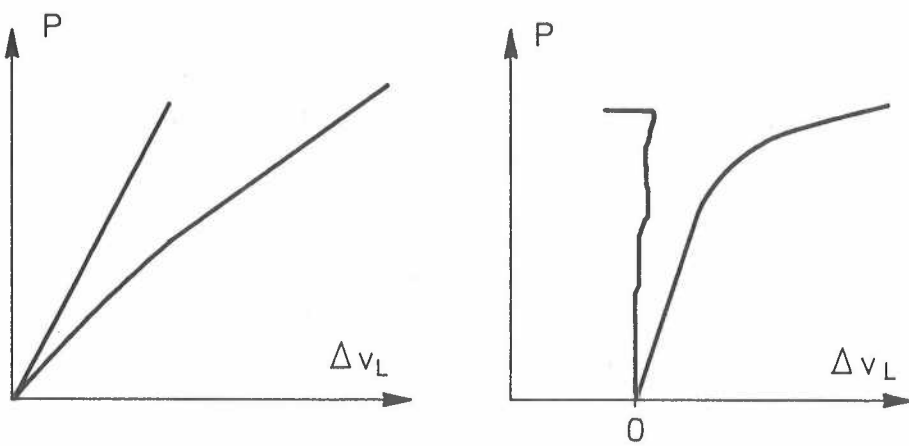
Figure 4.1.6　　Two examples of measurements of vertical strain, ΔV_1, by use of displacement transducers. Left: Systematic deviations between the measurements on the two sides. Right: Non–systematic irregularities.

The first, which can be considered as a systematic deviation from the expected, could perhaps be explained by the static behaviour of the cross section. This could for example be subjected to a torsional moment, see later explanation. Because even though the beam is centrally supported as shown in figure 4.1.2, the stiffness variation over the cross section results in an eccentricity as shown in figure 4.1.7.

wooden
cross—section

Analogue
steel profile
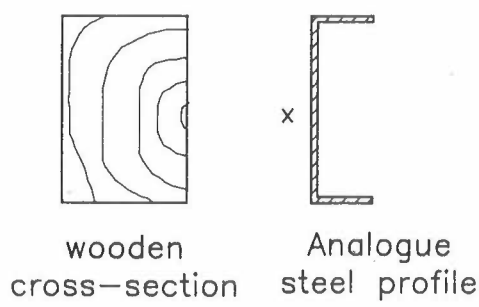
Figure 4.1.7　　Stiffness variation of the cross section results in a shift of the shear center as for the analogue steel profile.

An eccentricity at the support implies a torsional moment giving additional shear strains with different signs on the two sides. This torsional moment would reduce the strains on one side and increase the strains on the other, resulting in a systematic deviation between the two sides.

The irregularities, as shown in figure 4.1.6, are more difficult to explain. They must arise from local inhomogeneties or mechanical movements of the measuring devices originating in loose fittings.

Additional strains from torsions

In order to investigate whether torsion would be the reason for the systematic deviations, the strains from torsion were calculated theoretically. The rectangular cross-section in figure 4.1.8 is considered:
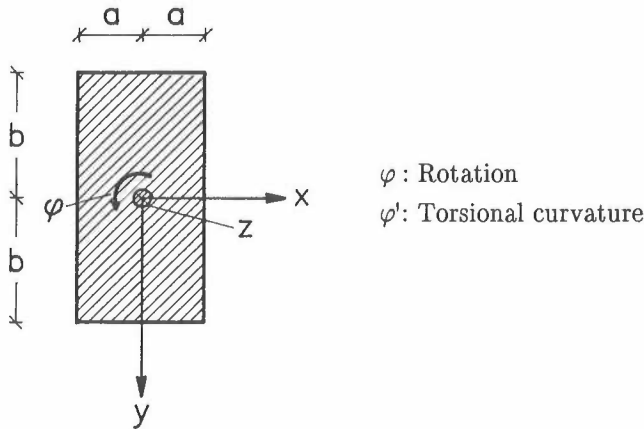
Figure 4.1.8 Geometry of rectangular cross-section.

The cross-section is assumed to be isotropic. We seek a solution to the following equation from /Timoshenko & Goodier/:

$$\frac{\partial^2 \Phi}{\partial x^2} + \frac{\partial^2 \Phi}{\partial y^2} = -2\ G\ \varphi' \tag{4.1.1}$$

where $\Phi(x,y)$ = Timoshenkos Stress Function
   G   = Shear modulus
   φ' = Torsional curvature

According to /Timoshenko & Goodier/ the following stress function is a solution to

equation (4.1.1) for the cross–section shown in figure 4.1.8:

$$\Phi = \frac{32\ G\ \varphi'\ a^2}{\pi^3} \sum_{n=1,3,5,\ldots}^{\infty} \frac{1}{n^3}(-1)^{\frac{n-1}{2}} \left[1 - \frac{\cosh(n\pi y/2a)}{\cosh(n\pi b/2a)}\right] \cos \frac{n\pi x}{2a} \qquad (4.1.2)$$

If the stress–function (4.1.2) is inserted in (4.1.1), it can be seen that (4.1.2) is only a solution if

$$\sum_{n=1,3,5}^{\infty} \frac{1}{n}(-1)^{\frac{n-1}{2}} = \frac{\pi}{4} \qquad (4.1.3)$$

This can be shown graphically.

The warping function $\omega(x,y)$ is found by

$$\frac{\partial \omega}{\partial x} = -\frac{\tau_{xz}}{G\varphi'} - y$$

$$\frac{\partial \omega}{\partial y} = -\frac{\tau_{yz}}{G\varphi'} + x \qquad (4.1.4)$$

where the shear stresses are found as

$$\tau_{xz} = \frac{\partial \Phi}{\partial y}$$

$$\tau_{yz} = -\frac{\partial \Phi}{\partial x} \qquad (4.1.5)$$

If the shear stress functions found from (4.1.5) are inserted in (4.1.4), this results in two warping functions $\omega(x,y)$, which are identical if

$$\sum_{n=1,3,5,\ldots}^{\infty} \frac{1}{n}(-1)^{\frac{n-1}{2}} \sin \frac{n\pi x}{2a} = \frac{\pi^2}{8} \frac{x}{a} \qquad (4.1.6)$$

This can also be shown graphically for different values of $\frac{x}{a}$.

The warping function for the cross–section shown in figure 4.1.8 is then given by

$$\omega(x,y) = \frac{32}{\pi^3} \frac{a^2}{} \sum_{n=1,3,5}^{\infty} \frac{1}{n^3} (-1)^{\frac{n-1}{2}} \left[\frac{\sin \frac{n\pi y}{2a}}{\cosh \frac{n\pi b}{2a}} \right] \sin \frac{n\pi x}{2a} - xy \qquad (4.1.7)$$

The cross–sectional displacements w along the axis are now found from the equation (4.1.8):

$$w(x,y) = -\varphi' \cdot \omega(x,y) \qquad (4.1.8)$$

The warping function $\omega(x,y)$ is shown graphically in figure 4.1.9, illustrating the form of the cross–sectional displacement field:
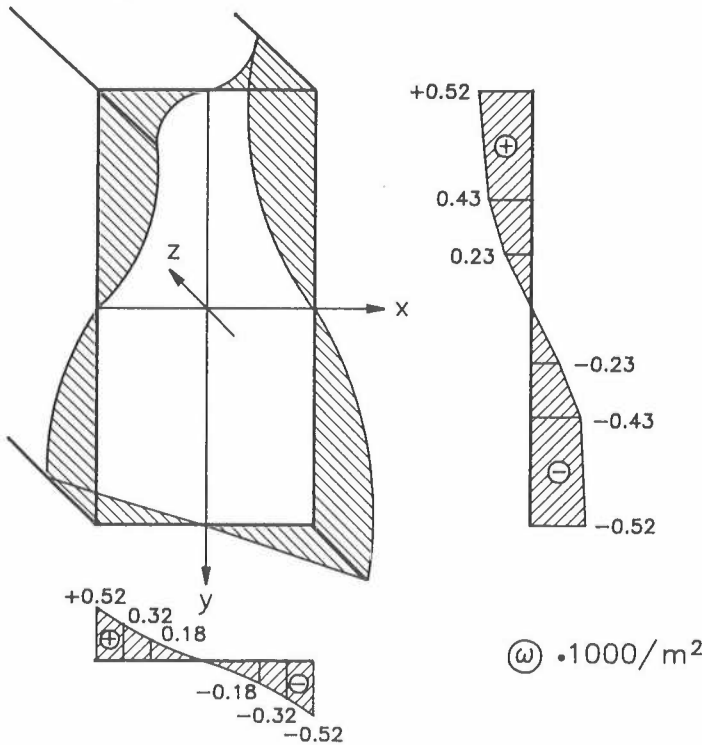
Figure 4.1.9 Warping function $\omega(x,y)$ for rectangular isotropic cross section.

The relation between the torsion moment, M_v and the torsion curvature, φ', is given by the following equation from /Timoshenko & Goodier/, still assuming the cross–section to be isotropic:

$$M_v = 0.23 \; G \quad \varphi' \; (2a)^3 \; (2b) \tag{4.1.9}$$

when $b/a = 2$. Equation (4.1.8) and (4.1.9) results in

$$w(x,y) = -\frac{M}{0.23 \cdot G \, (\, 2a)^3 \; (2b)} \cdot \omega(x,y) \tag{4.1.10}$$

To give an idea of the magnitude of the cross–sectional displacements along the axis due to a torsional moment, an example is calculated. The following is assumed:

Load $P = 10$ kN, reaction $V = 5$ kN, Eccentricity $e = 1$ cm
Torsional moment: $M_v = V \cdot e = 0.05$ kNm
Shear modulus $G = 700$ MPa
Cross–section $2a = 0.045$ m
$\qquad\qquad\quad\;\, 2b = 0.095$ m

From (4.1.10) the following is obtained

$$w(x,y) = -0.035 \cdot \omega(x,y)$$

This gives a maximum displacement at the corner

$$\underline{w_{corner} = \pm \; 18 \; \mu m}$$

At the notch the cross–section is reduced and according to /Timoshenko & Goodier/ the torsional moment now is given by

$$M_v = 0.15 \; G \quad \varphi'(2a)^3 \; (2b) \tag{4.1.11}$$

The corner displacement at the notch is calculated in the same way

$$\underline{w_{corner}^{notch} = \pm \; 57 \; \mu m}$$

Not surprising the displacements increase when the cross–section becomes smaller and the area available to distribute the torsional rotation is decreased.

There must be a zone between the reduced cross–section and the total cross–section, where only a part of the cross–section is effective as shown in figure 4.1.10.
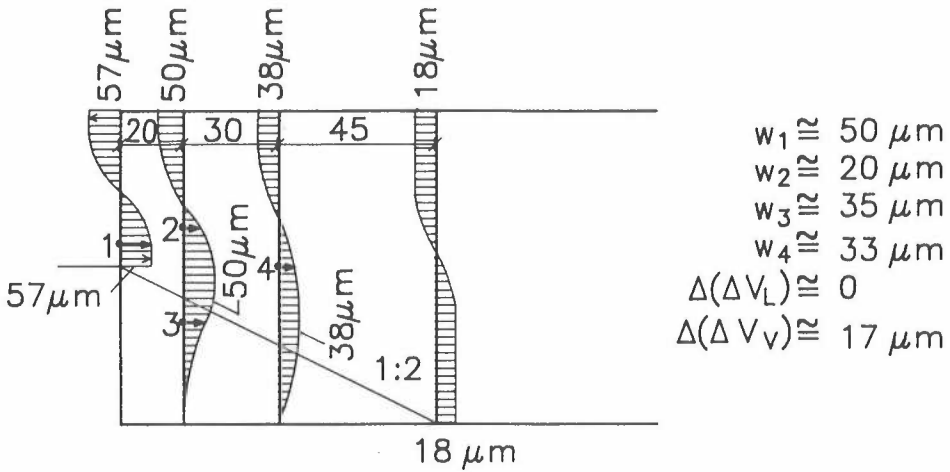
Figure 4.1.10   Cross section displacement along the axis due to a torsional mo-
                     ment $M_v = 0.05$ kNm

With the assumed numbers in figure 4.1.10, it can be seen that the torsional rotation
gives an additional strain $\Delta(\Delta V_v) = 17$ μm on each side. The strain will be positive
on one side and negative on the other. The difference between the two sides will there-
fore be the double: $\Delta(\Delta V_v) = 34$ μm. The vertical strain, ΔV_l, is not affected.

The example shows, though the method is approximative and the applied torsional mo-
ment is overestimated, that torsion could imply a systematic deviation between measu-
rements on the front and back side of the beam.

**Comparison between strain/deformations measured by displacement transducers and
strain gages:**

To investigate further the behaviour of the displacement transducers, it was decided to
carry out a number of tests, where the measurements from the transducers were compa-
red with simultaneous strain gages measurements.

The strain gages were fixed, so that they had the same direction as the transducers,
and covered the same area on both sides of the expected crack. As the strain gages on-
ly had a length of 17 mm, the measuring length was considerable smaller than for the
transducers, see figure 4.1.11.

91

Therefore the strain gage measurements of the relative displacements are expected to be a factor smaller than the transducer measurements.
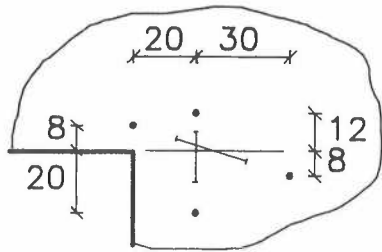
Figure 4.1.11   Simultaneous strain gage and transducer measurements of strains at the notch.

The results from 5 tests are shown in figure 4.1.12.

Figure 4.1.12 a) Test results from 5 tests. Vertical strain ΔV_v and diagonal strain ΔV_1 in notch area measured by partly displacement transducers, partly strain gages.

93
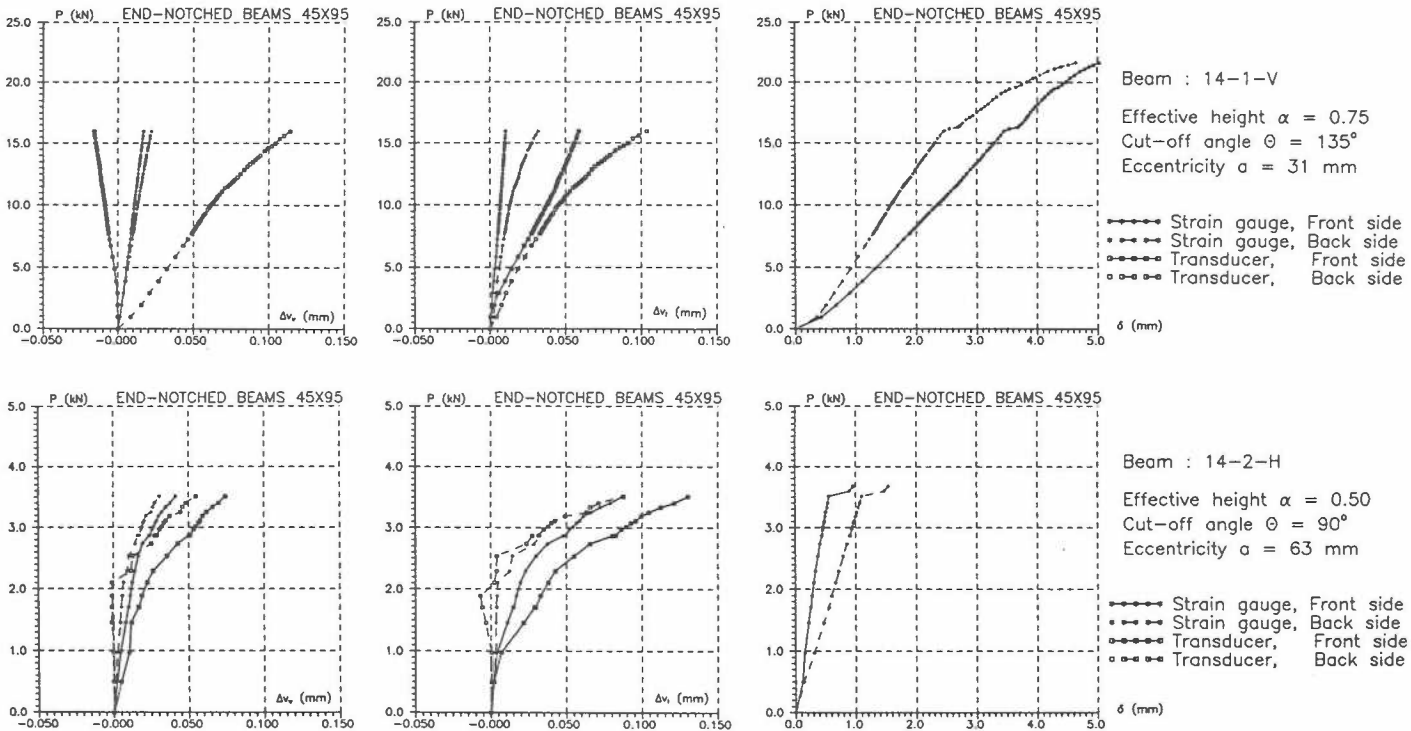
Figure 4.1.12 b) Test results from 5 tests. Vertical strain ΔV_1 and diagonal strain ΔV_v in notch area measured by partly displacement transducers, partly strain gages.

94
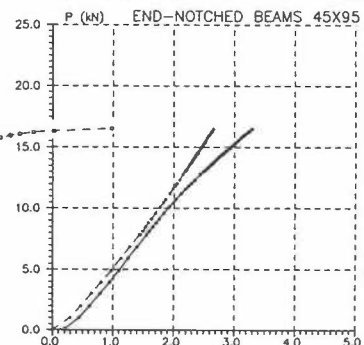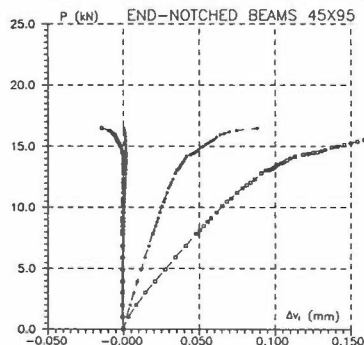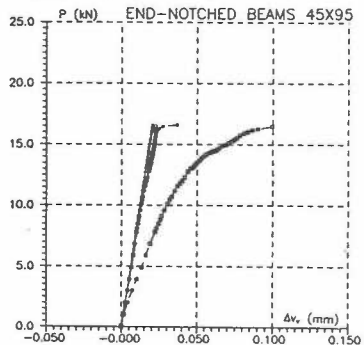
In general, there is good agreement between transducer and strain gage measurements, though a few transducer measurements seem unreasonable, f.ex. ΔV_v in test 14–1–V, ΔV_l in test 14–3–H and ΔV_l in test 14–2–H.

If the mean value between front and back side for the transducer and strain gage measurements is compared, then there is a good agreement, when it is considered, that the transducer measurements were expected to be larger than the strain gage measurements because of the longer gage length. In general however, the strain gage measurements seem more reliable and less sensitive to torsion.

Finally, a test was carried out, where the influence of increased lateral eccentricity at the support, as discussed earlier in this section, was attempted verified. In the test the relative displacements were measured for different eccentricities of the support. There was employed eccentricies in steps of 5 mm where the support was moved from 10 mm left to 10 mm right of the symmetric line, as shown in figure 4.1.13.
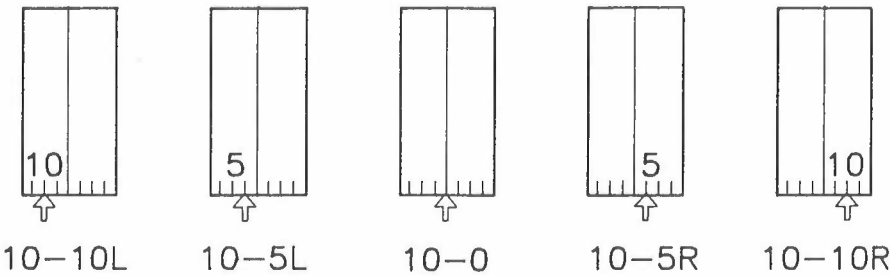
Figure 4.1.13   Test of the influence of possible eccentricities. Different eccentricities tested.

The beam was only loaded to a certain load level, approx. 25% of the expected failure load, and then unloaded again. This to secure, that all 5 tests with different eccentricities were carried out under the same elastic conditions.

This also means that the measured strains were small (5–10 μm) compared to the strain at failure load (50–150 μm). Especially the transducer measurements have previously proved to be inaccurate in the elastic area. This is probably due to local inhomogeneties which dominate in the elastic area, but for higher load levels become overruled by the global mode of operation. The results are shown in figure 4.1.14.
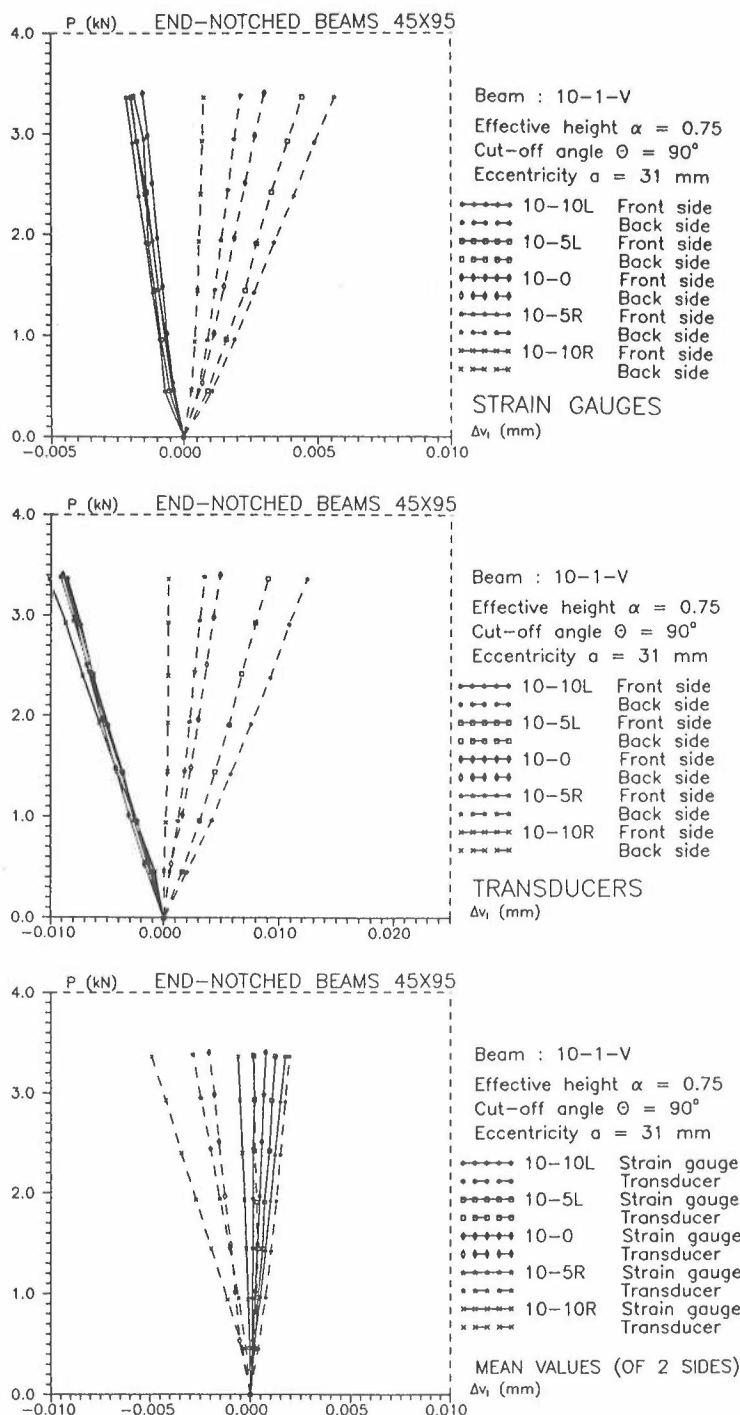
Figure 4.1.14a   Vertical strains or relative displacements. Results from tests with different eccentricies, Δv_v = Horizontal displacement and Δv_l = Vertical displacement. 10–10 R indicates that the support has been moved 10 mm to the right (10–10 L 10 mm to the left).

96
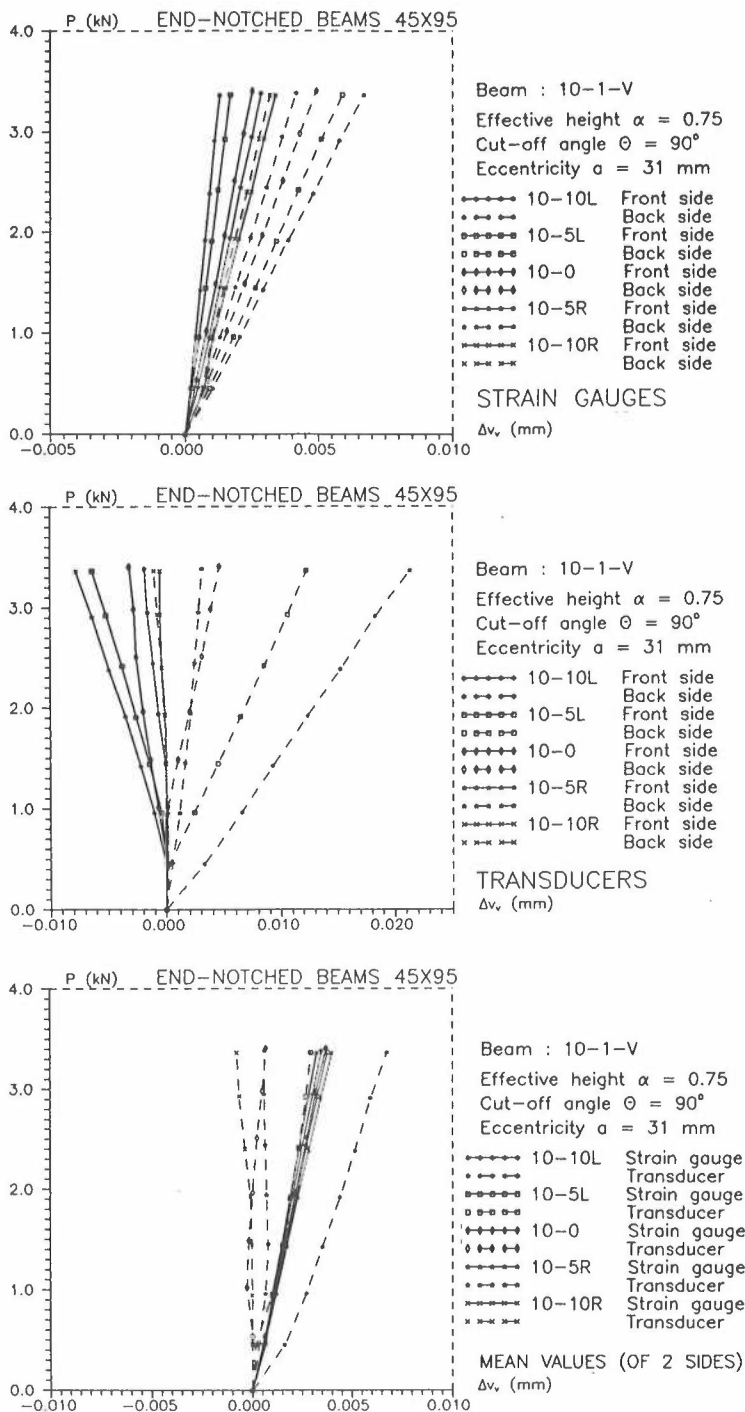
Figure 4.1.14b   Horizontal strains or relative displacements.   Results from tests
with different eccentricies, Δv_v = Horizontal displacement and
Δv_l = Vertical displacement.   10–10 R indicates that the support
has been moved 10 mm to the right (10–10 L 10 mm to the left).

97
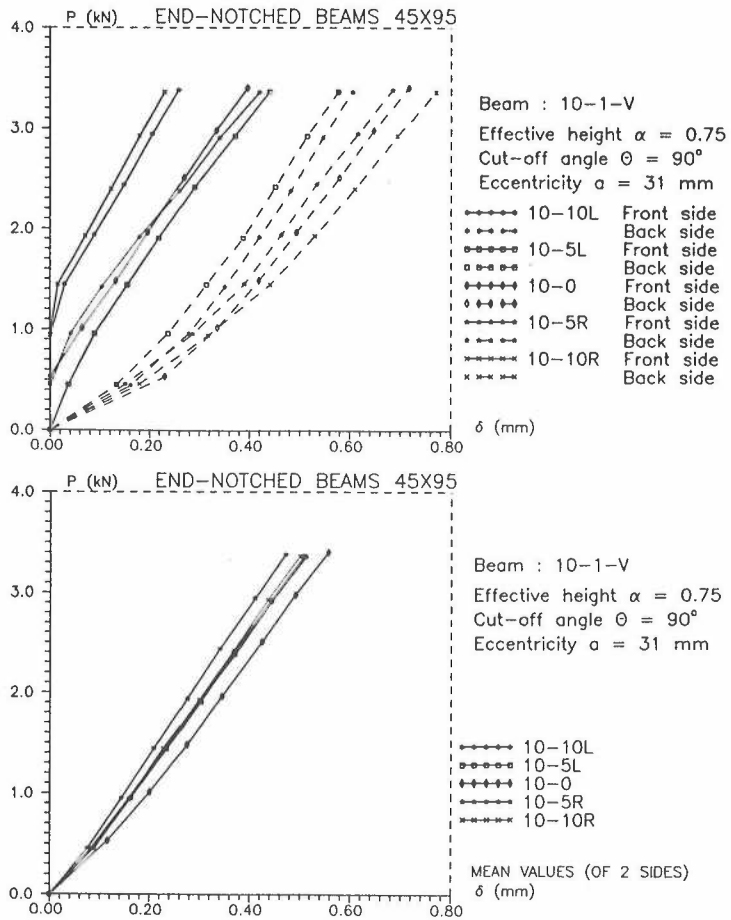
Figure 4.1.14c   Midspan deflections δ , both sides separately, mean values. Results from tests with different eccentricies. 10–10 R indicates that the support has been moved 10 mm to the right (10–10 L 10 mm to the left).

It can be seen from figure 4.1.14, that the measurement at the front and back side can be brought to be equal at a certain eccentricity for the ΔV_v–measurement. This is the case for both the strain gage and transducer measurements. When this is observed, it seems unreasonable, that the mean values at this eccentricity for the strain gage and transducer measurements do not correspond.

For the ΔV_1–measurement, it can be seen that equality between front and back side measurement can not be obtained for any eccentricity. On the other hand, a reasonable agreement between strain gage and transducer measurement can be observed.

In general, strain gages seem most reliable and what is most important, the mean value for strain gage measurements is most insensitive to variation in eccentricity.

Chosen test method and measuring methods

The test method in figure 4.1.2 was chosen. For this the position of the support force was known. The described method for measuring beam deflection is implemented.

The strains in the notch area were chosen to be measured by strain gages, as measurements with displacement transducers had proved to be unreliable, probably influenced by local inhomogeneties and more sensitive to torsional moments.

4.2 Selected test methods

The basic test method is shown in figure 4.1.1 and figure 4.1.2 Depending on the required force, two different arrangements were employed. For solid timber beams with cross sections b x h 45 x 95 mm and 45 x 195 mm a standard 60 Mp–universal testing machine was used. For the solid timber beams with cross section b x h 85 x 185 mm and the glued laminated beams of 90 x 200 mm, 90 x 300 mm and 160 x 567 mm, individual arrangements were set up on the strong floor.

The load application was controlled manually. The load was increased in steps and kept constant during the reading of the instruments. The time period from the beginning of the test to the final rupture was typical 5 min. to 10 min.

Testing in 60 Mp–universal testing machine

In this machine, the test specimen was placed on a traverse, which with an upward movement, pressed the beam against the pressure head at the middle point of the beam. In this way the desired mode of operation was obtained, see figure 4.2.1.
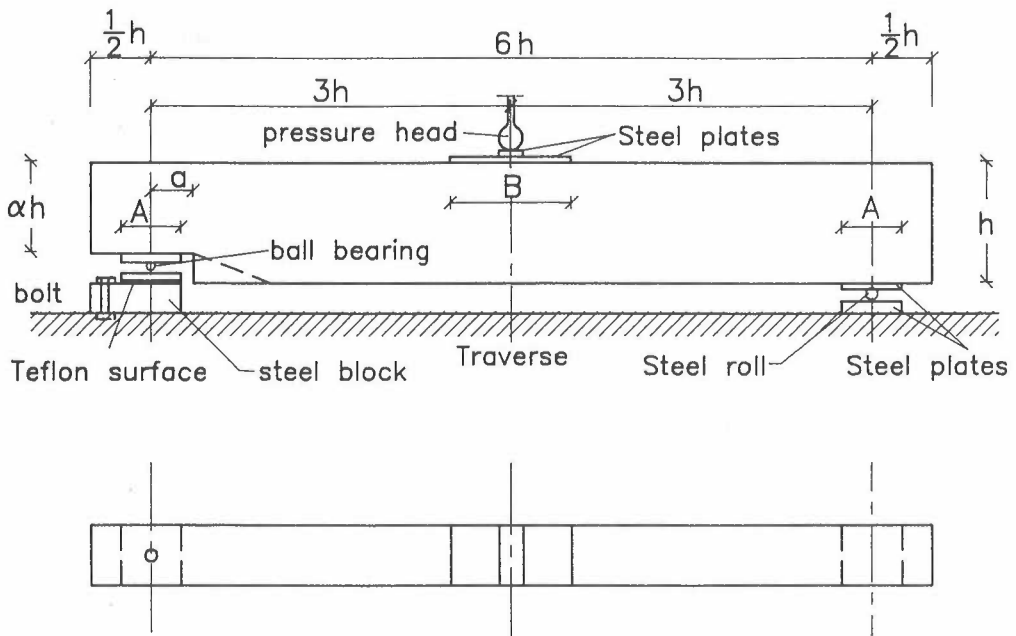
Figure 4.2.1   Test arrangement for 45 x 95 mm² and 45 x 195 mm² specimens.

The employed measuring range of the testing machine was with a maximum of 30 kN for both dimensions.

The load application was controlled manually. In this way measurements could be taken at appropriate chosen load levels where the force was constant in time. The measurements were intensified in the last non–linear stage with automatic data scans at intervals of a few seconds.

The beam displacement was measured by use of displacement transducers (HP 7 DCDT 1000, measuring area 50 mm, accuracy: 0.125 mm) as shown in figure 4.1.3. Displacements on both sides were registered, and in the following working up of the results, a mean value was calculated, representing the value for the assumed two–dimensional plane model.

The strains in the notch area were measured by use of strain gages (gages factor 2.27, gage length 17 mm). Both a vertical opening mode displacement (mode I), ΔV_l, and a diagonal (horizontal) displacement ΔV_v, an indirect measure of the horizontal sliding displacement (mode II), were measured. The strain gages were placed as close as possible to the notch. The position of the strain gages depending on the notch angle θ is shown in figure 4.2.2.

$\Theta = 90°$

$\Theta = 135° \sim 1:1$

$\Theta = 153° \sim 1:2$

$\Theta = 162° \sim 1:3$

$\Theta = 169° \sim 1:5$ undimensioned sizes in mm
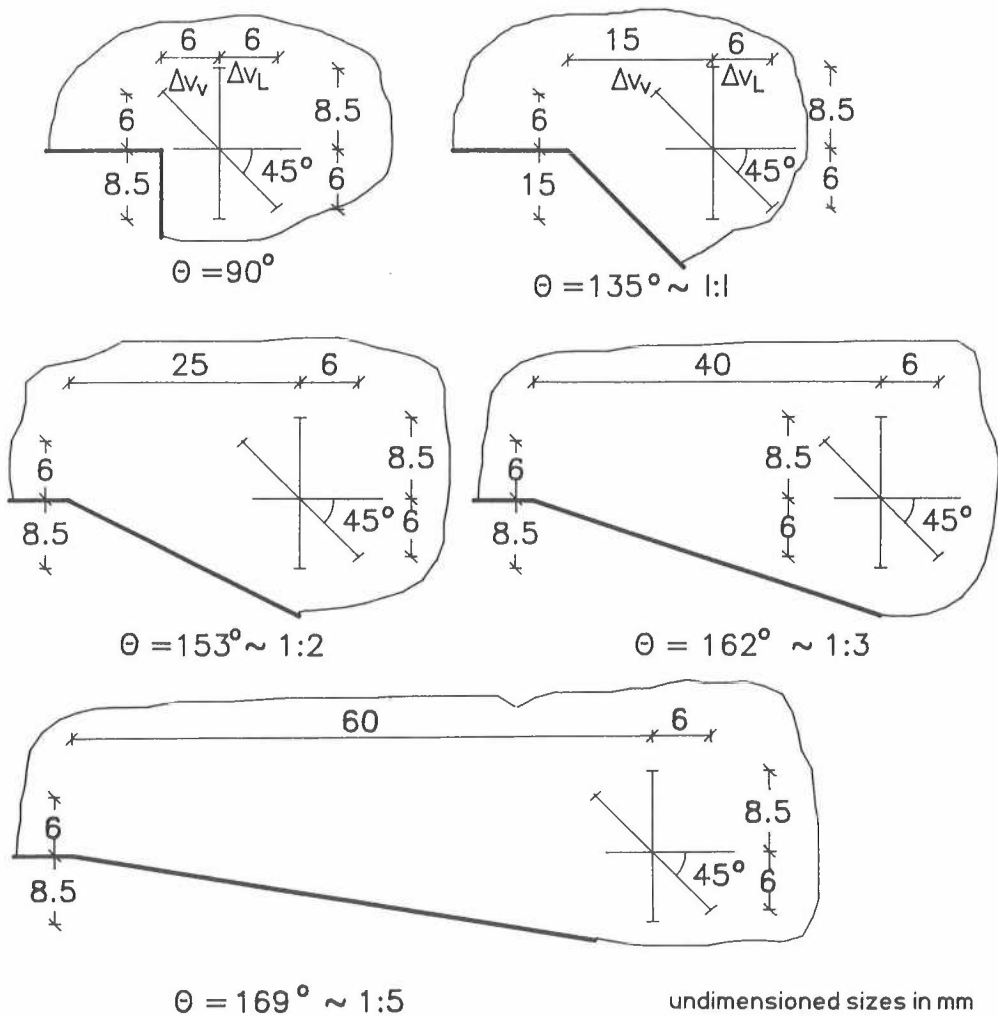
Figure 4.2.2   Position of strain gauges in the notch zone depending on the notch angle θ.

Strains were registered on both sides, and an average value was calculated in the following working up of the results.

For the beam with a large notch angle (flat notches), the strain gages had to be placed so far from the notch, that it's doubtfull, whether the strains were measured within the fracture zone.

As mentioned previously in section 3.3, the accuracy on the strain gauge measurements was $\Delta\epsilon = 0.038$ %o. As the length of the strain gages were 17 mm, the absolute accuracy on the strain gage measurements was 0.65 μm.

Individual testing arrangements for larger specimens

For the larger specimens the testing was performed on the strong floor of practical reasons. Bearings were arranged on the floor providing the appropriate support conditions. A hydraulic jack was hanging up over the beam. Different hydraulic jacks were used according to the required force. As for the smaller specimens, the force application was controlled manually. The test arrangement is shown in figure 4.2.3.

Cross sec. mm	A mm	B mm	h mm	a mm	force Mp
85 x 185	50	100[1]	185	31	5–20
90 x 200	50	250	200	35	10
90 x 300	70	250	300	45–90	10–20
160 x 567	100	250	567	70	25
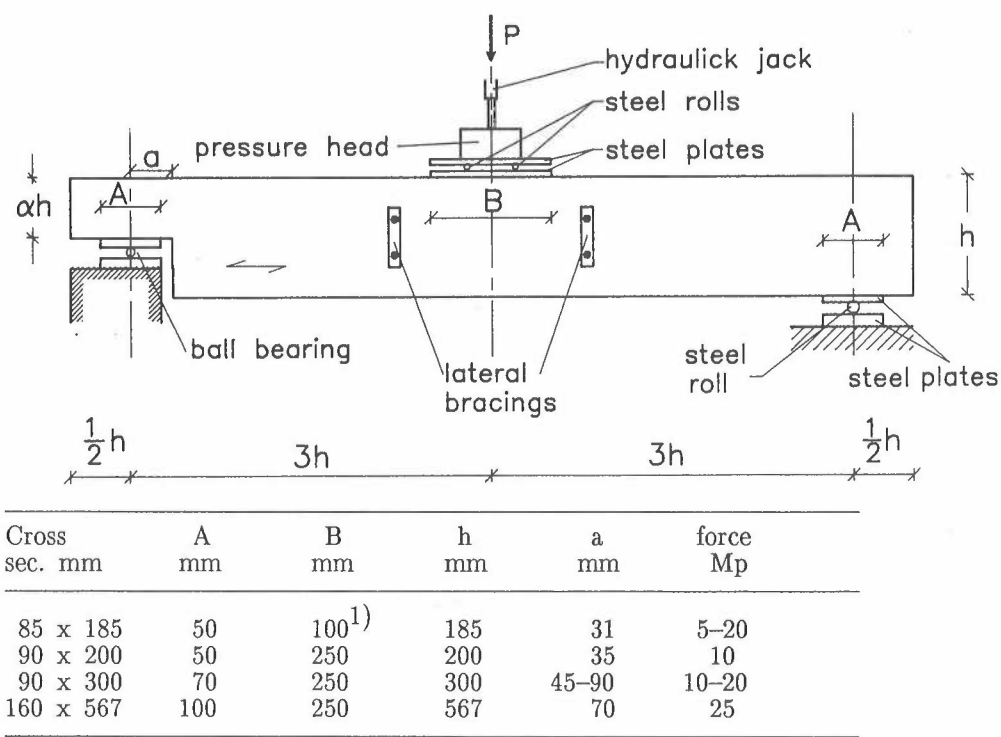
[1] Only steel plates were used at the load fixing point, as shown in figure 4.2.1.

Figure 4.2.3   Test arrangement for specimens with cross sections 85 x 185, 90 x 200, 90 x 300 and 160 x 567 mm².

The beam displacements and strains in the notch area were measured in the same way and with the same equipment as in the case with testing in the 60 Mp universal testing machine, see previous subsection.

Bracings were established in the middle of the span in order to prevent lateral deflection. The surface between the bracing and the beam was covered with teflon, so that displacements in the bearing plane were almost without friction.

4.3 Test results

Table 4.3.1 gives a review of the test results for each type of notched specimen. The results for every notched beam are given in Annex 1. The number of repetitive tests of similar specimens were:

Structural timber:	6 pieces
Glulam	4 pieces

The maximum shear capacity V_{max} of the notch is determined as half the applied force at the catastropic failure. Static equilibrium results in this. The dead load of the specimen has been disregarded as negligible. The catastropic failure was defined as an event where the crack propagated for decreasing applied force without any tendency to that the crack could be stable.

The average shear stress at the catastropic failure was calculated from

$$\tau_{max} = \frac{V_{cat}}{b(\alpha h)} = \frac{V_{cat}}{b\ h_e} \tag{4.3.1}$$

In some cases a pre–failure crack was visible. Table 4.3.3 gives the results for the cases, where this happened. In very few cases the catastropic crack propagation was blocked by a knot resulting in that the final failure occured at a higher level than the catastropic failure. These cases are also stated in table 4.3.3.

Table 4.3.1   Shear capacities at catastrophic failure of the notched beam for each type of notched beam.

Type no.	α h_e/h	Incli. of necking θ, deg	tan θ	Eccen. a, mm	Average shear stress at fail, MPa Mean	St.dev.	min	max
Structural timber 45 x 95 mm								
1	0.25	90	∞	31	1.44	0.24	1.17	1.87
2	0.50	90	∞	31	1.46	0.06	1.40	1.57
3		135	1:1		1.38	0.30	1.08	1.89
4		153	1:2		2.85	0.91	2.01	4.56
5		162	1:3		2.80	0.81	1.94	3.95
6		169	1:5		3.86	0.29	3.44	4.26
7	0.75	90	∞	31	2.22	0.48	1.79	2.93
8		135	1:1		2.29	0.36	1.67	3.79
9		162	1:3		3.14	0.57	2.59	3.90
10	0.875	90	∞	31	2.90	0.22	2.62	3.15
11	0.50	90	∞	63	1.07	0.19	0.87	1.38
12		162	1:3		1.51	0.53	1.68	3.20
13	0.75	90	∞	63	1.96	0.39	1.42	2.56
Structural timber 45 x 195 mm								
21S[1]	0.50	90	∞	31	0.99	0.16	0.79	1.20
21R[1]					1.04	0.11	0.88	1.16
22S[1]	0.75				1.52	0.17	1.28	1.70
22R[1]					1.45	0.29	1.00	1.75
Structural timber 85 x 185 mm								
31	0.50	90	∞	31	1.32	0.14	1.07	1.48
32		162	1:3		2.04	0.51	1.46	2.70
33	0.75	90	∞		2.29	0.65	1.59	3.00
34		162	1:3		2.01	0.45	1.51	2.79
Glulam 90 x 300 mm								
L1	0.50	90	∞	45	1.44	0.15	1.30	1.65
L2		135	1:1		1.66	0.41	1.31	2.19
L3		153	1:2		1.84	0.15	1.69	2.05
L4		169	1:5		2.77	0.49	2.41	3.46
L5		173	1:8		2.79	0.11	2.65	2.90
L6	0.722	90	∞	45	1.63	0.31	1.25	2.01
L7	0.833				2.06	0.34	1.63	2.43
L8	0.50	90	∞	90	1.27	0.19	1.10	1.47
L9		153	1:2		1.90	0.41	1.29	2.20
Glulam 90 x 200 mm								
L10	0.50	90	∞	35	1.59	0.27	1.22	1.87
L11	0.75				2.56	0.44	2.04	3.11
Glulam 160 x 567 mm								
L12	0.50	90	∞	70	0.97	0.16	0.85	1.19
L13		153	1:2		1.10	0.15	0.96	1.24

[1]   Signifies Standing or Round annual rings.

104

The measured shear strength values can be compared with those found in other research projects where timber of the same species and type has been employed. Some mean values have been stated in table 4.3.2. In /Gustafsson & Enquist, 1988/ there is stated some test results for some other wood types. The shear strength values in table 4.3.2 have been determined as the average shear stress at failure as defined in formula (4.3.1). So in the case where the Grashof shear stress distribution has been employed in the original test report the shear strength has been divided by 1.5.

Table 4.3.2   Mean values of the average shear stress τ_{max} at failure and the density ρ and moisture content ω of the wood.

Species	Cross section b x h, mm	h_e/h α	Incli. θ	Eccen. a, mm	τ_{max} MPa	Dens. ρ,kg/m³	Moist. ω, %
/Larsen & Riberholt, 1972/							
Spruce and	63 x 125	1	90	50	(3.0)	438	16
fir. Picea		0.75			1.9		
Abies and Pinces		0.50			1.4		
Sylvest.		0.25			1.2		
/Gustafsson & Enquist, 1988/							
Fir. Pinus	44 x 48	0.75	90	24	2.75	406	15
Sylvest.	44 x 192	0.75		96	1.30		
	45 x 50	0.50	90	25	2.00	−	12
	45 x 100	0.50		50	1.46		
	45 x 200	0.50		100	1.18		
	45 x 45	0.50	90	23	1.82	−	18
	45 x 195	0.50	90	98	0.95		18
/Möhler & Mistler, 1978/, Structural timber							
Spruce	32 x 120	0.917	90	30	2.36	440	15
		0.833			1.93		
		0.750			1.68		
		0.667			1.52		
		0.583			1.50		
		0.500			1.59		
		0.333			1.48		
/Möhler & Mistler, 1978/, Glulam							
Spruce	100 x 600	0.917	90	250	1.00	409	15
		0.833			1.61		
		0.750			0.88		
		0.667			0.86		
		0.500			0.75		

A comparison of the mean values in table 4.3.1 and table 4.3.2 shows that the shear stresses at failure are very similar.

In table 4.3.3 the tests where prefailure crack propagation took place, are listed. In

these tests a crack was observed at a load, V_{cra}, lower than the catastrophic load. In these cases the visible (by the naked eye) crack length was measured by yardstick and registered together with the applied force. After the formation of the crack the load could be increased until the catastrophic load, V_{cat}, defined previously.

In some tests the load could be increased further, until a higher level, V_{max}, was reached. This could be observed when the notch area was reinforced by knots. This can be seen from the load displacement curves in figure 4.3.1.1, which in some cases show similarities with the load–displacement curve in figure 4.3.1.

Shear force

V_{max}

V_{cat}

V_{cra}

Crack propagation
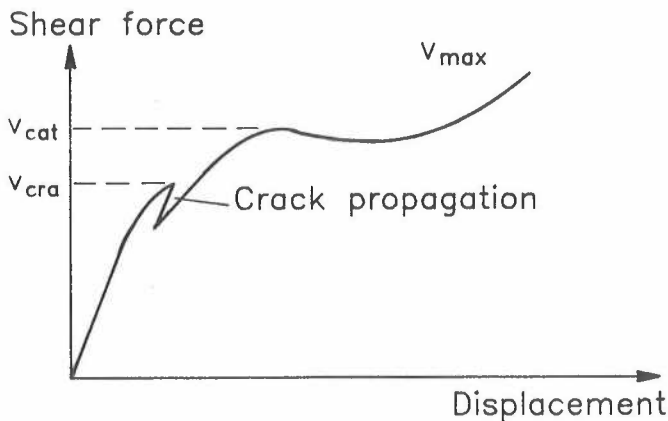
Displacement

Figure 4.3.1   Illustration of the principle load–displacement relation.

Table 4.3.3   Pre–failure crack propagation. Shear force V_{cra} at the prefailure crack formation and the corresponding crack length ℓ. Further maximum shear forces V_{max} larger than the registered catastrophic load V_{cat} in cases where this occured.

Identity	α	$\theta/$ incli.	a mm	V_{cra} kN	ℓ mm	V_{cat} kN	$\dfrac{V_{cra}}{V_{cat}}$	V_{max} kN	Comments
Timber 45 x 95 mm:									
type 1									
11–2–V	0.25	90	31	1.25	8	1.25	1.00	1.3	
type 2									
20–1–V	0.50	90	31	3.0	20	3.0	1.00	3.05	
3–1–V				2.9	20	3.15	0.91		
8–1–V				4.5	80	4.5	1.00	6.7	
9–2–H				3.05	10	3.05	<u>1.00</u>	3.1	
						Mean	0.98		
type 4									
20–2–V	0.50	153	31	3.95	20	4.3	0.92		
type 7									
22–1–V	0.75	90	31		5	8.7	0.95		
type 8									
20–2–H	0.75	135	31		10	7.65	0.80		
14–1–V				8.0		8.0	1.00	12.2	Knot prevents crack propagation until bending failure
15–1–V				12.15		12.15	<u>1.00</u>	12.4	Reinforced by knot
						Mean	0.93		
type 9									
42–3–H	0.75	162	31	8.85	15	8.85	1.00	9.0	
type 10									
10–1–H	0.875	90	31	10.9		10.9	1.00	11.1	
22–2–H				8.5	10	11.5	<u>0.74</u>	13.75	Reinforced by knot bending failure
						Mean	0.87		
type 11									
14–2–H	0.50	90	63	0.5		1.85	0.27		Not in Mean value
15–3–V				2.95		2.95	1.00	8.0	Bending failure
17–1–H				2.0		2.0	1.00	3.5	
30–2–H				1.5	3	2.35	<u>0.64</u>	2.4	
						Mean	0.89		
type 13									
16–3–H	0.75	90	63	6.45	25	8.05	0.80		Reinforced by knot
15–2–V				6.3		6.3	<u>1.00</u>	11.7	Bending failure
						Mean	0.90		

Identity	α	$\theta/$ incli.	a mm	V_{cra} kN	ℓ mm	V_{cat} kN	$\dfrac{V_{cra}}{V_{cat}}$	V_{max} kN	Comments
Timber 45 x 195 mm									
Standing annular rings: type 21S									
61–1–V	0.5	90	31	4.5		5.3	0.85		
Round annular rings: type 21R									
69–2–V	0.5	90	31	3.3	20	4.1	0.80		
68–2–V				3.85	10	3.85	1.00	4.6	ℓ = 200 and blocked by knot
64–1–V				4.5	25	4.9	0.92		
68–1–V				4.5	20	5.0	0.90		
71–1–V				3.8	5	4.45	0.85		
						Mean	0.89		
Standing annular rings: type 22S									
67–2–H	0.75	90	31	7.75		8.35	0.93	–	
60–1–V				10.75	15	11.2	0.96		
64–1–H				9.5	25	10.2	0.93		
65–1–V				9.5	20	10.5	0.90		
60–2–H				9.0	10	10.95	0.82		
63–1–V				7.2	20	8.45	0.90		
						Mean	0.90		
Round annular rings: type 22R									
69–1–V	0.75	90	31	5.0		6.6	0.76		
68–2–H				9.0	20	11.4	0.79		
69–2–H				7.5	30	8.1	0.93		
66–2–H				9.0	10	11.3	0.80		
62–1–H				8.25	10	10.7	0.77		
						Mean	0.81		
Timber 85 x 185 mm: type 31									
118–1–V	0.50	90	31	8.5	50	10.75	0.79	16.05	Crack 300 mm assumed as catastrophic load, V_{cat}. Beam turs over at V_{max}
115–1–V				8.85	50	10.4	0.85	–	Test stopped after catastrophic crack propagation. However, stable crack – possibility to increase load after V_{cat}
						Mean	0.82		
type 33									
110–1–V	0.75	90	31	18.1	(–)	34.2	0.53	–	Test stopped after catastrophic crack propagation. However, stable crack – possibility to increase load after V_{cat}
type 34									
110–2–V	0.75	162	31	27.7	(–)	32.9	0.84		
108–1–V				25.9		25.9	1.00	29.7	Partially Reinforced by knot. Bending Failure
						Mean	0.92		

Identi-ty	α	$\theta/$ incli.	a mm	V_{cra} kN	ℓ mm	V_{cat} kN	$\dfrac{V_{cra}}{V_{cat}}$	V_{max} kN	Comments
Glulam, 90 x 200 mm:									
No cracks registered for loads below V_{cat}									
Glulam, 90 x 300 mm:									
type L1									
L6–1–V	0.50	90	45	15.1		17.55	0.86		
type L2									
L2–1–V	0.50	135	45	17.7		18.6	0.95		
L6–1–H	0.50	135		17.65		17.65	1.00		
						Mean	0.97		
type L6									
L8–1–V	0.722	90	45	34.3	50	39.15	0.88		
L8–2–V				28.9		31.9	0.91		
						Mean	0.90		
Glulam 160 x 567 mm:									
type L12									
L13–1–V	0.50	90	70	48	100	54.0	0.89		
L12–1–H				44.5	100	38.7	0.63		
L13–1–H				41.5	300	45.0	0.92		
						Mean	0.81		
type L13									
L14–1–V	0.50	153 1:2	70	43		53.1	0.81		

A thorough analysis of the shear strength in dependency of the geometry will be given in section 4.4. But here some observations will be presented.

The cutting angle of the necking appears to influence the shear strength of the structural timber. For flatter neckings the shear strength increases up to the flattest cut–off 1:5. For the glulam this is also the case, but there is found a negligible increase in the shear strength when the inclination of the necking is altered from 1:5 to 1:8.

For the structural timber of a cross–sectional size of 45 x 195 it has been found that there is no influence on the shear strength from the pattern of the annual years. It does not matter whether they are standing or round in the cross section. This finding is in accordance with that the failure energy in tension perpendicular to the grain is independent of the annual ring pattern.

A comparison between specimens of almost the same cross–sectional height and force application shows that notched glulam beams have a higher shear strength than structural timber beams, see table 4.3.4. Further, from this table it can be seen that the

narrower cross section 45 x 195 mm has a lower shear strength than the wider 85 x 185 mm. The mean values of density and moisture content are also given in the table because there is a systematic difference between structural timber and glulam.

The reason for these relations could be that the drying cracks in glulam are smaller or positioned differently (they do not form crack surfaces perpendicular to the tensile stresses perpendicular to grain). Further, drying cracks of a certain depth result in a larger reduction in the shear strength of narrow cross section.

Drying cracks could be registered on the 85 x 185 mm² beams of structural timber (depth 2–5 mm). However, while cutting out the test specimens, it was ensured, that no cracks appeared within a considerable distance from the notch. In this way drying cracks had no influence on the test results.

Table 4.3.4   Mean values of shear strength τ_{max} at catastrophic failure. Structural timber and glulam notched beams of almost equal cross–sectional height. Further, means of density ρ and moisture content ω.

Type no	α	θ	$\overline{\tau}_{max}$ MPa	$\tau_{struc}/\tau_{glulam}$	ρ kg/m³	ω %
Structural timber 45 x 195 mm						
21S+21R	0.50	90	1.02	0.64	385	14.0
22S+22R	0.75	90	1.49	0.58	393	14.0
Structural timber 85 x 185 mm						
31	0.50	90	1.32	0.83	387	15.4
33	0.75	90	2.29	0.89	394	14.6
Glulam 90 x 200 mm						
10	0.50	90	1.59		426*	12.0
11	0.75	90	2.56		466*	11.2

* Density of the notch lamination.

Pre–failure crack propagation

From table 4.3.3 it appears that pre–failure cracking occurred in several cases, specially for the specimens of structural timber. It is also typical that pre–failure cracking occurred for "neckings" cut perpendicular to the grain, that is for $\theta = 90^0$. It can be seen from the table, that the pre–failure crack propagation in average occurred at stress levels from 0 to 19% lower than the catastrophic load.

Further, during the tests, cracking sounds from the beam occured from an earlier stage for the beams with perpendicular or steep neckings. Thus, for the beams with perpen-

dicular or steep neckings, the failure seems to be more ductile. See also table 4.3.5.

In a few cases a knot acted as a reinforcing element by stopping the crack propagation. The same effect is reported in /Larsen & Riberholt, 1972/. The final failure at V_{max} was in these cases a bending failure.

Characterization of fracture surface
The character of the fracture surface can roughly be separated into two cases as shown in figure 4.3.2, a "clean" fracture surface or an irregular fracture surface.
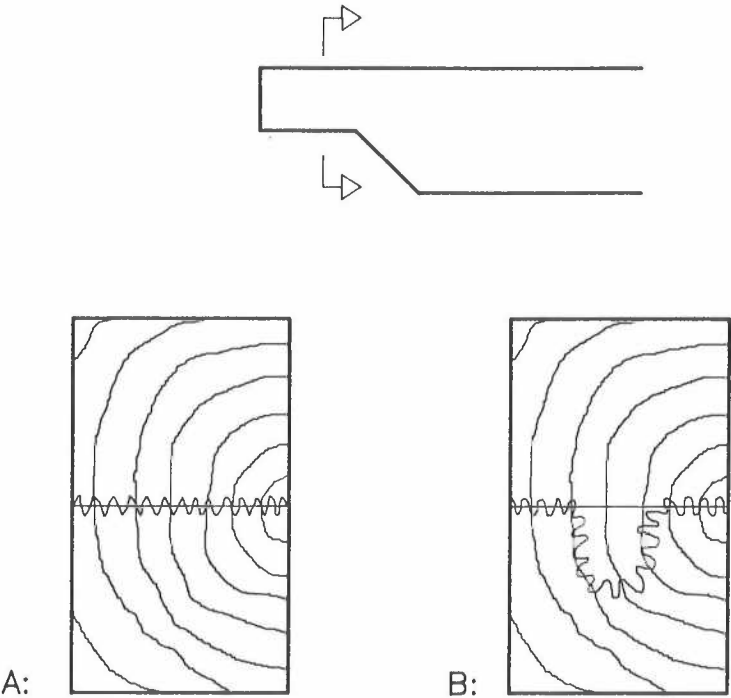
Figure 4.3.2   Characterization of fracture surface.
a. "clean" fracture surface.
b. irregular fracture surface.

Tests showed, that a clean fracture surface, where the crack ran from the notch horisontally through the beam, was obtained for beams with perpendicular neckings ($\theta = 90^0$). In the case of inclined neckings, the character of the fracture surface became more casual, both clean and irregular fracture could be observed. In table 4.3.5 observations from the tests concerning brittleness and fracture character are shown schematically.

Table 4.3.5: Observations concerning failure characteristics during tests.

Type	Dimension	Geometry $\alpha =$ h_e/h	θ (0)	incli (1:x)	eccen. a (mm)	Failure: Brittle[*]	Ductile[*]	Fracture Surface Clean	Irregular
	Structural timber								
1	45 x 95	0.25	90	–	31	x	x	x	
2		0.50	90	–	31		x	x	
3			135	1	31	x		x	
4			153	2		x	(x)	x	(x)
5			162	3		x		x	x
6			169	5		x		x	x
7		0.75	90	–	31		x	x	
8			135	1			x	x	
9			162	3		x	x		x
10		0.875	90	–	31	x	(x)	x	
11		0.50	90	–	63		x	x	
12			162	3		x		x	x
13		0.75	90	–	63	(x)	x	x	
21	45 x 195	0.50	90	–	31		x	x	
22		0.75	90	–	31		x	x	
31	85 x 185	0.50	90	–	31		x	x	
32			162	3		x		x	x
33		0.75	90	–	31		x	x	
34			162	3		x	x	x	x
	Glulam								
L1	90 x 300	0.50	90	–	45	x	x	x	
L2			135	1		x	x	x	x
L3			153	2		x		x	x
L4			169	5		x			x
L5			173	8		x			x
L6		0.722	90	–	45		x	x	
L7		0.833	90	–	45		x	x	
L8		0.50	90	–	90		x	x	
L9			153	2		x			x
L10	90 x 200	0.50	90	–	35		x	x	
L11		0.75	90	–	35		x	x	
L12	160x567	0.50	90	–	70		x	x	
L13			153	2		x			x

* Refers to measured load–deformation behaviour, see for example figures 4.3.1.3 to 4.3.1.6 and the typical curves in figure 4.3.1.14.

For the glulam beams groaning could be heard in all cases, independable of geometry and failure characteristics. The groaning seemed to be caused by internal fracture, possibly sliding fracture along the glued lamination surfaces.

4.3.1 Load–deformation relations

Midspan deflections on each side of the specimen
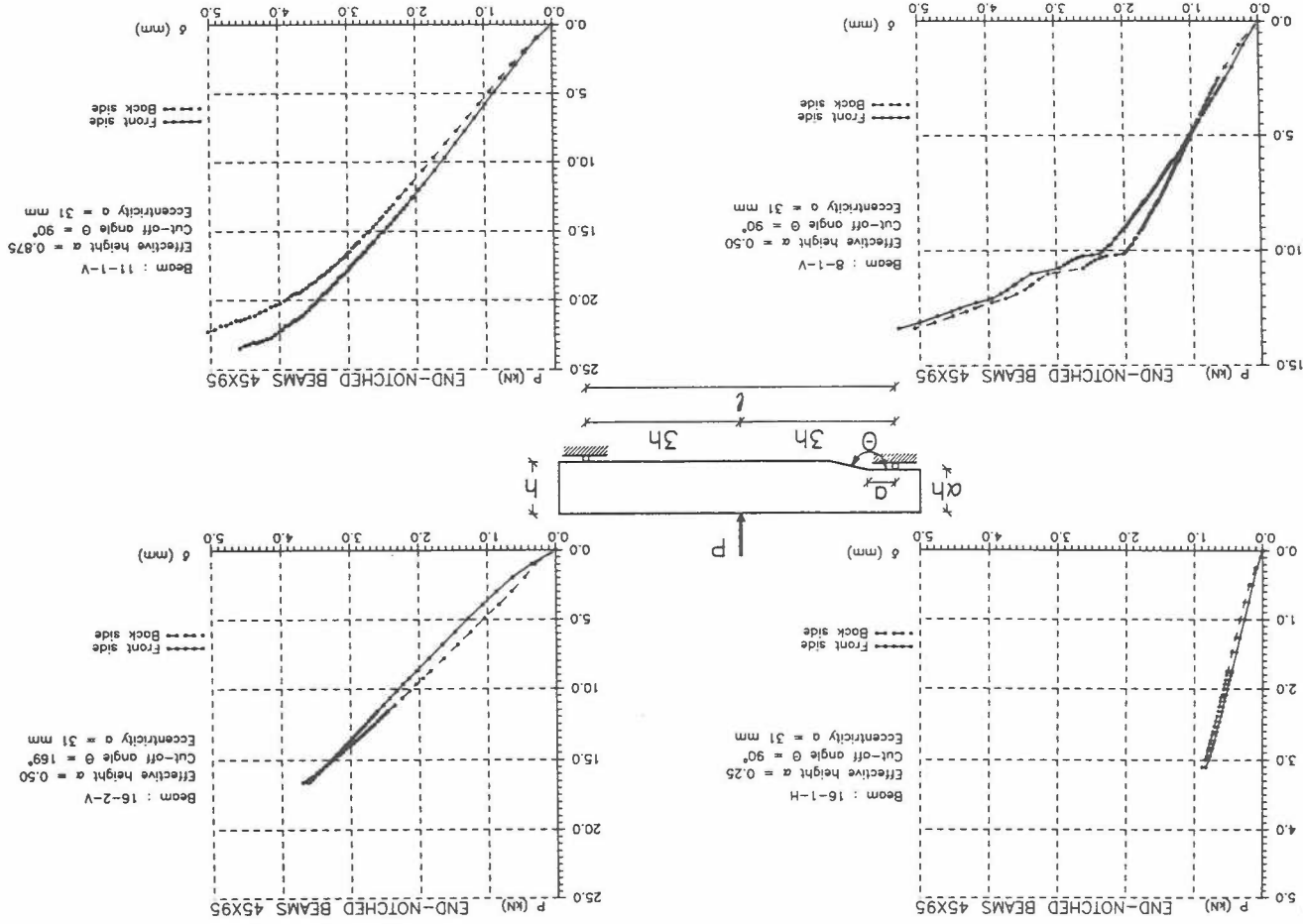
Figure 4.3.1.1   Structural timber. Typical mid span deflections on each side of the specimen.

113

Figure 4.3.1.2   Glulam. Typical mid span deflections on each side of the specimen.
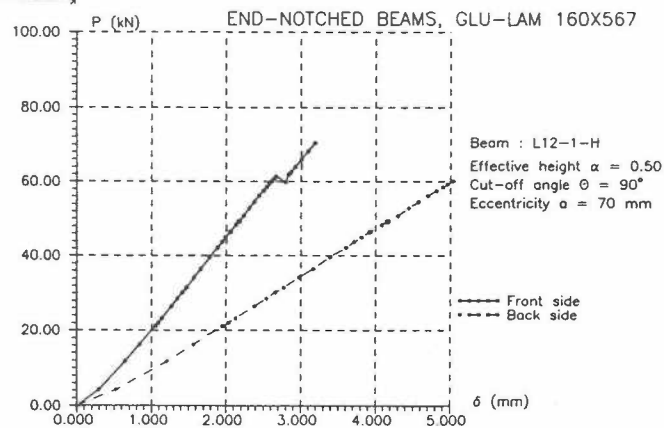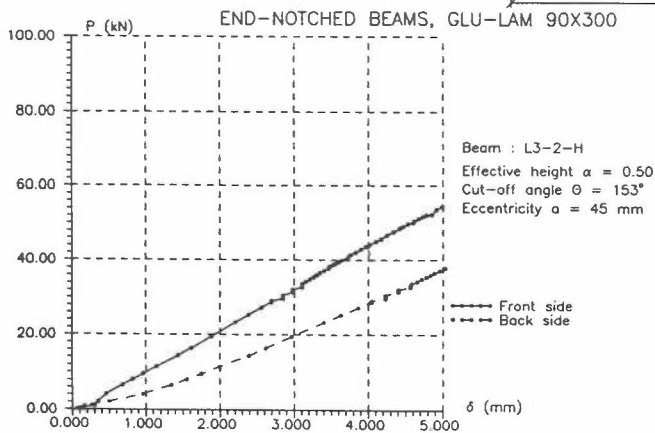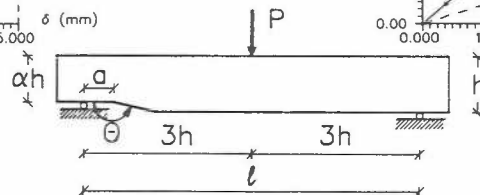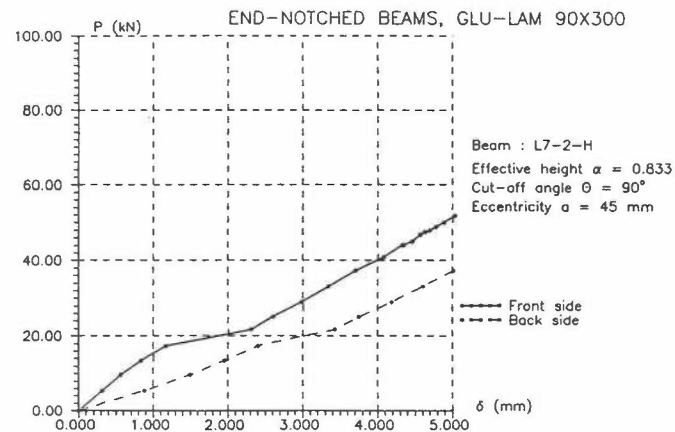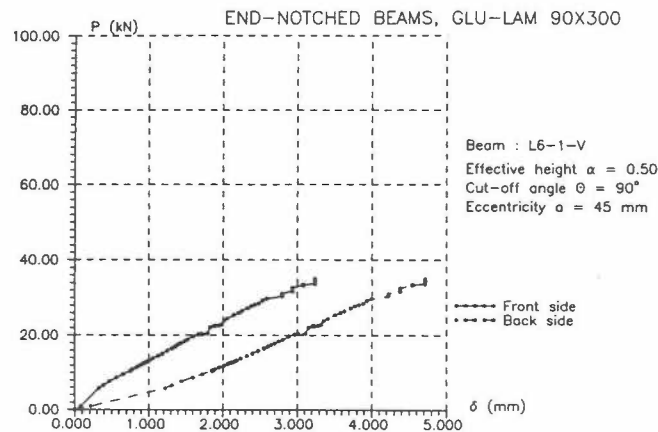
It can be seen from the figure 4.3.1.1 and 4.3.1.2 that there is a certain difference between the mid span deflections on each side of the specimen. Apparently some torsion takes place. But generally, non–linearities are observed in both deflections at the same load level.

Strains at the notch tip on each side of the specimen

The figures 4.3.1.3 to 4.3.1.6 show the load–elongation relations for the strain gage measurements at the notch tip. The elongation is equal to the average strain along the gage multiplied by the gage length 17 mm. It appears from them that the load–strain curves follow each other, but typical they are not identical. So the strain field is not plane, not constant in depth.
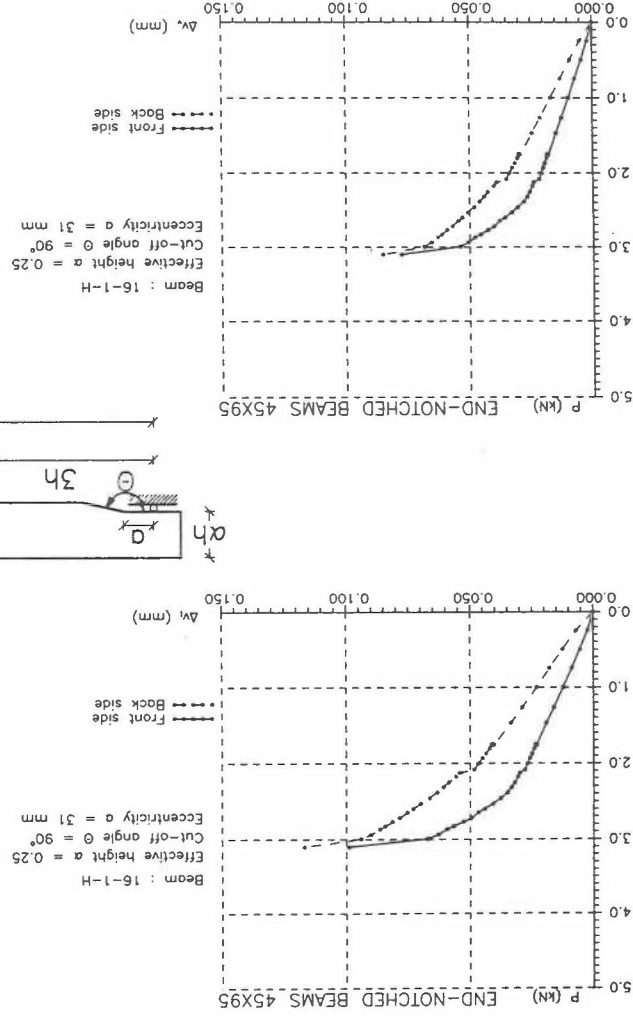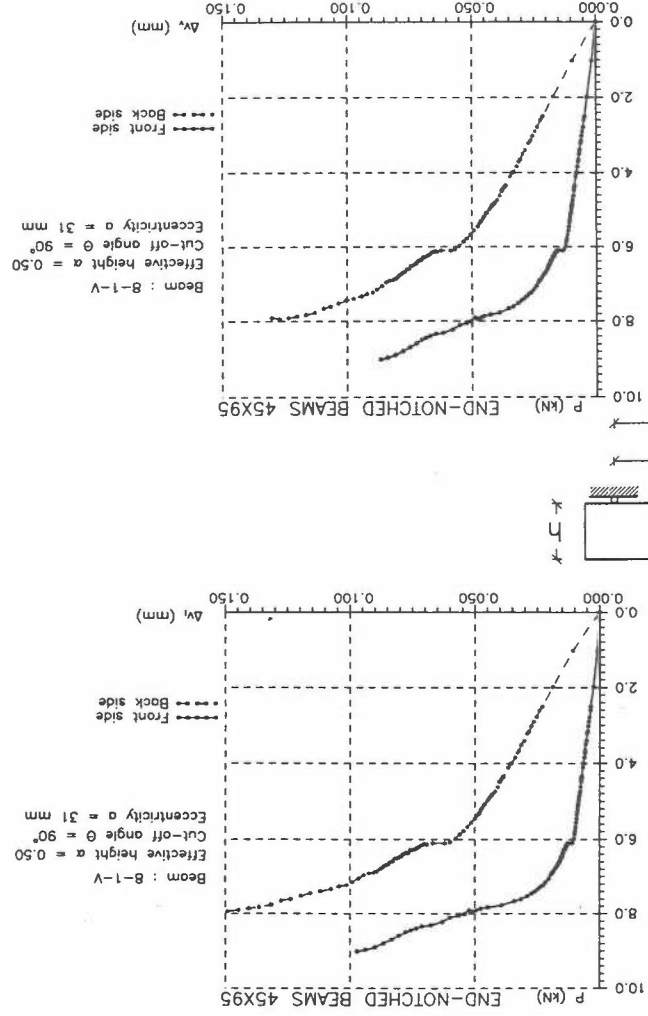
Figure 4.3.1.3

Structural timber. Load-elongation relations for strain gages close to the notch tip and positioned on each side of the specimen. Δv_l: vertical elongation, Δv_V: diagonal elongation (almost horizontal elongation).
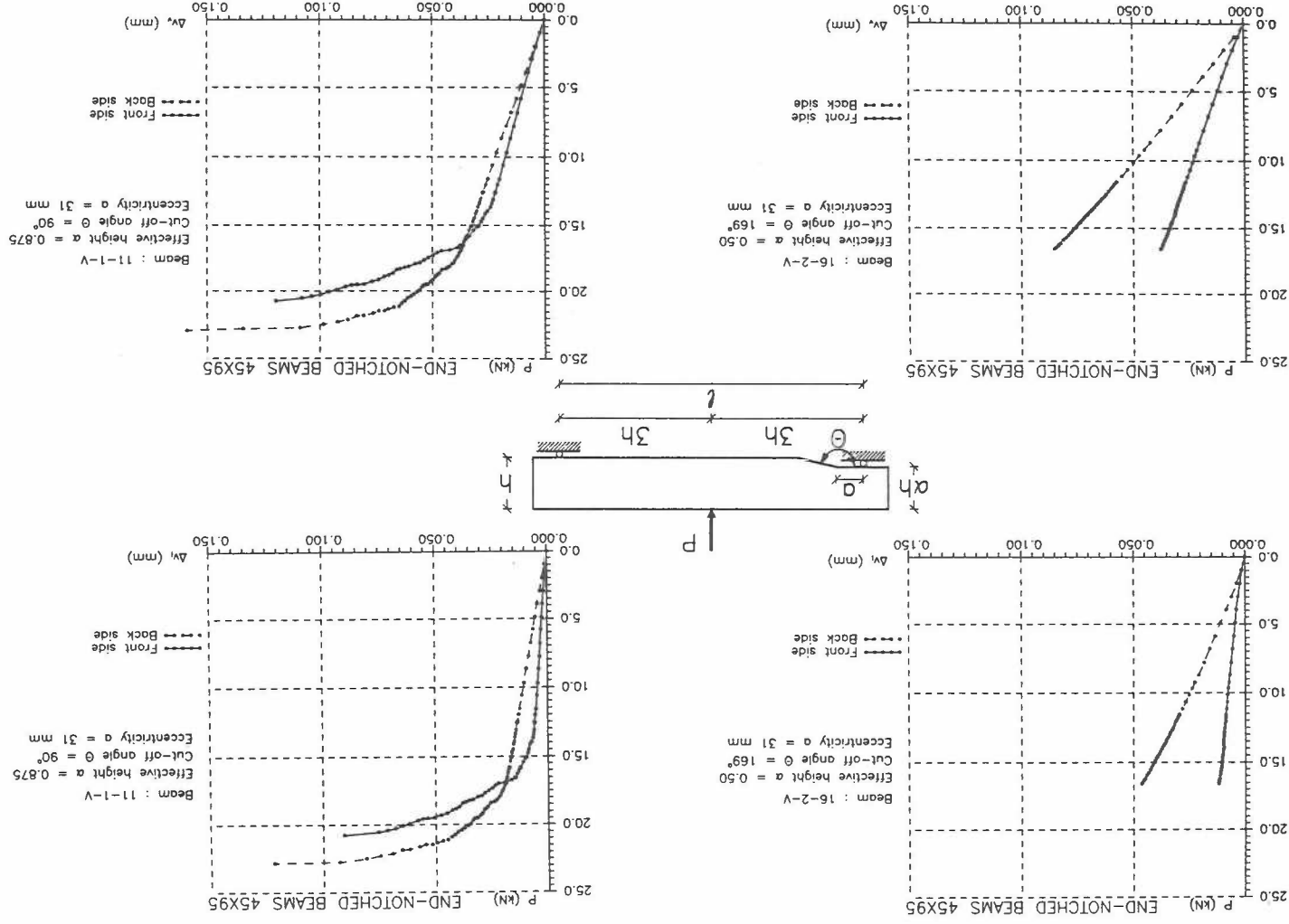
Figure 4.3.1.4   Structural timber. Load–elongation relations for strain gages close to the notch tip and positioned on each side of the specimen. Δv_I: vertical elongation, Δv_V: diagonal elongation (almost horizontal elongation).

117

END-NOTCHED BEAMS, GLU-LAM 90X300

P (kN)

Beam : L3-2-H
Effective height α = 0.50
Cut-off angle θ = 153°
Eccentricity a = 45 mm

Front side
Back side

Δv₁ (mm)

0.000   0.050   0.100   0.150

0.00   20.00   40.00   60.00   80.00   100.00

END-NOTCHED BEAMS, GLU-LAM 90X300

P (kN)

Beam : L6-1-V
Effective height α = 0.50
Cut-off angle θ = 90°
Eccentricity a = 45 mm

Front side
Back side

Δvₕ (mm)

0.000   0.050   0.100   0.150

0.00   20.00   40.00   60.00   80.00   100.00

END-NOTCHED BEAMS, GLU-LAM 90X300

P (kN)

Beam : L3-2-H
Effective height α = 0.50
Cut-off angle θ = 153°
Eccentricity a = 45 mm

Front side
Back side

Δv₁ (mm)

0.000   0.050   0.100   0.150

0.00   20.00   40.00   60.00   80.00   100.00

END-NOTCHED BEAMS, GLU-LAM 90X300

P (kN)

Beam : L6-1-V
Effective height α = 0.50
Cut-off angle θ = 90°
Eccentricity a = 45 mm

Front side
Back side

Δvₕ (mm)

0.000   0.050   0.100   0.150

0.00   20.00   40.00   60.00   80.00   100.00

l
3h   3h
h
αh
a
θ
P

Figure 4.3.1.5   Glulam. Load–elongation relations for strain gages close to the notch tip and positioned on each side of the specimen. Δv_l: vertical elongation, Δv_v: diagonal elongation (almost horizontal elongation).

END-NOTCHED BEAMS, GLU-LAM 90X300

Beam : L7-2-H
Effective height α = 0.833
Cut-off angle Θ = 90°
Eccentricity a = 45 mm

END-NOTCHED BEAMS, GLU-LAM 160X567

Beam : L12-1-H
Effective height α = 0.50
Cut-off angle Θ = 90°
Eccentricity a = 70 mm

END-NOTCHED BEAMS, GLU-LAM 90X300

Beam : L7-2-H
Effective height α = 0.833
Cut-off angle Θ = 90°
Eccentricity a = 45 mm

END-NOTCHED BEAMS, GLU-LAM 160X567

Beam : L12-1-H
Effective height α = 0.50
Cut-off angle Θ = 90°
Eccentricity a = 70 mm

Figure 4.3.1.6   Glulam. Load-elongation relations for strain gages close to the notch tip and positioned on each side of the specimen. Δv_l: vertical elongation, Δv_v: diagonal elongation (almost horizontal elongation).

119
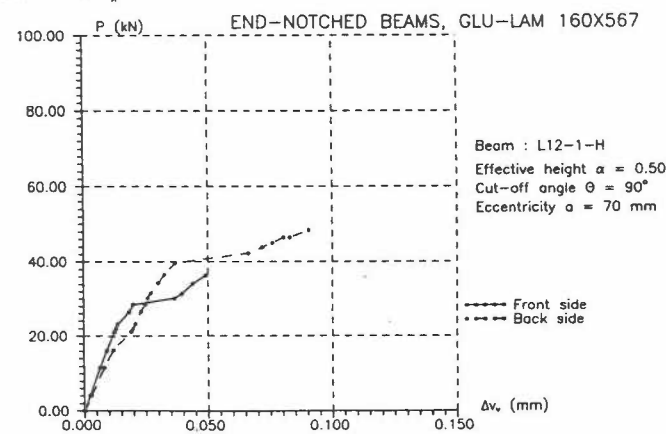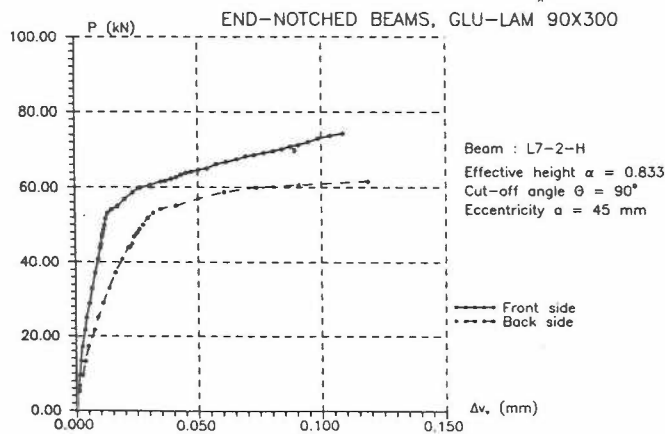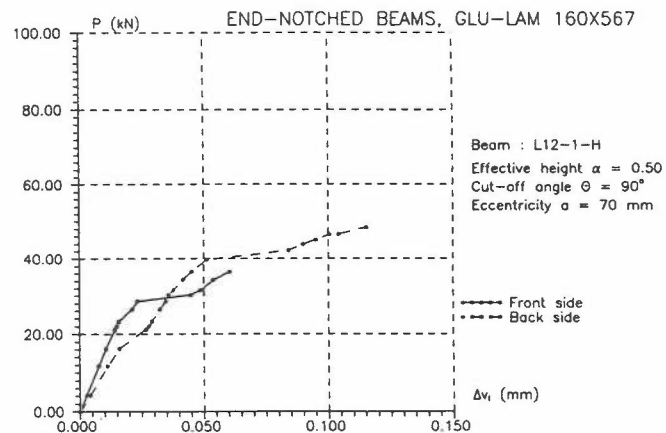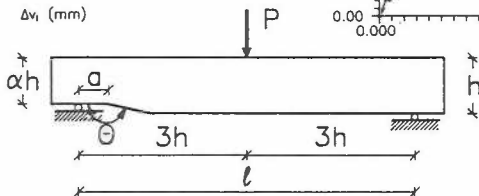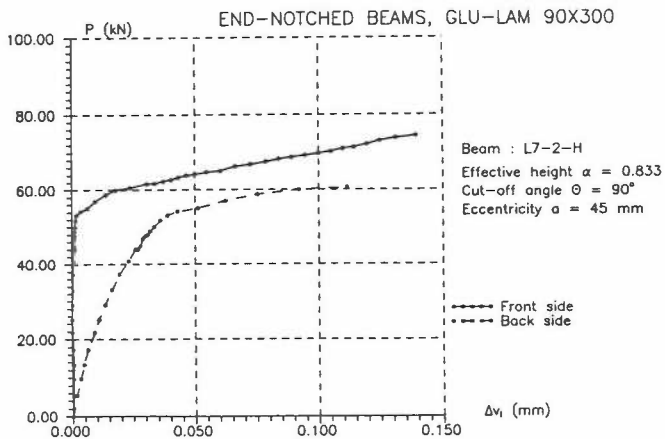
Load—deformation relations for structural timber

The following figures show the load—deformation relations for the mean values measured on both sides of the specimens. The figures show the relations for mid span deflection δ , vertical elongation (vertical strain) Δv_l and diagonal (horizontal) elongation Δv_v .
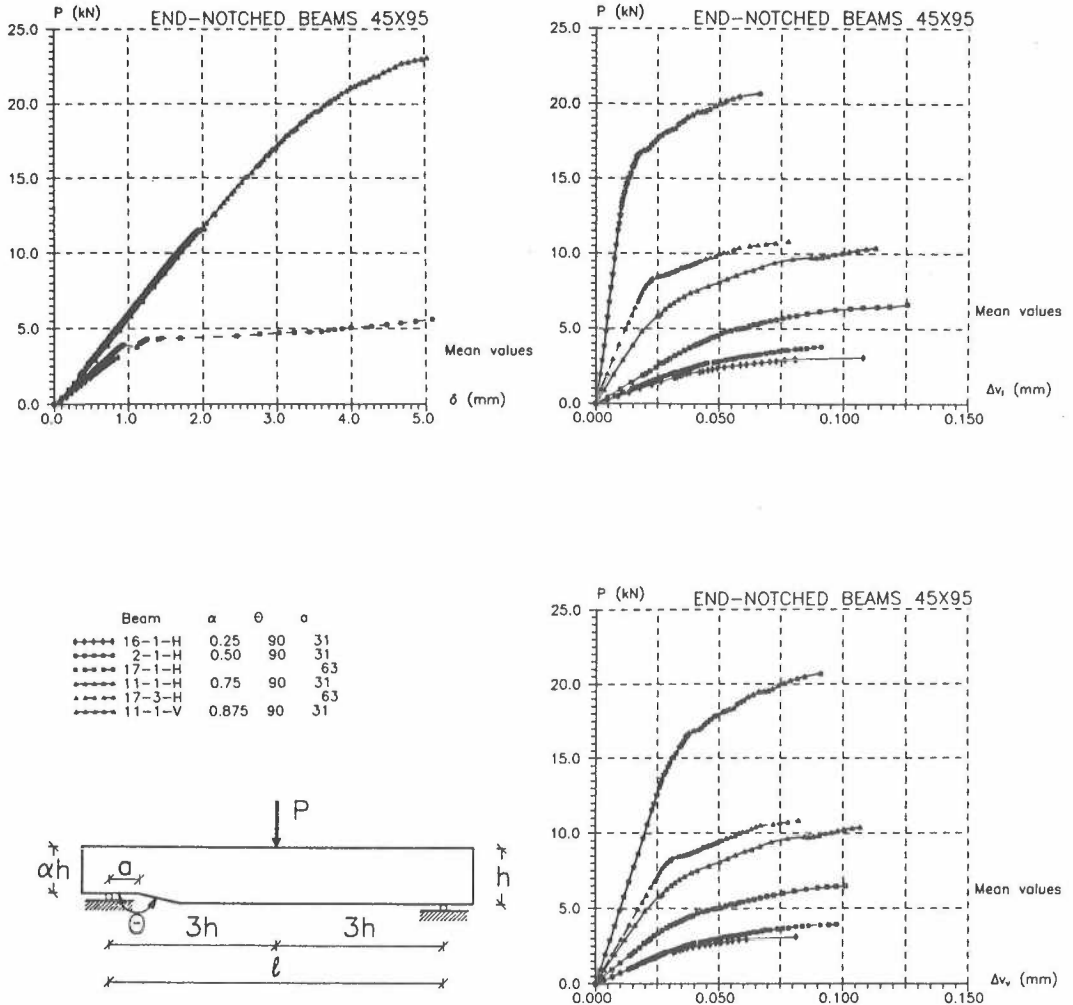
Figure 4.3.1.7   Load—deformation relations for structural timber of cross section 45 x 95 mm. The cut—off angle θ is constant, 90^0 and the relative effective depth α varies.

Beam	α	Θ	a
2-1-H	0.50	90	31
17-1-H			63
8-1-H		135	31
8-2-V		153	31
8-2-H		162	31
17-2-H			63
16-2-V		169	31
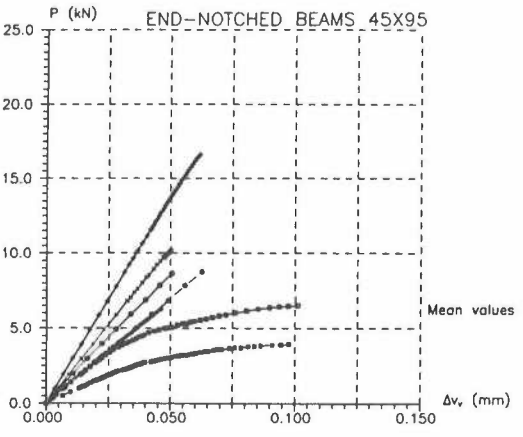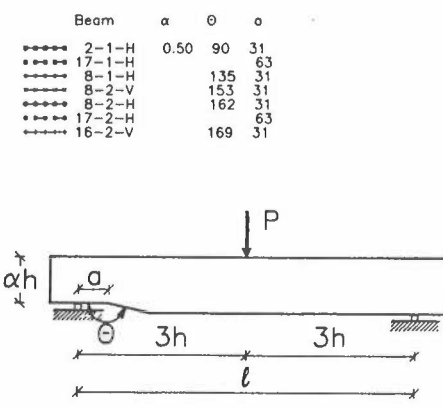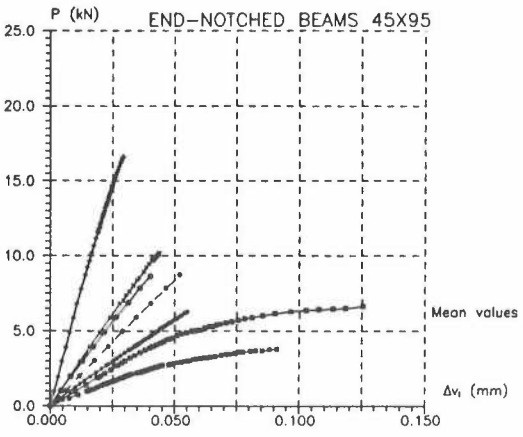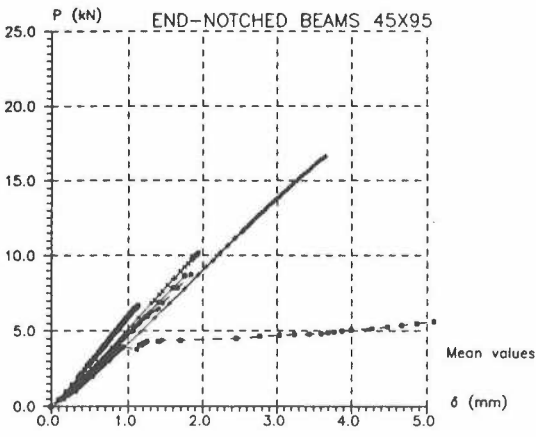
Figure 4.3.1.8 Load–deformation relations for structural timber of cross section 45 x 95 mm. The relative effective depth α is 0.50 and the inclination angle θ varies.

121

Figure 4.3.1.9 Load–elongation relations for structural timber of the cross sections 45 x 95 mm and 45 x 195 mm.

122
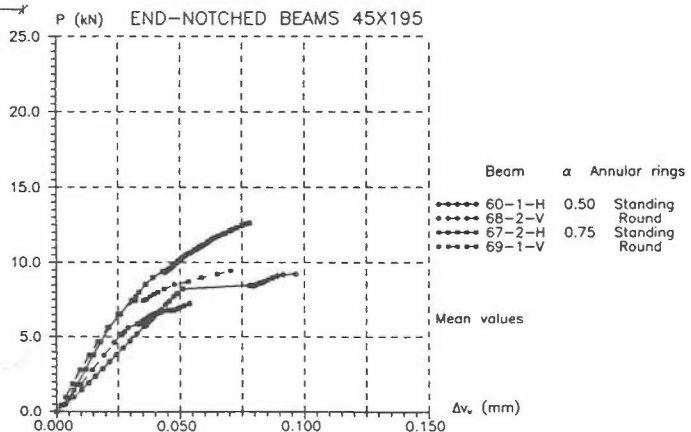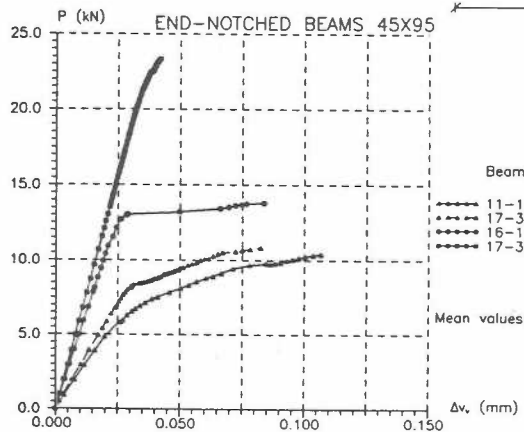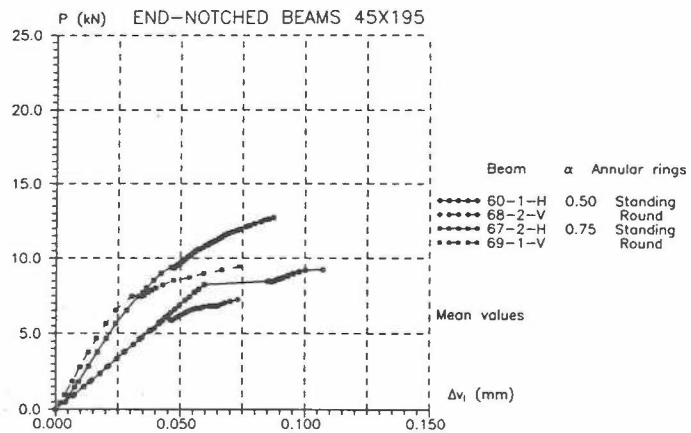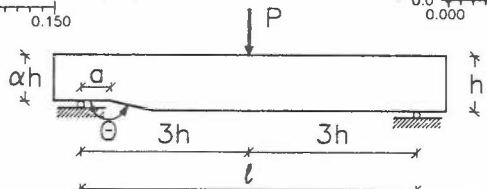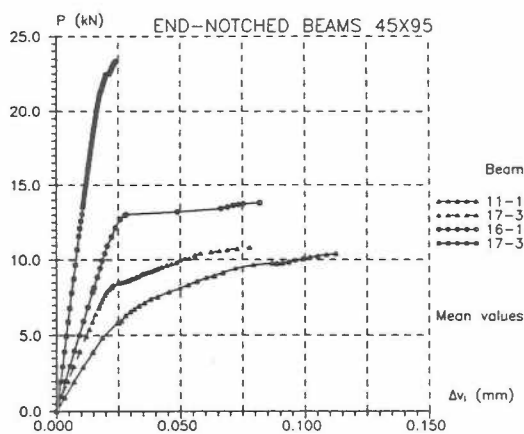
It appears from the two figures, that the load–deformation curves tends to become straight lines when the inclination of the necking becomes flatter. The failure seems to be more brittle for flat neckings.

It is also remarkable that the elongations are so alike for the different geometries of the specimens. In this context it must be remembered that for the flattest neckings it was not possible to position the strain gages as close to the crack tip as for the steeper neckings. So these strain gage measurements become more or less linear because the gages were not positioned directly over the process zone at the crack tip.
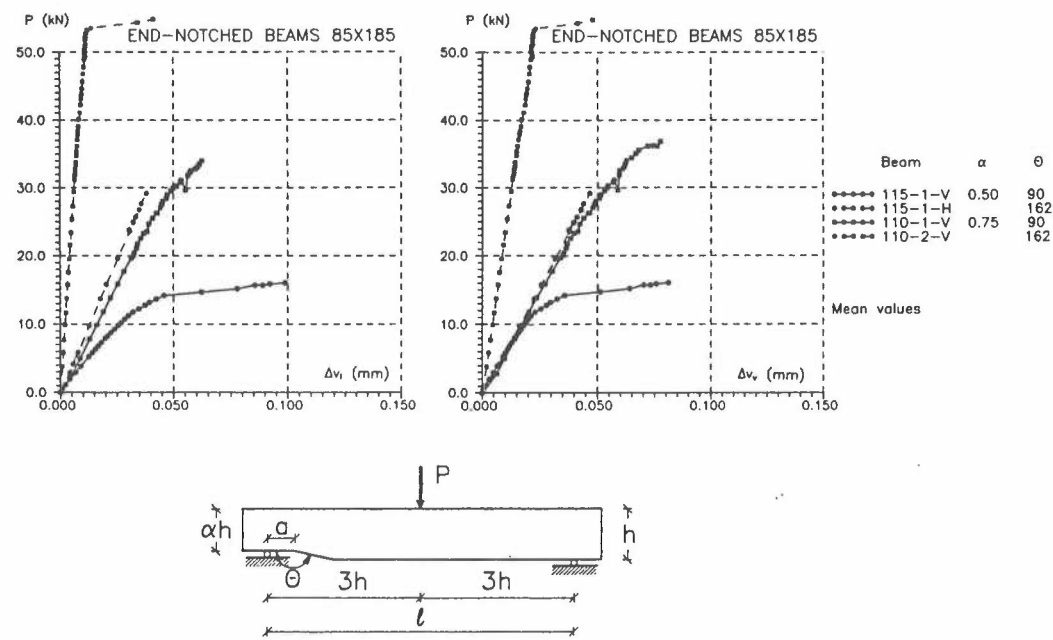
Figure 4.3.1.10   Load–elongation relations for structural timber of the cross section 85 x 185 mm.

Figure 4.3.1.11   Load-deformation relations for glued laminated timber, glulam

Load-elongation relations for glulam of the cross sections 90 x 200 mm and 90 x 300 mm.

124
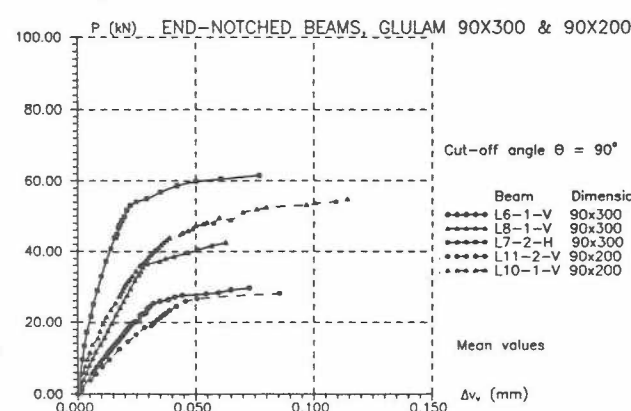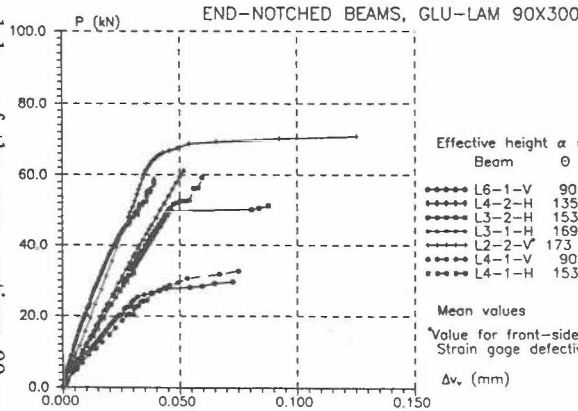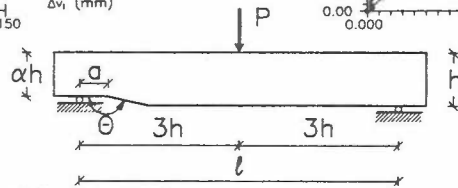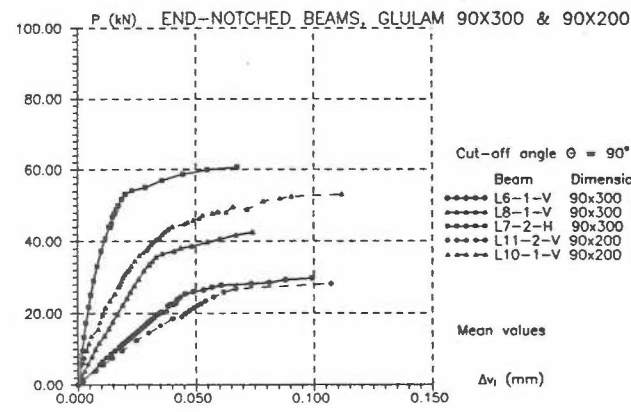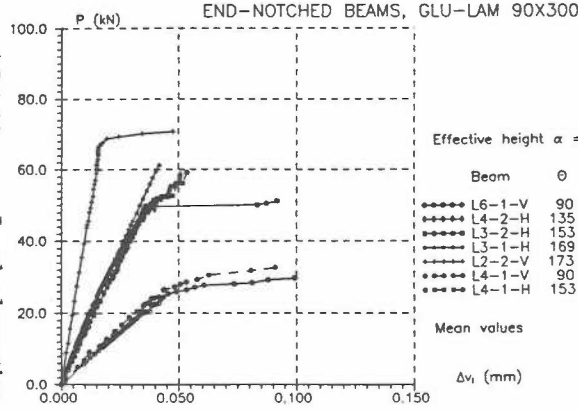
It appears from figure 4.3.1.11 that the same observations can be done for glulam as for structural timber
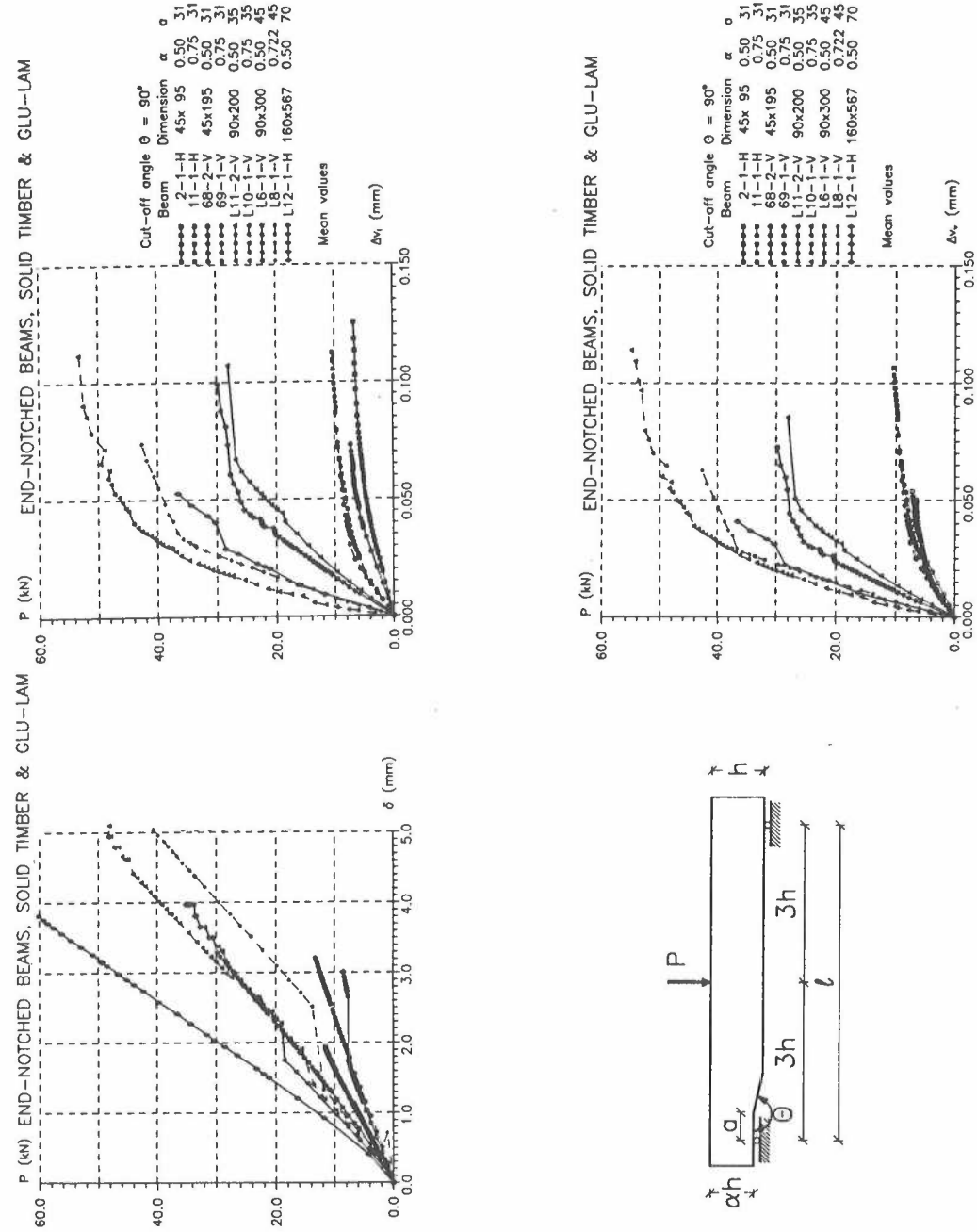
Figure 4.3.1.12   Load–deformation relations for structural timber and glulam.
The cut–off angle θ is constant 90^0, and the relative effective
depth α varies.

125

Figure 4.3.1.13 Load–deformation relations for structural timber and glulam. Relative flat cut–off angles θ 1530–1620 and the relative effective depth α is either 0.50 or 0.75.

126
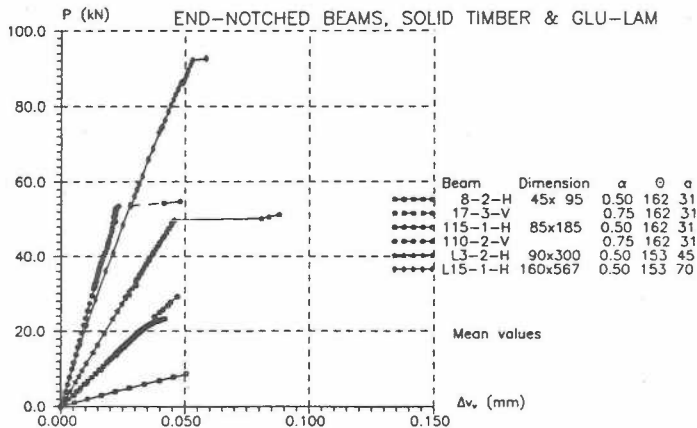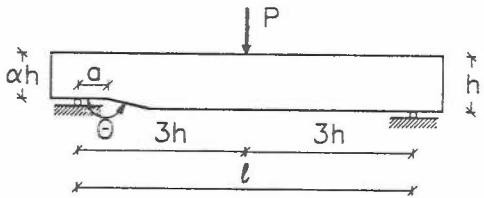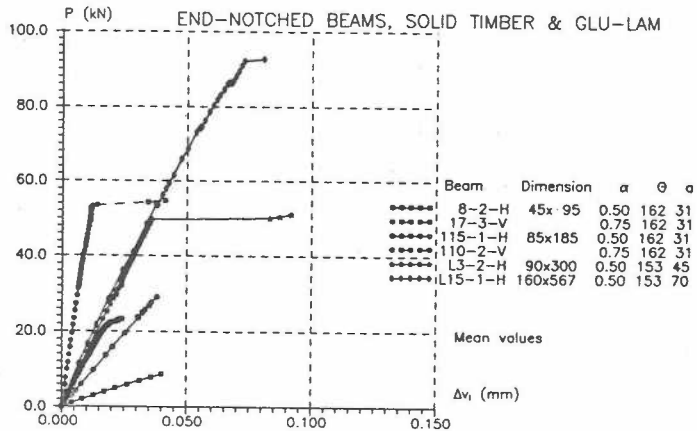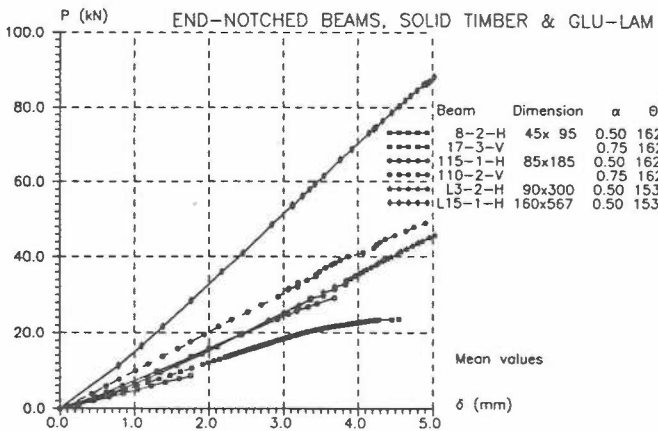
A comparison between the figures 4.3.1.12 and 4.3.1.13 gives that the flat cut–off results in relatively brittle failures. This is observed for all specimens independently of that the wood is structural timber or glulam. The general load–deformation relation depending on the geometry is shown in figure 4.3.1.14:
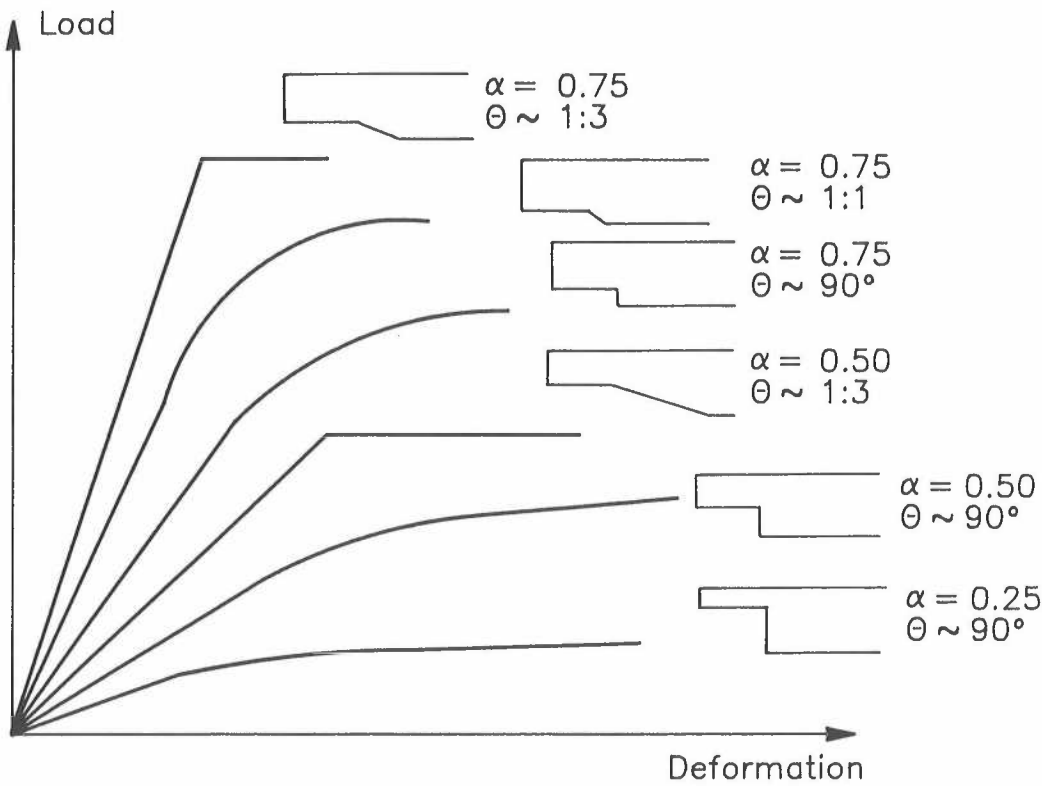
Figure 4.3.1.14 Load–deformation curves in dependency of geometry.

For the perpendicular cut–off notches and those with steep inclination the load–elongation curves indicate that a non–linear process takes place in the vicinity of the notch tip. From visual observations it is known that in some cases a crack became visible at a certain load level and it increased slowly but jumping in size until the catastrophic failure occurred with a rapid crack propagation. Based on table 4.3.3 it can be stated that in those cases where a crack was of a visible size this occurred at load levels from 80% to 100% of the catastrophic failure load.

Comparisons with FEM–analyses

The finite element method is described in section 5.3. The notched beam has been mo-

delled by orthotropic linear elastic elements and some specially developed cracked elements simulating the non–linearity in the process zone.

In the FEM–calculations the relation between the load and the length of the developed crack could be found. Three basic cases could occur as shown in figure 4.3.1.15. The three cases are pre–failure crack propagation, normal crack propagation and post–failure crack propagation.
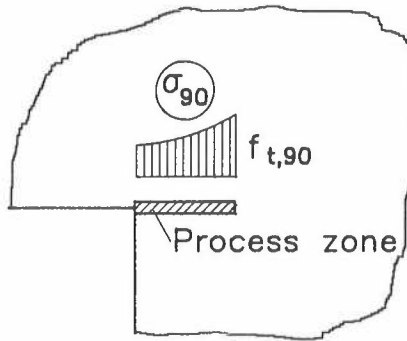
a_{notch} = distance between cracktip and notch
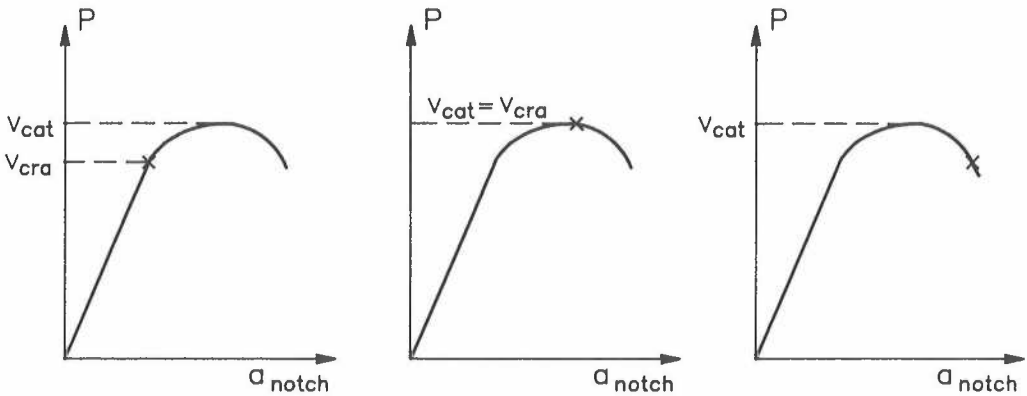
A. **Pre–failure crack propagation**
Crack fully developed at load level V_{cra}. Crack begins to move through beam leaving an open crack. Load can be increased until load level, V_{cra}, the catastrophic load level

B. **Normal crack propagation**
Crack fully developed at catastrophic load level, V_{cra}

C. **Post–failure crack propagation**
Crack fully developed after catastrophic load level, V_{cat}

Figur 4.3.1.15   Three basic cases of failure. Pre–failure crack propagation, normal crack propagation and post–failure crack propagation.

129
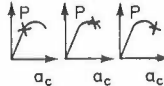
The difference between the three cases is whether the crack is fully developed before, at, or after the catastrophic failure. By a fully developed crack is meant, that the stress at the tip is equal to the material strength and that the stress further out in the crack becomes zero.

Case A, Pre–failure crack propagation corresponds to the ductile failure mode described previously. In this case a crack is visible at a certain load level, V_{cra}, before the catastrophic load–level, V_{cra}.

Case B and C, Normal and Post–failure crack propagation corresponds to the brittle failure mode described previously. In these cases, once the crack is fully developed, the shear capacity is reached and the load cannot be increased.

In table 4.3.6 test observations and FEM–calculations are compared and there is seen to be good agreement, when the above physical explanation is considered.

Table 4.3.6: Comparison between test observations and FEM–calculations

Type	Dimension	$\alpha = h_e/h$	θ (0)	incli (1:x)	eccen. a (mm)	Brittle	Ductile	Measured Load–deformation		FEM Calculation		
	Structural timber											
1	45 x 95	0.25	90	–	31	x	x	x			x	
2		0.50	90	–	31	x		x			x	
3			135	1			x		x			x
4			153	2		(x)	x		x			x
5			162	3			x		x			x
6			169	5			x		x			x
7		0.75	90	–	31	x		x		x		
8			135	1		x			x	x		
9			162	3		x	x		x			x
10		0.875	90	–	31	(x)	x	x		x		
11		0.50	90	–	63	x		x			x	
12			162	3			x		x			x
13		0.75	90	–	63	x	(x)	x		x		
21	45 x 195	0.50	90	–	31	x		x			x	
22		0.75	90	–	31	x		x		x		
31	85 x 185	0.50	90	–	31	x		x		x		
32			162	3			x		x			x
33		0.75	90	–	31	x		x		x		
34			162	3		x	x		x			x
	Glulam											
L1	90 x 300	0.50	90	–	45	x	x	x			x	
L2			135	1		x	x		x			x
L3			153	2			x		x			x
L4			169	5			x		x			
L5			173	8			x		x			
L6		0.722	90	–	45	x		x		x		
L7		0.833	90	–	45	x		x		x		
L8		0.50	90	–	90	x		x			x	
L9			153	2			x		x			x
L10	90 x 200	0.50	90	–	35	x		x			x	
L11		0.75	90	–	35	x		x		x		
L12	160x567	0.50	90	–	70	x		x		x		
L13			153	2			x		x			x

From table 4.3.6 a general picture can be drawn. For beams with perpendicular neckings the failure is often ductile, in some cases pre—failure crack propagation can be observed.

For beams with inclined neckings the failure is often brittle and no crack propagation is observed before failure.

4.4 Analyses of the shear capacity in dependence on the geometry.

By the planning of the experiments with the structural timber members there was aimed at that all timber should have the same moisture content and that the specimens had a density with a rather narrow range. The 6 specimens of a certain type/geometry was selected as 2 with medium density, 2 with a little higher and 2 with a little lower density. The groups of specimens of each type should thus match each other. So within the same cross—sectional dimension the mean values can be compared directly.

By comparing results from tests with specimens of different cross section it must be considered that the timber differs slightly in density and moisture content. Further, the pattern of the annual rings differs.

For the glulam there is also a difference in density between the specimens of a thickness of 90 mm and those of 160 mm.

The mean values for each cross section are stated in table 4.4.1, and those for each specimen type can be found in annex 2.

Table 4.4.1   Mean values of density and moisture content for the wood of different cross—sectional sizes. For the glulam it is the density measured from the whole notched specimen.

Cross section b x h	Density kg/m^3	Moist. content %
Structural timber		
45 x 95	429	12.8
45 x 195	388	14.0
85 x 185	389	15.1
Glulam		
90 x 20 and 90 x 300	442	12.0
160 x 567	418	12.8

In the following there is in some figures shown the dependency between the failure shear stress and partly the necking angle θ, partly the relative effective depth $\alpha =$

132

h_e/h. The failure shear stresses are mean values for each specimen type.
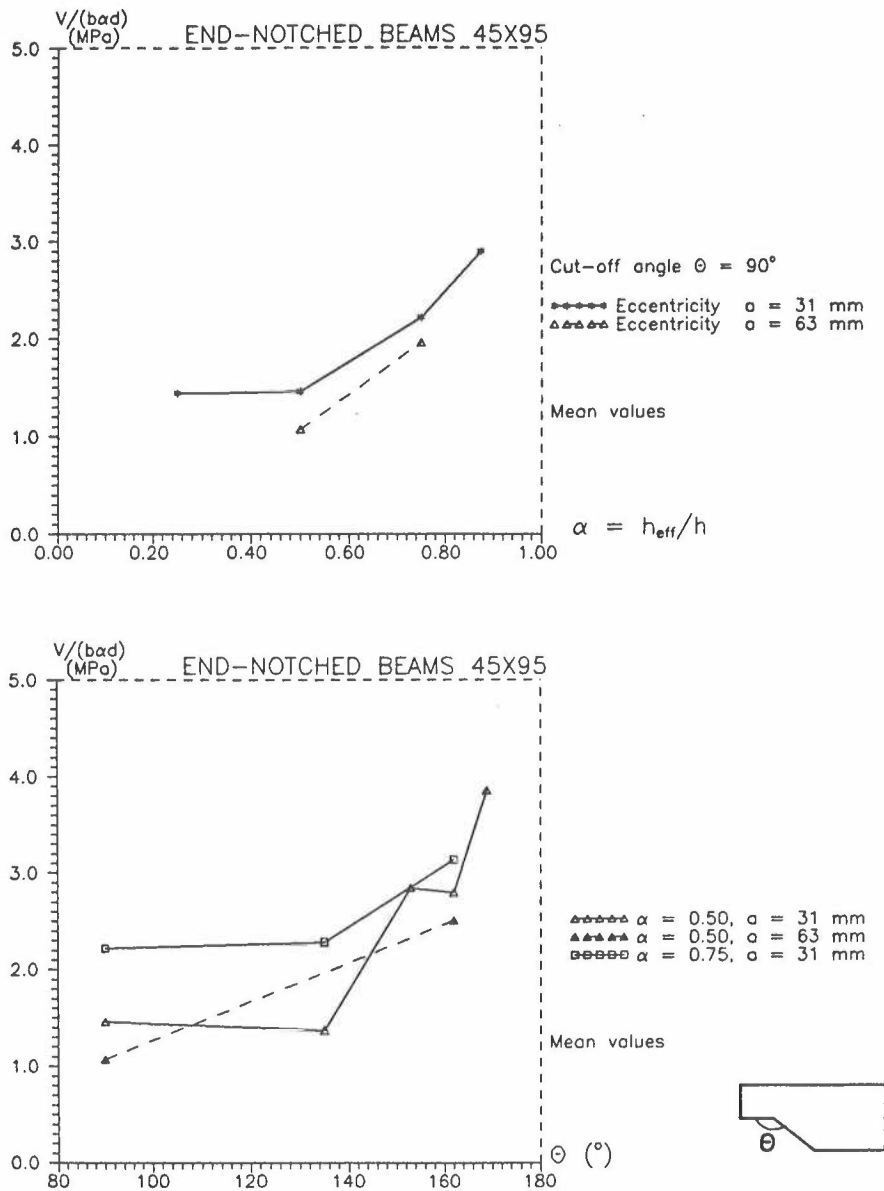
Figure 4.4.1   Mean failure shear stress for structural timber with cross section 45 x
                95 mm. Top: In dependence on the relative effective depth, perpen-
                dicular cut–off. Bottom: in dependence on the necking angle θ, re-
                lative effective depth: 0.50 and 0.75 and for 2 eccentricities a = 31
                and 63 mm.

133
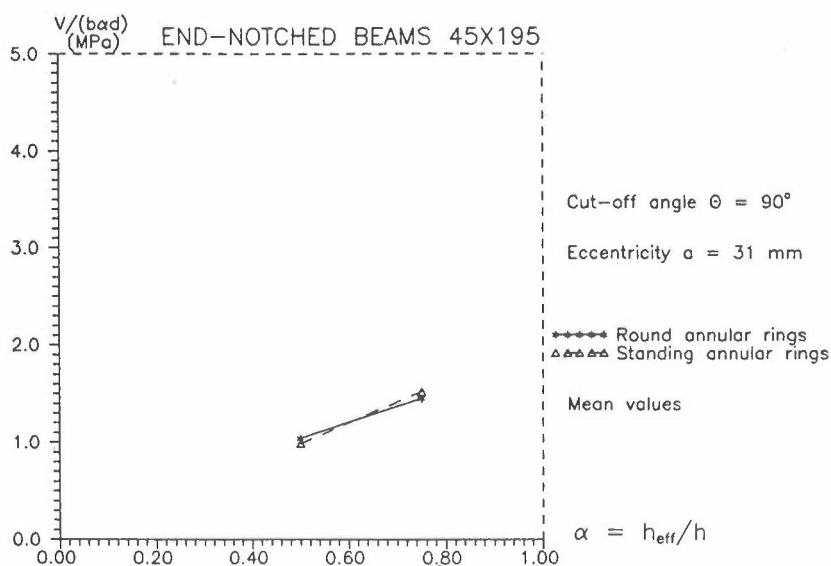
Figure 4.4.2   Mean failure shear stress for structural timber with cross section 45 x 195 mm in dependence on the relative effective depth. Perpendicular cut–off.
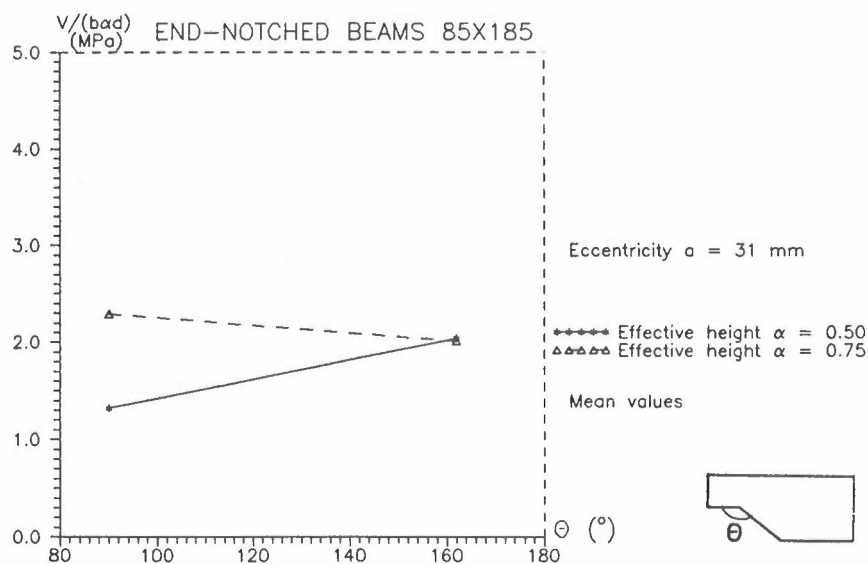
Figure 4.4.3   Mean failure shear stress for structural timber with cross section 85 x 185 mm in dependence on the necking angle θ. Effective depth: 0.50 and 0.75.
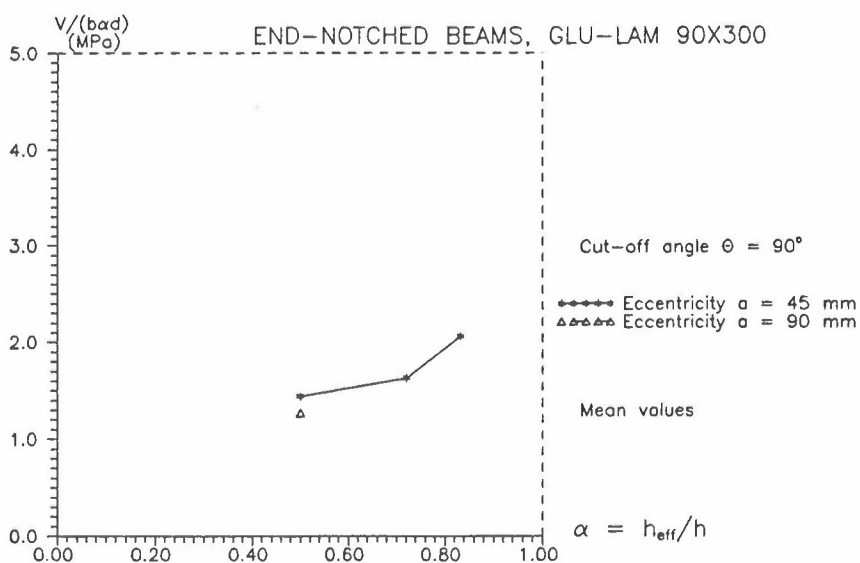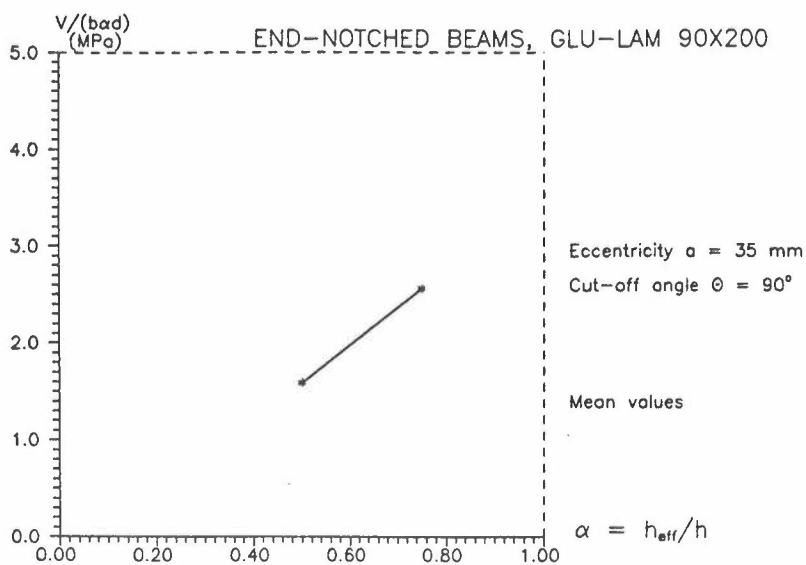
Figure 4.4.4   Mean failure shear stress for glulam with a cross–sectional width b = 90 mm in dependence on the relative effective depth. Perpendicular cut–off.
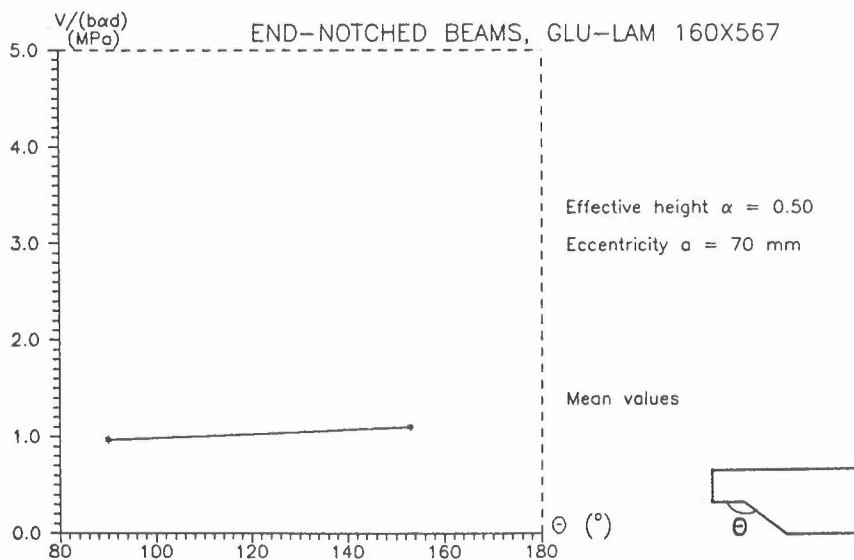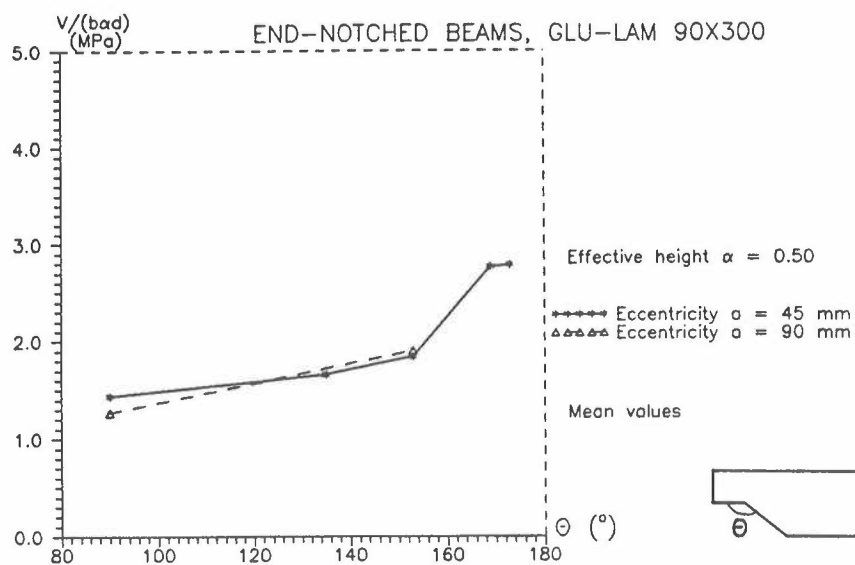
Figure 4.4.5   Mean failure shear stress for glulam in dependence on the necking angle θ. Effective depth $= 0.50$. Top: For a cross section 90 x 300 mm. Bottom: For a cross section 160 x 567 mm.

Relative effective depth α

It appears from the figures that the failure shear stress (shear strength) increases with increasing relative effective depth. This applies to both perpendicular cut—offs and inclined neckings. A phenomenological explication could be that for a large relative effective depth the "separate beam" that will be peeled of at failure is small so it will be flexible and the necessary tensile stresses perpendicular to the grain to curve the "separate beam" are small. So the eventual splitting failure will occur at a larger curvature level, that is at a relatively higher load level.

Inclination of the necking θ

From the figures it can be seen that the flatter inclination of the necking the larger becomes the shear capacity of the notch. This effect is explicable as the previous. But for glulam there is apparently no increase in the shear strength when the inclination is changed from 1:5 to 1:8, see figure 4.4.5.

Sizes b x h

Figure 4.4.1 and figure 4.4.3 show that the shear strength of the so—called half—timber 45 x 95 mm and 85 x 185 mm approximately are equal. It must here be remembered that the timber 45 x 95 mm has a higher density than 85 x 190, see table 4.4.1. But the planks 45 x 195 mm have a lower shear strength.

For the glulam specimens there is a pronounced tendency to that the larger size 160 x 567 mm has a lower shear strength than the smaller sizes. Further, the size 90 x 200 mm tends to have a higher shear strength than the size 90 x 300 mm, see figure 4.4.4.

See also the subsection: Structural timber — Glulam.

Support eccentricity a

When the support eccentricity a from the force application to the notch tip is doubled it results in a minor decrease in the shear strength of the notch. See the figures 4.4.4 and 4.4.5.

Structural timber — Glulam

In figure 4.4.6 there is shown all mean values of the shear strength for variations in partly the relative effective depth, partly the necking inclination. It appears from this that the glulam specimens have a little lower shear strength than those of structural timber.

A comparison between strength properties and fracture energies of partly structural timber, partly glulam shows, that there are no essential differences between these properties. The only exception is the tensile strength perpendicular to grain for glulam of the size 160 x 567 mm, and this has most likely contributed the low shear strength of the glulam.

But anyhow, considering the figure 4.4.6 there appears to be a tendency to that the shear strength decreases with increasing cross section. Specially that the shear strength decreases with increasing slenderness h/b of the cross section. The structural timber dimension 45 x 195 mm is a pronounced example, because the mechanical properties of the wood of this size do not deviate essential from those of the other sizes.

So apparently the differences in shear strength between structural timber and glulam cannot be attributed to the kind of wood, timber or glulam. It seems more controlled by the very size of the cross section, specially the slenderness h/b.
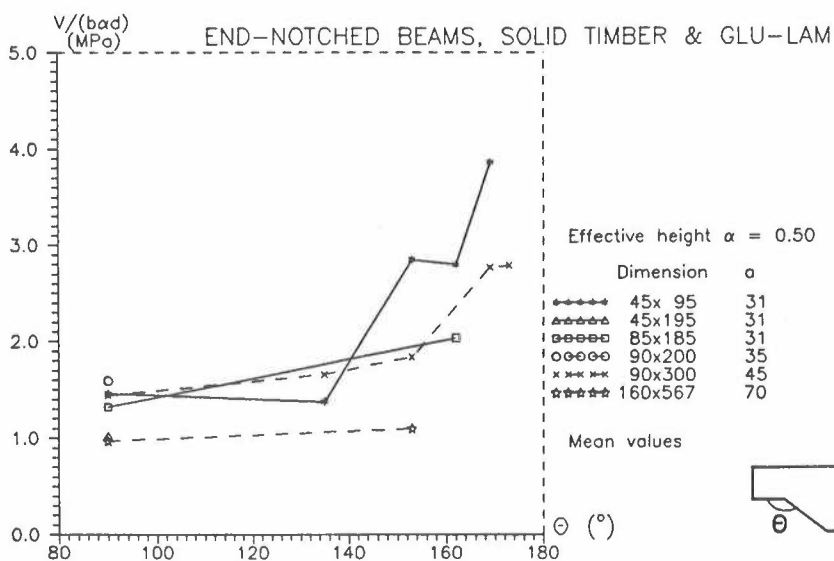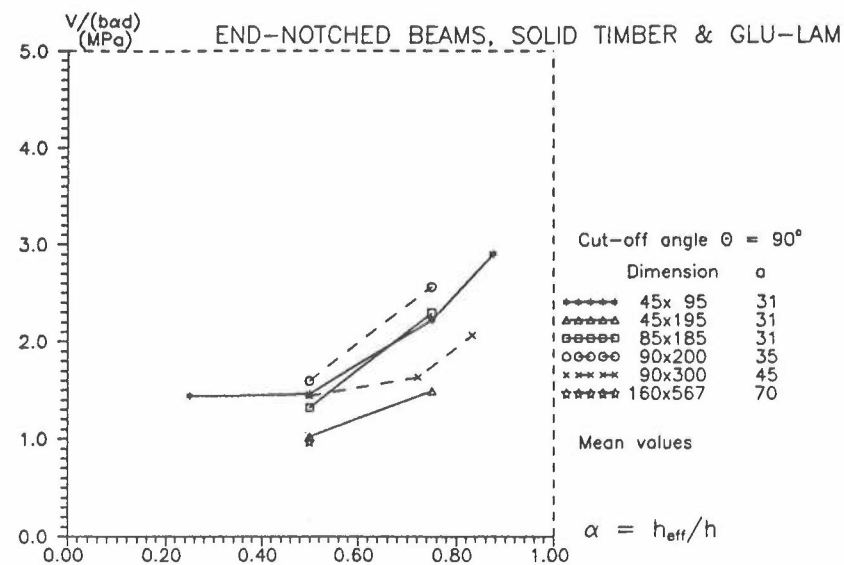
Figure 4.4.6   Mean failure shear stress for structural timber and glulam. Top: In dependence on the relative effective depth, perpendicular cut–off. Bottom: In dependence on the necking inclination, relative effective depth 0.50.

139

4.5 Analysis of the shear capacity in dependence on geometry and material properties.

The analyses in section 4.4 do only consider the geometry of the specimen as variable, other material properties have not been included. So in this section there is given a report of regression analyses in which both material properties and geometry has been included.

4.5.1 Shear capacity in dependence on geometry, wood density and moisture content.

Analyses clearly showed that the moisture content of the wood is not a significant variable in the tests. The reason why is most likely that the range of the moisture content is too narrow.

From the figures in section 4.4 it can be seen that the shear capacity appears to vary non linear with the relative effective height α and the necking angle θ. So regression analyses have been carried out with the following free variables

b,h	cross–sectional dimensions, mm
a	force eccentricity, mm
ω	density, kg/m^3
$\alpha, \alpha^2, \alpha^3$	relative effective depth, h_e/h
i, i^2, i^3	inclination, cot θ

Structural timber

The specimens of structural timber were analyzed and the non–linear regression analyses resulted in coefficients of correlation in the range of 0.80 to 0.88 depending on the combination of free variables and the set of cross–sectional dimensions. It appears from the analyses that incorporation of the non–linear terms of α and i does not result in an essential improvement in the coefficient of correlation.

So from a linear regression analysis the following formula for the estimation of the shear capacity of a notched beam of structural timber has been determined.

$$\tau_{max} = V_{cat}/(bh_e)$$
$$= -0.79 - 0.0121\, a - 0.00471\, h + 0.00552\, \rho + 1.98\, \alpha + 0.344\, i$$

Coef. of correl. = 0.82 (4.5.1.1)

In table 4.5.1.1 there is for the structural timber specimens given the mean value and the predicted value for each specimen type together with the minimum and maximum of the residual = $\tau_{max} - \tau_{predict}$. Further there is stated the mean and standard devia

tion plus minimum and maximum values of the following variable, which can be interpreted as the relative residual since it is the normalized residual of the shear capacity.

$$\tau_{\mathrm{rel,resi}} = \tau_{\mathrm{residual}}/\tau_{\mathrm{max}} = (\tau_{\mathrm{max}} - \tau_{\mathrm{predict}})/\tau_{\mathrm{max}} \qquad (4.5.1.2)$$

Table 4.5.1.1   Structural timber. Measured and predicted shear capacity of the notched cross section together with the minimum and maximum values of the residual. Mean value, standard deviation, minimum and maximum of the relative residual.

b x h Eccen. a,mm	Annual rings	α	incli.	Shear capacity, MPa Mean: Meas.	Estim.	Residual: Min	Max	Relative residual, % Mean	St. dev.	Min	Max
45x95 31	R	0.25	0	1.44	1.32	−0.07	0.35	8	11	−6	23
type 2		0.50	0	1.44	1.75	−0.40	−0.18	−20	6	−28	−12
3			1	1.38	2.05	−1.09	−0.17	−54	33	−101	−9
4			2	2.85	2.41	−0.47	2.00	10	22	−23	44
5			3	2.80	2.73	−0.87	1.22	−4	30	−45	31
6			5	3.86	3.52	−0.04	0.78	9	7	1	18
type 7		0.75	0	2.22	2.30	−0.65	0.43	−7	21	−36	16
8			1	2.29	2.55	−0.54	0.04	−13	13	−32	1
9			3	3.14	3.22	−0.71	0.68	−5	19	−27	17
type 10		0.875	0	2.90	2.53	0.10	0.68	13	7	4	22
type 11 63	R	0.5	0	1.07	1.27	−0.48	0.22	−21	24	−56	17
12			3	2.51	2.38	−0.34	0.66	2	17	−20	21
type 13		0.75	0	1.96	1.89	−0.39	0.47	1	17	−28	21
45x195 31	R	0.5	0	1.04	1.03	−0.22	0.15	1	15	−25	15
type 22R		0.75	0	1.45	1.57	−0.45	0.30	−10	19	−32	18
type 21S	S	0.5	0	0.99	1.03	−0.30	0.11	−6	17	−38	11
22S		0.75	0	1.52	1.56	−0.37	0.17	−4	17	−18	10
85x185 31	R	0.5	0	1.32	1.09	−0.02	0.49	17	14	−2	36
type 32			3	2.04	2.14	−0.71	0.67	−10	29	−49	25
type 33		0.75	0	2.29	1.62	−0.23	1.48	24	25	−15	50
34			3	2.01	2.60	−0.97	0.18	−34	26	−65	6

From table 4.5.1.1 it appears that the regression formula (4.5.1.1) generally can estimate the mean values within an error of approximately ± 20%. But for 2 test results the error is bigger, they are:

Type no.	b x h	a	α	incl.	θ
3	45 x 95	31	0.50	1	135
34	85 x 185	31	0.75	3	162

It has been investigated why these two test types have resulted in such low shear capacities, but no convincing explanation has been found.

It is remarkable that the standard deviation of the relative residual is large, typical between 15% and 30%. From annex 2 it also appears that the standard deviation of τ_{max} is large. So the statistical deviation of the shear capacity is relatively large.

Glulam

For glulam there has been carried out the same regression analysis as for structural timber. For a multiple, linear regression the following relation was found where ρ_{nl} is the density of the notch lamination.

$$\tau_{max} = 1.34 - 0.00187a - 0.00235h - 0.000143\,\rho_{nl} + 1.98\alpha + 0.192\,i$$
Coef. of correl $= 0.86$ (4.5.1.3)

Meanwhile, the 2 variables: force eccentricity a and the density of the notch lamination ρ_{nl} were not significant at a 15% level. By omitting them the following is obtained. It is remarkable that the coefficient of correlation is the same.

$$\tau_{max} = 1.15 - 0.00244\,h + 2.07\,\alpha + 0.194\,i$$
Coef. of correl $= 0.86$ (4.5.1.4)

Further, it has been checked that a substitution in (4.5.1.3) of the density of the notch lamination with the density of the beam does not alter the coefficient of correlation, and this density is not significant.

For the glulam specimens there has also been performed an analysis of the residuals, see table 4.5.1.2.

Table 4.5.1.2   Glulam. Measured and predicted shear capacity of the notched cross section together with the minimum and maximum values of the residual. Mean value, standard deviation, minimum and maximum of the relative residual.

b x h	Eccen. a,mm	α	incli.	Shear capacity, MPa				Relative residual, %			
				Mean:		Residual:		Mean	St.	Min	Max
				Meas.	Estim.	Min	Max			dev.	
90x200	35	0.50	0	1.59	1.69	−0.47	0.17	−9	21	−39	9
type 11		0.75		2.56	2.21	−0.17	0.90	12	15	−8	29
90x300	45	0.50	0	1.44	1.45	−0.15	0.20	−2	10	−12	12
type 2			1	1.66	1.64	−0.34	0.55	−3	24	−26	25
3			2	1.84	1.84	−0.15	0.21	0	8	−9	10
4			5	2.77	2.42	−0.01	1.04	11	14	0	30
5			8	2.79	3.00	−0.36	−0.10	−8	4	−14	−4
type 6		0.722	0	1.63	1.91	−0.66	0.10	−20	24	−52	5
7		0.833		2.06	2.14	−0.51	0.29	−6	19	−31	12
type 8	90	0.50	0	1.27	1.45	−0.35	0.02	−16	18	−32	2
9			2	1.90	1.84	−0.55	0.36	−2	28	−43	17
160x567	70	0.50	0	0.97	0.80	0.05	0.39	16	13	6	33
type 13			2	1.10	1.19	−0.22	0.05	−8	13	−23	4

From table 4.5.1.2 it appears that the simple regression formula based on geometry variables (4.5.1.4) can estimate the mean values with an error of ± 20%.

The standard deviation is large as for structural timber, typical in the range of 10% to 25%.

5. WORKING UP OF TEST RESULTS

This chapter contains some comparisons between measured shear capacities and theoretical estimated capacities. The data have been processed by the statistical analysis system SAS, versions 5.18 and 6.06, see /SAS, 1979/.

Further, there is presented a new method based on Taylor series expansion. With this method the comparison can be carried out considering the measured values of the individual tests. Further, if discrepancies are observed the method enables to suggest the terms in the theoretical formula which should be modified.

5.1 A method to compare test results with theoretical estimations.

5.1.1 General description

The method is based on a comparison between the terms in a Taylor series expansion of the theoretical formula with the terms in a multiple regression analysis. The mathematical description of the method is given in the following.

The comparison between the terms for each variable gives an indication of how well the formula fits the measured results. Further, if discrepancies are observed, then they can indicate where the theory should be modified to fit the measurements better.

The method is applicable to a series of tests where the variation of the variables are limited, so that the error by expanding the theoretical formula in a Taylor series can be disregarded.

The method is recommended instead of other methods based on linearization by certain transformations of the theoretical formula. The disadvantage by transformations is that the statistical analysis typical is carried out on variables in the transformed space. So the least squares method is applied in this space resulting in a minimization of the transformed errors, not the direct errors.

Mathematical description
The theoretical formula is given by (5.1.1.1) and it depends on a number of variables $v_1, v_2, ...v_n$.

$$F_{theo} = F(v_1, v_2, ...v_n) \qquad (5.1.1.1)$$

144

This formula is expanded into (5.1.1.2) in which $\bar{v}_1$ are the values of the variables in the point from which the formula is expanded.

$$F_{ex} = F(\bar{v}_1, \bar{v}_2, ... \bar{v}_n) + \sum_{i=1}^{n} \left[\frac{\partial F}{\partial v_i}(v_i - \bar{v}_i) \right] + error$$

(5.1.1.2)

$$= F((\bar{v}_1, \bar{v}_2, ... \bar{v}_n) - \sum_{i=1}^{n} \left[\frac{\partial F}{\partial v_i} \bar{v}_i \right] + \sum_{i=1}^{n} \left[\frac{\partial F}{\partial v_i} v_i \right] + error$$

It should be noticed that the first two twems are constant in the sense that they only depend on point $(\bar{v}_1, \bar{v}_2, ... \bar{v}_n)$ from which the formula is expanded.

The similarity between (5.1.1.2) and a regression equation is obvious, see formula (5.1.1.3).

$$F_{reg} = Intercept + \sum_{i=1}^{n} [k_i \, v_i] + error$$

(5.1.3)

The Intercept and the parameters k_i are determined by a least squares method.

5.1.2 Application of the method

The method is applied to a theoretical formula proposed in /Gustafsson & Enquist, 1988/. The average shear stress at failure in a notch cut perpendicular to the beam axis is determined from the following expression, which has been derived from linear elastic theory and by assuming zero size of the fracture process zone. A corresponding alternative expression in which non–zero fracture region size is considered is somewhat lengthier and gives a lower shear capacity of small beems.

$$\bar{f}_v = \frac{V_f}{b\,\alpha h} = \frac{\sqrt{G_{f\,t}/h}}{\sqrt{0,6(\alpha - \alpha^2)/G} + \beta\sqrt{6(1/\alpha - \alpha^2)/E}}$$

(5.1.2.1)

where

$\bar{f}_v$		Average shear stress at failure
V_f		Shear force at failure
b		Width
h		Depth

α Relative effective height. $h_e = \alpha h$

β Relative eccentricity a/h

G_{ft} Fracture energy in tension perpendicular to grain

G Shear modulus

E_o E–modulus parallel to grain

The series expansion of formula (5.1.2.1) was carried out from some approximate mean values. These mean values and the results are given in table 5.1.2.1 and table 5.1.2.2 for structural timber and glulam respectively. In both cases only the results from tests with notches cut perpendicular to the beam axis have been considered in this section.

These two tables give also the results of the statistical analyses. One where only variables significant at the 15% level are incorporated, and one with all relevant variables.

Table 5.1.2.1   Structural timber, $\bar{f}_v$ (variables). Comparison between terms in a linear series expansion and a multiple linear regression analysis.

Variab. or terms		15% significant var. Param.	p{f>F}	All relevant var. Param	p{t>T}	Series expansion Param.	expa.point
Constant term	MPa	1.58	0.0016	1.73	0.0028	1.15	
E_0	MPa			$-16.7 \cdot 10^{-3}$	0.48	$28.0 \cdot 10^{-6}$	13,400
E_{90}	MPa	$-1.34 \cdot 10^{-3}$	0.009				
G	MPa	$510 \cdot 10^{-6}$	0.14	$457 \cdot 10^{-6}$	0.23	$739 \cdot 10^{-6}$	767
$f_{t,90,}$ ABK	MPa	$122 \cdot 10^{-3}$	0.05				
G_{ft}	Nmm/mm^2			0.841	0.33	3.28	0.287
h	mm	$-9.5 \cdot 10^{-3}$	0.0001	$-9.89 \cdot 10^{-3}$	0.0001	$-6.28 \cdot 10^{-3}$	150
α		2.43	0.0001	2.46	0.0001	1.07	0.50
β				-1.83	0.0001	-2.27	0.33
Correl. coef.		0.84		0.82			

Table 5.1.2.2 Glulam, $\tilde{f}_v$ (variables). Comparison between terms in a linear series expansion and a multiple linear regression analysis.

Variab. or terms	15% significant var. Param.	p{f>F}	All relevant var. Param	p{t>T}	Series expansion Param.	expa.point
Constant term MPa	0.30	0.52	1.95	0.13	0.53	
$E_{0,beam}$* MPa			$-112 \cdot 10^{-6}$	0.41	$14.9 \cdot 10^{-6}$	13,500
$E_{90,nl}$* MPa	$877 \cdot 10^{-6}$	0.05				
G MPa			$-1.18 \cdot 10^{-3}$	0.18	$788 \cdot 10^{-6}$	741
G_{ft} Nmm/mm²			2.19	0.12	2.58	0.304
h mm	$-1.83 \cdot 10^{-3}$	0.003	$-2.25 \cdot 10^{-3}$	0.003	$-2.28 \cdot 10^{-3}$	350
α	26	0.0001	2.28	0.002	1.10	
β			-0.91	0.54	-2.02	
Correl. coef.	0.85		0.85			

* E–moduli for the beam as a whole and for the notch lamination respectively.

From the two tables it can be seen which variables are significant at the 15% level. All other variables, except the slenderness h/b of the cross section, have not been significant at this level. The cross–sectional slenderness is dealt with later.

Further, from the two tables it can be stated for the properties relevant for formula (5.1.2.1) that the effect is predicted:

	Correct for	Not good for	Wrong for
Fracture energy G_{ft}	Glulam	Struc. timber*	
Depth h	Glulam Struc. timber		
Relative depth α	Glulam Struc. timber		
Relative eccen.	Struc. timber	Glulam*	
Shear modulus G		Struc. timber*	Glulam*
E–modulus E_0			Glulam* Struc. timber*

It should be noticed that the properties, with a correct effect prediction, are all significant variables at the 15% level. The other properties are not significant at this level and they have been marked with * to indicate an uncertain conclusion.

The parameter values in the tables 5.1.2.1 and 5.1.2.2 can be used as guidelines for a modification of the theoretical formula (5.1.2.1). This formula is based on the compliance of the notched beam. Since the total deflection is a sum of a number of deflection

contributions, these can adjusted based on the parameter values given in the two tables.

It can be seen that some of the parameters or factors of the relevant variables have been found significant and of approximately the same value in the regresesion analysis and the series expansion. By approximate equal values is meant that the proportion between the values is less than 2.5. These values are stated in table 5.1.2.3. In this table there is also referred to relevant parameters, that is parameters relevant to the proposed theoretical formula (5.1.2.1).

Table 5.1.2.3   Significant variables in a linear multiple regression $\bar{f}_v(x_1, x_2, ...x_n)$. Classification on conformity of parameter values.

Structural timber			Glulam		
Significant relevant parameters of approximately equal value determined by regression analysis and series expansion:					
h	α	β	G_{ft}	h	α
Relevant parameters of approximately equal value determined by regression analysis and series expansion:					
G			β		
Parameters significant at the 15% level					
E_{90}	G	$f_{t,90,}$ABK h α	$E_{90,nl}$	h	α

From the table it can be seen that almost all relevant parameters are significant in the test with structural timber or glulam. Meanwhile, the two stiffness variables G and E_0 are not significant, but the parameter for G is of approximately the same value in the regression analysis and the series expansion.

The E–modulus E_0 in the direction of grain is neither a significant variable nor is the parameter found by regression equal to that determined by series expansion. Both for structural timber and glulam they are of different sign, meaning that the effect of an increase in the E–modulus theoretically should result in an increase of the shear capacity whereas the regression analyses predict a decrease. For the structural timber the E–modulus has been determined from tests with mean value 13,400 MPa, St.dev 2,100 MPa, max 18,000 MPa and min 8,700 MPa. So the range has been relatively wide. But for the glulam the range was rather narrow, because the E–modulus was estimated

148

based on the density of the whole beam specimen. In general the results indicate a discrepancy between the theoretical description and the measured results of the effect of E_0 on the shear capacity. For the shear modulus G there is also a tendency.

From table 5.1.2.3 it can further be seen that 2 material properties, E–modulus perpendicular to grain E_{90} and the tensile strength $f_{f,90}$ perpendicular to grain, are significant at the 15% level but they are not included in the theoretical formula. But may be they should be incorporated.

Slenderness of cross section

In section 4.4, subsection: Structural timber – Glulam it is pointed out that the shear capacity of the notch decreases with increasing slendernes h/b of the cross section. The reason for this could be that the stress states are different for a narrow and slender cross section and a wide one.

Multiple linear regressions analyses of partly all structural timber specimens, partly all glulam specimens show that in both cases the slenderness is significant at the 0.01% level. So the slenderness is a significant variable in the statistical sense. But it must be remembered that the wood is from different sources, so the significance could be caused by differences in the wood properties which have not been measured. Table 5.1.2.4 gives the variables found to be significant at the 15% level in a multiple linear regression analysis.

Table 5.1.2.4   Significant variables, the values of parameters and $p\{f>F\}$ in a multiple linear regression analysis. Only square notches.

	Intercept MPa	$E_{90,ABK}$ MPa	$f_{t,90,ABK}$ MPa	h mm	1/Slender b/h	α	Coef. of Correl.
Structural timber							
Parameter	−0.19	$623\cdot10^{-6}$	0.145	$3.3\cdot10^{-3}$	2.7	2.4	0.87
$p\{f>F\}$	0.74	0.10	0.02	0.08	0.0001	0.0001	
Glulam							
Parameter	−1.26				3.7	2.7	0.85
$p\{f>F\}$	0.0026				0.0001	0.0001	

It is remarkable to see that with the variables in table 5.1.2.4 a larger or equal coefficients of correlation have been obtained than for the other regression analyses.

Regression analyses of the combined data for structural timber and glulam

Regression analyses similar to those described previously in this section have been carried out on the combined data set consisting of those for structural timber and glulam. The results are given in table 5.1.2.5. In this there is the results of an analyses, where the slenderness intentionally is omitted, so this analysis corresponds to a plane state situation.

Table 5.1.2.5 — Significant variables, the values of parameters and $p\{f>F\}$ for multiple linear regression analyses of the combined data for structural timber and glulam. Only square notches.

	Coef. of Correl.	Interc. MPa	E_0 MPa	G MPa	$f_{t,90,\text{ABK}}$ MPa	G_{ft} N/mm	1/Slender b/h	h mm	α	β
Only Significant variables at the 15% level										
Parameter	0.85	−1.26			0.125		3.45		2.44	−1.06
$p\{f>F\}$		0.0001			0.003		0.0001		0.0001	0.0001
Only significant variables at the 15% level. Slenderness omitted										
Parameter	0.73	−0.11				2.00		−0.00139	2.34	
$p\{f>F\}$		0.69				0.01		0.001	0.0001	
Only relevant variables										
Parameter	0.73	−0.22	20.2	65,5·10⁻⁶		1.98		−0.00171	2.27	−0.42
$p\{t>T\}$		0.63	0.43	0.87		0.015		0.0009	0.0001	0.20

It is a bit strange to see that depending on whether or not the slendernes of the cross section is considered then completely different variables become significant. The only variable, which is common for all three analyses, is the relative effective height α.

Further, it can be observed from table 5.1.2.5 that the slenderness of the cross section is a very significant variable. If it is omitted then the coefficient of correlation drops essentially. So there seems to be an influence which cannot be considered by a plane static model of the notched beam.

As remarked in subsection Structural timber − Glulam of section 4.4, it is apparently possible to obtain an equally high value of the coefficient of correlation for the combined data set as for structural timber and glulam treated separately. In all cases the coefficient of correlation is in the range of 0.82 to 0.87.

5.2 Comparison between predicted and measured values of the average shear stress at failure.

The predicted values of the average shear stress at failure in a notched beam with a

perpendicular cut—off have been computed from formula (5.1.2.1). They have been compared with the measured values by determining the proportion between the predicted and measured shear capacity. So the following variables have been computed:

$$\tau_{pred} = \bar{I}_v \qquad \text{see } (5.1.2.1)$$
$$\tau_{pro} = \tau_{pred}/\tau_{meas}$$
$$\tau_{presi} = \tau_{pro} - 1$$

The mean values, standard deviation, min— and max—values are for each type of test specimen stated in table 5.2.1.

Table 5.2.1   Mean values, standard deviations, min— and max—values for each type of test specimen. $\theta = 90^0$

Ty-pe	b mm	h mm	α	a mm	Mean values τ MPa	τ_{pred} MPa	τ_{pro}	τ_{resi}	Standard dev. τ MPa	τ_{pred} MPa	τ_{pro} %	Min τ_{pro} %	Max τ_{pro} %
Structural timber													
1	45	95	0.25	31	1.44	2.08	1.44	0.44	0.24	0.35	8	135	153
2			0.50		1.46	2.46	1.68	0.68	0.06	0.33	19	141	190
7			0.75		2.22	3.25	1.52	0.52	0.48	0.35	39	106	216
10			0.875		2.90	4.22	1.46	0.46	0.22	0.26	11	124	154
11			0.50	63	1.07	1.72	1.64	0.64	0.19	0.24	38	117	230
13			0.75		1.96	2.39	1.25	0.25	0.39	0.30	25	96	167
21	45R	195	0.50	31	1.04	1.96	1.90	0.90	0.12	0.18	20	172	226
22			0.75		1.45	2.44	1.71	0.71	0.29	0.43	32	142	220
21	45S	195	0.50	31	0.99	1.75	1.80	0.80	0.16	0.17	20	161	210
22			0.75		1.52	2.40	1.59	0.59	0.17	0.33	23	126	176
31	85	185	0.50	31	1.32	2.15	1.64	0.64	0.14	0.32	24	126	193
33			0.75		2.29	1.52	1.19	0.19	0.65	0.29	37	76	163
All							1.57				32	76	230
Glulam													
L10	90	200	0.50	35	1.59	2.17	1.38	0.38	0.27	0.46	28	111	171
L11			0.75		2.56	2.70	1.10	0.10	0.44	0.44	32	66	143
L1	90	300	0.50	45	1.44	1.68	1.17	0.17	0.15	0.26	19	101	142
L6			0.722		1.63	1.92	1.20	0.20	0.31	0.10	18	97	141
L7			0.833		2.06	2.25	1.11	0.11	0.34	0.15	18	88	132
L8			0.50	90	1.27	1.43	1.15	0.15	0.19	0.09	23	88	137
L12	160	567	0.50	70	0.97	1.29	1.35	0.35	0.16	0.02	20	109	153
All							1.21				23	66	171

Based on table 5.2.1 it can be stated that the formula (5.1.2.1) overestimates the average shear stress at failure. In average the values are 57% to large for structural timber and 21% for glulam. But the formula predicts reasonably the variations in the shear stress. So, if the presently measured material properties are used then the formula should be adjusted to give smaller failure values.

5.3 Comparison between measured and FEM—predicted values of the shear capacity.

The notched beams were analyzed as plane structures with a triangular diaphram element with orthotropic material properties and 10 nodes enabling the use of a complete cubic displacement field.

The process zone was modelled by specially developed cracked elements. These elements can model the material non—linearities in the proces zone as proposed by Hillerborg with the introduction of fictitious cracks.

The cracked element was given the linear relation between stress and relative crack displacement as shown in figure 5.3.1. This relation was determined by the material strength f (tensile or shear strength) and the fracture energy G_f (tensile or shear). The maximum relative crack displacement δ_0 , which occurs when the stress becomes zero, was calculated from

$$\delta_0 = 2 \, G_f / f \tag{5.3.1}$$
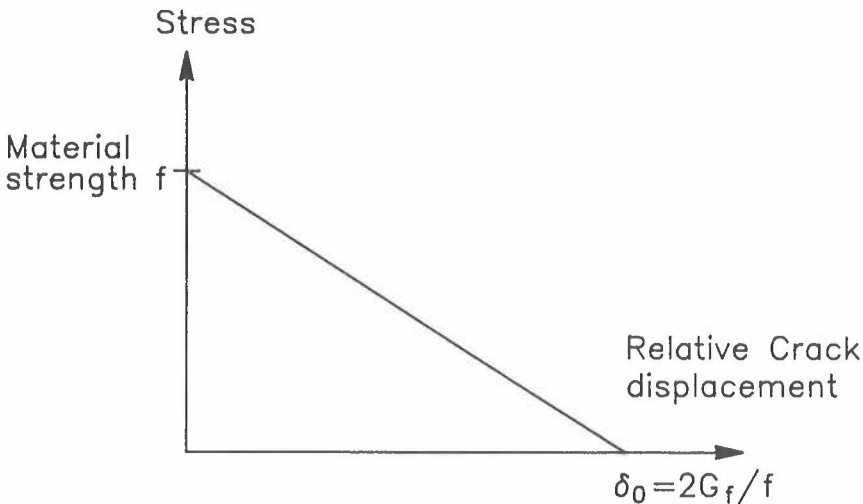
Figure 5.3.1 Relation between stress in crack and relative crack displacement.

The element can model both mode I and mode II displacements. They are modelled separately and they are independent of each other. But it appeared that the best agreement with the measured shear capacities was obtained when the relative shear displacements in the process zone were locked, e.g. they were disregarded. Further description will emerge in a report intended published by ABK.
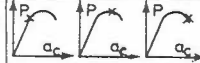
The employed material properties for the analyses are the mean values for each test type. They are listed in table 5.3.1.

The model number employed in the FEM–analysis refers to a certain topology, which will be explained in the above mentioned report.

In the table there is shown 3 curves for the relation between the crack length a_c and the applied force P at the middle of the beam. The "x" on the curves indicates where the process zone has been fully developed. This occurs when the tensile stress perpendicular to the cracked surfaces varies from zero at the outer end of the crack to tensile strength at the inner process zone. So the 3 curves (columns) indicate that the process zone was fully developed before, at or after catastrophic failure. The position of the "x" in the table indicated the situation for each FEM–analysis.

Table 5.3.1 Comparison between applied force F_{cat} at catastrophic failure measured from tests, mean values and finite element analyses.

Type	Sizes b x h mm	Geometry α = h_e/h	θ	incl. 1:x	eccen. a,mm	E_0 GPa	E_{90} MPa	G_{xy} MPa	$f_{t,90}$ MPa	$G_{f,t}$ N/mm	Test P_{cat} kN	Model No.	P_{cat} kN	(1)	(2)	(3)	Full zone P,kN	a_c, mm	Diff. $\frac{\Delta P}{P_{cat}}$ %
1	45x95	0.15	90	–	31	13.6	425	764	3.0	276	3.30	1	3.53	x			3.53	13.8	7
2		0.50	90	–	31	14.0	454	782	4.2	304	6.70	1	8.15	x			8.15	8.7	22
3			135	1		13.2	417	739	3.9	282	6.34	1	8.80		x		8.7	7.5	-39
4			153	2		14.0	380	695	3.6	287	13.10	1	11.95			x	11.5	6.8	9
5			162	3		14.5	413	707	3.5	311	12.86	1	17.95			x	16.9	5.7	40
7		0.75	90	–	31	13.9	278	774	3.0	328	15.30	2	17.5	x			15.95	11.0	14
8			135	1		14.5	310	742	2.8	267	15.78	2	15.5	x			14.64	10.0	-2
9			162	3		13.6	350	792	3.0	301	21.64	2	24.6			x	23.7	6.8	14
10		0.875	90	–	31	14.8	373	796	3.9	295	23.32	2	33.6	x			29.7	6.7	44
11		0.50	90	–	63	13.4	486	792	3.2	296	4.92	1	6.4		x		6.4	14.3	30
12			162	3		13.3	432	822	2.9	313	11.54	1	12.2			x	11.8	8.3	6
13		0.75	90	–	63	14.3	415	877	3.1	298	13.50	2	15.4	x			15.1	12.7	14
21	45x195	0.50	90	–	31	13.5	420	734	2.9	210	8.68	3	10.25	x			10.21	12.0	18
22		0.75	90	–	31	13.5	340	792	2.8	256	20.00	3	25	x			19.82	12.0	25
31	85x185	0.50	90	–	31	12.3	337	802	2.5	301	20.8	3	21.5	x			21.38	20.0	3
32			162	3		12.2	347	842	2.8	292	32.0	3	53.8			x	51.0	8.0	68
33		0.75	90	–	31	11.6	483	702	3.2	296	54.0	3	50	x			42.1	12.3	-7
34			162	3		12.1	483	679	2.8	309	47.4	3	86.5			x	82.9	8.0	82
L1	90x300	0.50	90	–	45	13.9	508	727	3.5	292	38.8	4	31.3	x			31.3	13.5	-19
L2			135	1		13.6	543	728	3.6	311	44.8	4	42.6		x		42.3	11.5	-5
L3			153	2		14.2	558	683	3.8	303	49.6	4	69.5			x	67.3	7.0	40
L6		0.722	90	–	45	13.8	562	727	3.3	275	44.0	4	64	x			52.0	13.5	45
L7		0.833	90	–	45	13.8	557	717	3.6	258	55.6	4	98	x			74.0	9.8	76
L8		0.50	90	–	90	13.8	580	741	4.0	313	34.2	4	32.1		x		32.07	12.2	-6
L9			153	2		14.1	680	733	3.6	314	51.4	4	65.1			x	63.7	9.0	27
L10	90x200	0.50	90	–	35	12.6	670	835	2.9	323	28.6	3	27.6		x		27.6	23.5	-3
L11		0.75	90	–	35	13.9	713	708	3.5	368	46.0	3	67	x			60.0	16.0	46
L12	160x567	0.50	90	–	70	12.9	556	733	1.6	298	88.0	5	77.0	x			76.6	60.0	-13
L13			153	2		13.0	581	733	1.7	306	99.8	5	139.5			x	134.6	37	40

[1] Applied force and crack length (to the tip of the process zone) for a fully developed process zone.

[2] Relative difference between measured and calculated force at catastrophic failure.

154

In the table there are given some definitions. The applied force is that in the middle of the beam, $(= 2V.)$:

P$_{cat}$ Applied force at catastrophic failure. Mean value of the repetitive tests in a series type.

P$_{cat}$ Applied force catastrophic failure. Determined from FEM—analyses.

P   Applied force for a fully developed crack in which the tensile stress perpendicular to grain at the tip of the process zone is equal to the tensile strength perpendicular to the grain and where the stress further out in the crack becomes zero.

a$_c$ Crack length measured from the tip of the process zone for the fully developed crack.

It can be seen from table 5.3.1 that there is a reasonable agreement between the measured and calculated failure forces. There is a certain amount of scatter and in average the FEM—analysis overestimated the capacities with 20%, both for structural timber and for glulam separately.

For the test types 6, L4 and L5 with inclinations of 1:5 and 1:8 it was not possible to determine a process zone by the FEM—analysis. This has been taken as an indication of that the nature of the fracture changes for very flat inclinations. For these it is no longer the notch—effect which controls the failure, instead it could be that the tensile-stresses from bending takes over. The bending stresses have a tensile component perpendicular to the grain so the failure is of the same nature as in cambered beams.

In table 5.3.1 it is also shown whether the process zone determined by the FEM—analysis was fully developed before, at catastrophic failure, or after catastrophic failure. A comparison between the test observations in table 4.3.6 and those in table 5.3.1 shows a reasonable agreement.

The calculated crack lengths in table 5.3.1 show the same trends as those observed, see table 4.3.3. The crack lengths increase with increasing size, they decrease with increasing relative depth α and inclination angle θ.

References

Larsen, H.J. and Riberholt, H. 1972. Forsøg med uklassificeret konstruktions. Rapport R31, Dept. Struc. Eng. Technical University of Denmark.

Gustafsson, P.J. and Enquist, B., 1988. Träbalks hållfasthet vid rätvinklig urtagning. Report TVSM–7042, Div. of Struct. Mech., Lund Inst. of Tech., Sweden.

Timoshenko and Goodier. Theory of Elasticity.

Möhler, K. and Mistler, H.L. 1978. Untersuchungen über den Einfluss von Ausklinkungen in Auftagerbereich von Holzbiegeträgern auf die Tragfestigkeit. Rapport, Lehrstuhl für Ingenieurholzbau und Baukonstruktionen, Karlsruhe Universität.

ISO 3130 Wood–Determination of moisture content for physical and mechanical tests.

Larsen, H.J. and Gustafsson, P.J., 1990. The fracture energy of wood in tension perpendicular to the grain. CIB–W18A/23–19–21.

Wernersson, H.I. 1990. Wood adhesive bonds – fracture softening properties in shear and in tension. Report TVSM–3012, Div. of Struct. Mech., Lund Inst. of Tech., Sweden.

SAS, 1979. SAS users guide.

The following pages contains the individual results for every notched beam.

The following notation has been employed.

OBS	Observation no.
TNR	Test number. If it is larger than 1000 then it has been rejected and substituted with another notched beam.
ID	Identity
B	Width of cross section, mm
H	Depth of cross section, mm
ALFA	Relative effective depth $\alpha = h_e/h$
THETA	θ = Inclination angle of necking, degrees
A	Eccentricity of the support force, distance from notch tip, mm
MOIST	Moisture content, %
DENSI	Density of structural timber beam (dry mass/wet volume), kg/m^3
DENSBEAM	Density of glulam beam (wet mass/wet volume), kg/m^3
DENSNL	Density of notch lamination (wet mass/wet volume), kg/m^3
AR	Pattern of annular rings in structural timber beams. R: Round with pith in the centre. S: Standing (mainly vertical) annular rings
EO	E_0. Modulus of Elasticity parallel to grain, GPa
EONL	$E_{0,nl}$. Modulus of Elasticity parallel to grain of the notch lamination, GPa.
EOBEAM	$E_{0,beam}$. Modulus of Elasticity parallel to grain of the glulam beam. Estimated from the correlation $E_{0,nl}$(density, moist.) MPa.
E90	E_{90}. Modulus of Elasticity in tension perpendicular to grain of wood near the notch tip. Narrow specimen, MPa.
E90NL	$E_{90,NL}$. Modulus of Elasticity in tension perpendicular to grain for notch lamination. Full width specimen, MPa.
E90ABK	E_{90}. Modulus of Elasticity in tension perpendicular to grain in structural timber. Full width specimen, MPa.
G	Shear modulus, MPa.

1

FT90	$f_{t,90}$. Tensile strength perpendicular to grain. For structural timber: Narrow specimen, for glulam: Full width specimen. MPa.
FT90ABK	$f_{t,90}$. Tensile strength perpendicular to grain. Full width specimen. Measured at ABK, MPa.
FV	f_v shear strength, MPa
GFT	$G_{f,t}$. Fracture energy in tension perpendicular to grain, Nm/m^2.
GFV	$G_{f,v}$. Fracture energy in shear, Nm/m^2
PMAX	Max applied force at catastrophic failure, kN.
TAU	$\tau = \frac{1}{2} \cdot PMAX/(bh_e)$. Average shear stress at catastrophic failure, MPa.

Further, for several variables there is linked a variable of the almost same name but added "AK", for example FT90AK. These AK–variables contain only 1 character, which characterizes the stated variable in the following ways:

A: Actual measurement

B: Actual measurement in a neighbouring specimen but for another α–value, that is at a level in the cross section different from that of the notch tip.

E: Estimated.

K: Measured for another α–value. For E_{90} and $f_{t,90}$ a correction has been carried out on the basis of the inclination of annular rings.

N Measurement in a neighbouring specimen.

T Doubtful measurement.

The data are available on diskets. The format of the data is given below, a SAS notation has been employed, see /SAS 1979/.

Structural timber:

```
DATA ALLE;
 INFILE HAKBJ;
 INPUT
  TNR ID Å 5–12 B H ALFA THETA INCLI A MOIST DENSI PMAX 48–54
  AR Å 55–55 #2 EO 1–16 EOAK Å 17–17 E90 18–22 E90AK Å 23–23
  G 24–29 GAK Å 30–30 FT90 31–35 FT90AK Å 36–36 FV 37–41
  FVAK Å 42–42 GFT 43–47 GFTAK Å 48–48 GFV 49–54 GFVAK Å 55–55
  FT90ABK 56–60 FT90ABKA Å 61–61 E90ABK 62–66 E90ABKAK Å 67–67;
 CARDS;
```

Glulam:

```
DATA ALLE;
  INFILE HAKBJL;
  INPUT
    TNR ID Å 5–12 B H ALFA THETA INCLI A DENSNL EONL 46–50
    MOIST 51–55 DENSBEAM #2
    E90NL 5–12 E90NLAK Å 13–13 G 14–19 GAK Å 20–20 FT90 25–29
    FT90AK Å 30–30 FV 31–35 FVAK Å 36–36 GFT 37–44 GPTAK Å 45–45
    GFV 46–51 GFVAK Å 52–52 PMAX 53–60;
  CARDS;
```

STRUCTURAL TIMBER

```
1                          The SAS System                          1
                                    15:41 Monday, October 7, 1991
```

```
                          T  I     M  D                              E
                      A   H  N     O  E    P           E          E  9
 O    T               L   E  C     I  N    M          0       E   9  0
 B    N   I           F   T  L     S  S    A  A   E   A   9    0  A
 S    R   D   B   H   A   A  I  A  T  I    X  R   0   K   0    A  K

 1    1 5-2-V  45 95 0.25  90 0 31 12.9 453  3.1 R 15.4 A 157.000 A
 2    2 23-1-V 45 95 0.25  90 0 31 11.6 438  2.8 R 15.0 A 346.000 A
 3    3 11-2-V 45 95 0.25  90 0 31 13.1 427  2.5 R 12.5   197.000 A
 4    4 4-2-H  45 95 0.25  90 0 31 13.5 481  4.0 R 15.2   229.618 E
 5    5 16-1-H 45 95 0.25  90 0 31 12.8 410  3.2 R 11.7 A 151.000 A
 6    6 22-2-V 45 95 0.25  90 0 31 12.9 435  2.9 R 11.9   256.000 A
 7    7 20-1-V 45 95 0.50  90 0 31 13.6 438  6.0 R 14.4   353.000 A
 8    8 2-1 H  45 95 0.50  90 0 31 13.0 470  6.7 R 15.0 A 248.000 A
 9    9 3-1-V  45 95 0.50  90 0 31 12.2 439  6.3 R 14.7   293.000 A
10   10 12-1-V 45 95 0.50  90 0 31 12.7 425  6.3 R 14.8   371.000 A
11   11 1-1-V  45 95 0.50  90 0 31 12.6 403  6.1 R 11.8   423.000 A
12   12 9-2-H  45 95 0.50  90 0 31 13.1 409  6.1 R 13.3   180.000 A
13 1012 8-1-V  45 95 0.50  90 0 31 13.0 400  9.0 R 11.2   148.000 A
14   13 20-1-H 45 95 0.50 135 1 31 13.2 443  4.6 R 14.4 A 353.000 A
15   14 30-1-H 45 95 0.50 135 1 31 12.9 432  5.4 R 12.2 A 188.000 A
16   15 3-1-H  45 95 0.50 135 1 31 12.4 433  5.9 R 14.7 A 293.000 A
```

```
                              F     E
                        F     T     9
                   F    T     9  E  0
                   T    9     0  9  A
          F        9    0  A  A  0  B
 O    G  T         0    V  G  T  G  V   A  B  A  K   T       B
 B       A  9   A  V    A  F  A  F  A   B  K  B  A   A       E
 S    G  K  0  K  V     K  T  K  T  K   K  A  K  K   U       T

 1  872.00 N 3.9 A  9.1000 A 246 A 1150 A 2.94 A 493 A 1.45029 0.32632
 2  492.36 E 3.0 B  7.3000 B 235 B  850 B 2.51 A 381 A 1.30994 0.32632
 3  653.00 N 3.5 A  8.0000 A 224 B 1660 B 3.13 E 326 E 1.16959 0.32632
 4 1003.62 E 3.6 A 11.8000 A 388 A 1250 A 3.53 A 443 A 1.87135 0.32632
 5  755.00 N 3.3 B  8.3390 E 282 B  999 E 2.63 A 371 A 1.49708 0.32632
 6  809.10 E 4.5 A  9.4000 A 283 A  943 A 3.33 A 536 A 1.35673 0.32632
 7  984.36 E 2.5 A  8.0000 A 287 A  814 A 3.91 A 394 E 1.40351 0.32632
 8  869.40 E 3.7 A  8.3000 A 399 A  693 A 3.56 A 373 E 1.56725 0.32632
 9  640.98 E 3.5 A 10.6000 A 236 A 1013 A 4.58 A 394 A 1.47368 0.32632
10  663.00 N 3.0 A  8.1000 A 362 A 1056 A 3.99 A 586 A 1.47368 0.32632
11  702.66 E 3.8 A  9.1000 A 276 A 1189 A 5.09 A 571 A 1.42690 0.32632
12  831.78 E 3.3 A  8.5000 A 261 A  789 A 3.93 A 406 E 1.42690 0.32632
13  765.00 A 3.1 A  6.1000 A 342 A 1114 A 2.35 A 405 E 2.10526 0.32632
14  891.06 E 2.5 A  8.0000 A 287 A  814 A 3.91 A 396 E 1.07602 0.32632
15  704.00 N 3.4 A  8.3000 A 222 A  896 A 2.93 A 384 A 1.26316 0.32632
16  684.06 E 3.5 A 10.6000 A 236 A 1013 A 4.58 A 394 E 1.38012 0.32632
```

```
1                          The SAS System                          2
```

STRUCTURAL TIMBER

15:41 Monday, October 7, 1991

```
                              T  I     M  D
                           A  H  N     O  E  P           E                  E
   O      T                L  E  C     I  N  M     E     9                  9   0
   B      N      I         F  T  L     S  S  A  A  E  A  9        E          0   A
   S      R      D    B  H A  A  I  A  T  I  X  R  O  K  0        O      A   K

   17     16 12-2-V 45 95 0.500 135 1 31 12.6 424  8.1 R 13.0 A 335.000 A
   18     17 1-1-H  45 95 0.500 135 1 31 12.7 402  4.9 R 11.8 A 423.000 A
   19     18 8-1-H  45 95 0.500 135 1 31 12.8 397  6.5 R 12.8   148.000 A
   20     19 20-2-V 45 95 0.500 153 2 31 12.2 437  8.6 R 16.8 A 286.886 E
   21     20 30-1-V 45 95 0.500 153 2 31 12.9 453 19.5 R 13.0   188.000 A
   22     21 3-2-V  45 95 0.500 153 2 31 12.3 427 12.9 R 14.3 A 248.000 A
   23     22 12-2-H 45 95 0.500 153 2 31 12.4 431 11.8 R 13.0   335.000 A
   24     23 1-2-V  45 95 0.500 153 2 31 12.8 397 10.1 R 13.0 A 487.000 A
   25     24 8-2-V  45 95 0.500 153 2 31 12.8 399 10.2 R 14.1 A 139.000 A
   26     25 20-3-H 45 95 0.500 162 3 31 12.3 435  8.3 R 17.8 A 278.830 E
   27     26 30-2-V 45 95 0.500 162 3 31 12.5 438 14.7 R 13.9 A 223.000 A
   28     27 3-2-H  45 95 0.500 162 3 31 12.5 419 10.3 R 14.3   248.000 A
   29     28 12-1-H 45 95 0.500 162 3 31 12.3 420 16.9 R 14.8 A 371.000 A
   30     29 1-2-H  45 95 0.500 162 3 31 12.8 405 13.1 R 13.0   487.000 A
   31     30 8-2-H  45 95 0.500 162 3 31 13.0 401  8.6 R 13.3   139.000 A
   32     31 5-1-V  45 95 0.500 169 5 31 13.3 466 17.6 R 15.2 A 203.000 A
```

```
                              F  E
                              F  T  9
                              T  9  0  E
                        F     9  0  9  A
           F     F      9  E  9  A  0
   O    G  T  F  V  G   F  V  A  B  A          B
   B    A  9  A  A  F   A  F  B  K  B   T      E
   S    G  K  K  K  T   K  V  K  A  K   A      T

   17 663.00 A 3.3 A  9.9000 A 331 A  904 A 4.23 A 351 A 1.89474 0.32632
   18 726.24 E 3.8 A  9.1000 A 276 A 1189 A 5.09 A 571 A 1.14620 0.32632
   19 765.00 N 3.1 A  6.1000 A 342 A 1114 A 2.45 A 405 E 1.52047 0.32632
   20 638.94 E 2.9 A  6.9000 A 275 A  653 A 3.59 E 393 E 2.01170 0.32632
   21 704.00 N 3.4 A  8.3000 A 222 A  896 A 2.93 A 384 A 4.56140 0.32632
   22 653.34 E 3.1 A 12.2000 A 266 A 1377 A 3.69 A 313 A 3.01754 0.32632
   23 663.00 N 3.3 A  9.9000 A 331 A  904 A 4.23 A 351 A 2.76023 0.32632
   24 745.74 E 3.1 A  8.3000 A 268 A  686 A 3.34 A 560 A 2.36257 0.32632
   25 765.00 N 3.1 A  7.3000 A 362 A  802 A 3.87 A 276 A 2.38596 0.32632
   26 661.50 E 3.0 A  7.5000 A 297 A 1032 A 2.80 A 348 A 1.94152 0.32632
   27 704.00 A 3.9 A  8.3000 A 308 A  811 A 3.60 E 393 E 3.43860 0.32632
   28 694.38 E 3.1 A 12.2000 A 266 A 1377 A 3.69 A 313 A 2.40936 0.32632
   29 663.00 N 3.0 A  8.1000 A 362 A 1056 A 3.99 A 586 A 3.95322 0.32632
   30 753.90 E 3.1 A  8.3000 A 268 A  686 A 3.34 A 560 A 3.06433 0.32632
   31 765.00 N 3.1 A  7.3000 A 362 A  802 A 3.87 A 276 A 2.01170 0.32632
   32 872.00 A 3.2 A  9.9000 A 426 A  999 E 2.74 A 379 A 4.11696 0.32632
```

1   The SAS System   3

15:41 Monday, October 7, 1991

STRUCTURAL TIMBER

```
                              T  I        M  D                        E
                           A  H  N        O  E  P           E         9
      O    T               L  E  C        I  N  M        O  E         0
      B    N   I      B  H  F  T  L        S  S  A  A  E  A  9         A
      S    R   D            A  A  I  A  T  I  X  R  O  K  O  K

      33    32 23-1-H 45 95 0.500 169 5 31 11.8 432 14.7 R 15.0 A 346.000 A
      34    33 11-2-H 45 95 0.500 169 5 31 12.5 447 16.2 R 12.7   197.000 A
      35    34 4-2-V  45 95 0.500 169 5 31 13.0 432 18.2 R 15.2 A 229.896 E
      36    35 16-2-V 45 95 0.500 169 5 31 12.8 420 16.6 R 11.7 A 223.000 A
      37    36 22-1-H 45 95 0.500 169 5 31 13.0 434 15.8 R 12.3 A 239.000 A
      38    37 5-1-H  45 95 0.750  90 0 31 13.3 466 11.5 R 14.1 A 203.000 B
      39    38 10-1-V 45 95 0.750  90 0 31 12.8 480 18.8 R 15.2 A 285.000 B
      40    39 11-1-H 45 95 0.750  90 0 31 13.2 431 11.6 R 13.9 A 177.000 A
      41    40 4-1-H  45 95 0.750  90 0 31 12.7 420 12.9 R 15.2 A 282.000 A
      42    41 13-2-V 45 95 0.750  90 0 31 12.4 402 13.3 R 12.2 A 187.000 B
      43    42 22-1-V 45 95 0.750  90 0 31 13.1 436 17.4 R 12.7 B 239.000 B
      44    43 20-2-H 45 95 0.750 135 1 31 13.3 440 15.3 R 16.8   215.220 E
      45  1043 15-1-V 45 95 0.750 135 1 31 13.7 464 24.3 R 16.7   108.000
      46    44 23-2-V 45 95 0.750 135 1 31 10.8 445 17.1 R 15.7 A 386.110 E
      47    45 17-1-V 45 95 0.750 135 1 31 13.4 420 16.5 R 13.5   276.000 B
      48    46 10-2-V 45 95 0.750 135 1 31 13.5 468 14.8 R 16.4   236.000 B
```

```
                                                F    E
                                           F    T    9
                                      F    T    9    0
                          F               T    9    0    9    A
               G    T     0         G     G    9    0    9    A           B
      O        T    9     A    F    V   G T   G V  A    B    A    K    T  E
      B        A    9     A    F    A   F    A F   B    K    B    A  T  T
      S    G   K    O     K    V    K T  A K  V K  K    A    K    K  U  A

      33  535.44 E 3.0 A  7.3000 A 235 A  850 A 2.51 A 338 K 3.43860 0.32632
      34  653.00 A 3.5 A  8.0000 A 224 A  999 E 3.67 E 399 E 3.78947 0.32632
      35  830.64 E 3.6 B 11.8000 B 388 B 1250 B 3.53 A 344 A 4.25731 0.32632
      36  755.00 N 2.6 A  7.1000 A 293 A  999 E 3.99 A 320 A 3.88304 0.32632
      37  832.68 E 3.9 A  8.2000 A 321 A  818 A 4.08 A 286 A 3.69591 0.32632
      38  872.00 N 3.2 B  9.9000 B 426 B  999 E 2.80 K 365 K 1.79337 0.32632
      39  830.40 E 2.1 B 10.0120 E 274 B  999 E 3.64 A 271 A 2.93177 0.32632
      40  653.00 N 3.4 E  8.2000 A 291 A 1235 A 2.33 A 184 A 1.80897 0.32632
      41  744.60 E 3.8 A  8.6000 A 342 A  933 A 3.14 A 238 A 2.01170 0.32632
      42  683.00 N 4.2 B  9.2000 B 314 B  890 B 2.31 A 297 A 2.07407 0.32632
      43  859.32 E 3.9 B  8.2000 B 321 B  818 B 3.90 K 310 K 2.71345 0.32632
      44  912.60 E 2.9 B  6.9000 B 275 A  653 A 2.80 E 346 E 2.38596 0.32632
      45 1102.00 N 2.9 A 10.4000 A 249 A  999 E 3.27 E 396 E 3.78947 0.32632
      46  302.70 E 3.1 A  9.4000 A 291 A  978 A 3.50 A 196 A 2.66667 0.32632
      47  808.00 N 4.5 A  7.6000 B 232 A  999 E 2.91 E 374 E 2.57310 0.32632
      48  990.36 E 3.3 B  8.6000 B 300 A  999 E 3.24 A 259 A 2.30799 0.32632
```

STRUCTURAL TIMBER

OBS	TNR	ID	B	H	ALFA	THETA	INCLI	A	MOIST	DENSI	PMAX	AR	EO
49	1046	14-1-V	45	95	0.750	135	1	31	13.0	441	16.0	R	13.7
50	47	16-1-V	45	95	0.750	135	1	31	12.5	412	13.8	R	12.7
51	48	42-1-H	45	95	0.750	135	1	31	12.7	361	10.7	R	11.6
52	49	15-1-H	45	95	0.750	162	3	31	13.2	453	21.4	R	16.7
53	50	23-2-H	45	95	0.750	162	3	31	11.8	434	16.6	R	15.7
54	51	17-3-V	45	95	0.750	162	3	31	12.6	428	23.5	R	13.5
55	52	14-2-V	45	95	0.750	162	3	31	13.1	429	16.6	R	13.3
56	53	16-2-H	45	95	0.750	162	3	31	13.1	419	25.0	R	11.1
57	54	42-3-H	45	95	0.750	162	3	31	12.8	354	17.7	R	11.1
58	55	5-2-H	45	95	0.875	90	0	31	13.0	435	19.6	R	15.7
59	56	10-1-H	45	95	0.875	90	0	31	13.2	476	21.8	R	15.6
60	57	11-1-V	45	95	0.875	90	0	31	13.1	424	23.5	R	14.3
61	58	4-1-V	45	95	0.875	90	0	31	12.6	425	21.5	R	14.7
62	59	13-1-V	45	95	0.875	90	0	31	12.3	395	20.2	R	12.2

OBS	EOAK	E90	E90AK	G	GAK	FT90	FT90AK	FV	FVAK	GFT
49		139.000	A	839.82	E	3.20000	A	8.9000	A	224.000
50		151.000	A	755.00	N	3.30000	A	8.3868	E	282.000
51	A	122.000	A	684.42	E	2.50000	A	8.0000	A	221.000
52	A	108.000	A	1102.00	N	2.90000	A	10.4000	A	249.000
53		311.652	E	537.48	E	3.10000	A	9.4000	A	291.000
54	A	137.000	A	806.00	N	3.60000	A	8.7692	E	311.000
55	A	241.000	B	852.18	E	3.90000	B	9.9000	B	379.000
56	A	223.000	B	755.00	A	2.60000	B	7.1000	B	293.000
57		145.000	B	701.88	E	2.90000	B	6.7000	B	280.000
58		157.000	B	872.00	N	3.90000	B	9.1000	B	246.000
59		285.000	A	924.72	E	2.10000	B	9.9164	E	274.000
60		177.000	B	653.00	N	3.40000	E	8.2000	B	291.000
61	A	282.000	B	725.10	E	3.80000	A	8.6000	B	342.000
62		281.000	B	685.00	N	3.40000	B	9.5000	B	317.000

OBS	GFTAK	GFV	GFVAK	FT90ABK	FT90ABKA	E90ABK	E90ABKAK	TAU	BETA
49	A	794.00	A	2.08	A	266	A	2.49513	0.32632
50	A	999.00	E	2.40	K	373	K	2.15205	0.32632
51	A	1480.00	A	2.11	A	309	A	1.66862	0.32632
52	A	1222.00	A	3.27	E	396	E	3.33723	0.32632
53	A	978.00	A	3.50	A	196	A	2.58869	0.32632
54	A	999.00	E	2.74	A	340	A	3.66472	0.32632
55	B	999.00	E	2.42	A	607	A	2.58869	0.32632
56	B	830.00	A	4.00	K	311	K	3.89864	0.32632
57	B	841.00	B	2.21	A	247	A	2.76023	0.32632
58	B	1150.00	B	2.94	B	517	K	2.61988	0.32632
59	B	999.00	E	4.80	K	290	K	2.91395	0.32632
60	B	1235.00	B	2.50	K	200	K	3.14119	0.32632
61	B	933.00	B	4.10	K	254	K	2.87385	0.32632
62	B	736.00	B	4.40	K	710	K	2.70008	0.32632

1   The SAS System   5

OBS	TNR	ID	B	H	ALFA	THETA	INCLI	A	MOIST	DENSI	PMAX	AR	EO

FILE: SASPRINT TEMP   A1   VM/SP Conversational Monitor System

OBS	TNR	ID	B	H	ALFA	THETA	INCLI	A	MOIST	DENSI	PMAX	AR	EO
63	60	10-2-H	45	95	0.875	90	0	31	13.2	464	23.6	R	16.4
64	1060	22-2-H	45	95	0.875	90	0	31	13.2	443	23.0	R	12.7
65	61	15-3-V	45	95	0.500	90	0	63	13.2	459	5.9	R	15.9
66	62	30-2-H	45	95	0.500	90	0	63	13.0	434	4.7	R	13.3
67	63	17-1-H	45	95	0.500	90	0	63	12.6	407	4.0	R	14.3
68	64	14-2-H	45	95	0.500	90	0	63	13.0	427	3.7	R	13.9
69	65	13-1-H	45	95	0.500	90	0	63	12.4	397	4.2	R	12.8
70	66	42-2-V	45	95	0.500	90	0	63	12.5	358	5.0	R	10.2
71	67	15-3-H	45	95	0.500	162	3	63	13.8	456	13.7	R	15.9
72	68	2-2-V	45	95	0.500	162	3	63	13.0	480	10.9	R	15.2
73	69	17-2-H	45	95	0.500	162	3	63	12.9	435	9.3	R	13.0
74	70	14-3-V	45	95	0.500	162	3	63	13.1	424	12.3	R	13.3
75	71	13-2-H	45	95	0.500	162	3	63	12.3	404	11.0	R	11.2
76	72	42-3-V	45	95	0.500	162	3	63	12.4	363	7.2	R	11.3

OBS	EOAK	E90	E90AK	G	GAK	FT90	FT90AK	FV	FVAK	GFT
63	A	236.000	B	912.48	E	3.30000	B	8.6000	B	300.000
64		256.000	B	891.06	E	4.50000	B	9.4000	B	283.000
65	A	201.000	A	1102.00	A	3.70000	A	9.0000	A	304.000
66		223.000	A	704.00	N	3.90000	A	8.3000	A	308.000
67	A	276.000	A	806.00	A	4.50000	A	7.6000	A	232.000
68	A	241.000	A	825.54	E	3.90000	A	9.9000	A	379.000
69	A	281.000	A	685.00	N	3.40000	A	9.5000	A	317.000
70	A	137.000	A	632.16	E	3.20000	A	6.5000	A	238.000
71		201.000	A	1102.00	N	3.70000	A	9.0000	A	304.000
72	A	284.000	A	879.60	E	4.30000	A	9.3000	A	351.000
73	A	176.000	A	806.00	N	4.00000	A	10.5000	A	342.000
74	A	150.000	B	847.08	E	4.00000	B	7.4000	B	285.000
75		187.000	A	683.00	A	4.20000	A	9.2000	A	314.000
76	A	145.000	A	612.66	E	2.90000	A	6.7000	A	280.000

OBS	GFTAK	GFV	GFVAK	FT90ABK	FT90ABKA	E90ABK	E90ABKAK	TAU	BETA
63	B	999.00	E	4.50	K	269	K	3.15455	0.32632
64	B	943.00	B	3.33	B	585	K	3.07435	0.32632
65	A	1412.00	A	3.82	A	529	A	1.38012	0.66316
66	A	811.00	A	3.60	E	393	E	1.09942	0.66316
67	A	999.00	E	3.35	E	377	E	0.93567	0.66316
68	A	1374.00	A	2.70	K	575	K	0.86550	0.66316
69	A	736.00	A	3.54	A	668	A	0.98246	0.66316
70	A	1354.00	A	2.32	A	376	A	1.16959	0.66316
71	A	1412.00	A	3.82	A	529	A	3.20468	0.66316
72	A	1010.00	A	4.55	A	647	A	2.54971	0.66316
73	A	1154.00	A	2.44	A	414	A	2.17544	0.66316
74	B	940.00	B	2.30	K	488	K	2.87719	0.66316
75	A	890.00	A	1.90	K	281	K	2.57310	0.66316
76	A	841.00	A	2.50	K	235	K	1.68421	0.66316

1   The SAS System   6
                                              15:41 Monday, October 7, 1991

OBS	TNR	ID	B	H	ALFA	THETA	INCLI	A	MOIST	DENSI	PMAX	AR	EO
77	73	15-2-V	45	95	0.75	90	0	63	13.0	454	12.6	R	17.9
78	74	2-1-V	45	95	0.75	90	0	63	13.1	474	16.4	R	13.7

8

STRUCTURAL TIMBER

79	75	17-3-H	45	95	0.75	90	0	63	12.6	427	11.6	R	13.3
80	76	14-3-H	45	95	0.75	90	0	63	13.2	421	9.1	R	14.7
81	77	9-2-V	45	95	0.75	90	0	63	12.8	407	14.1	R	12.7
82	1077	16-3-H	45	95	0.75	90	0	63	13.4	418	16.1	R	12.2
83	78	9-1-V	45	95	0.75	90	0	63	13.0	430	11.7	R	13.3
84	79	61-1-H	45	195	0.50	90	0	31	13.9	409	9.4	S	12.1
85	80	61-1-V	45	195	0.50	90	0	31	13.8	418	10.6	S	12.4
86	81	70-2-H	45	195	0.50	90	0	31	14.2	350	8.3	S	13.3
87	82	60-1-H	45	195	0.50	90	0	31	13.8	393	9.3	S	13.6
88	83	65-1-H	45	195	0.50	90	0	31	14.2	394	6.9	S	15.8
89	84	70-1-V	45	195	0.50	90	0	31	13.7	345	7.4	S	13.7
90	85	71-1-V	45	195	0.50	90	0	31	14.2	355	8.9	R	11.3

OBS	EOAK	E90	E90AK	G	GAK	FT90	FT90AK	FV	FVAK	GFT
77	A	171.000	A	1102.00	N	3.10000	A	9.9000	A	294.000
78		248.000	B	898.08	E	3.70000	B	8.3000	B	399.000
79		137.000	A	806.00	N	3.60000	A	8.7453	E	311.000
80		150.000	A	868.62	E	4.00000	A	7.4000	A	285.000
81	A	180.000	B	755.94	E	3.30000	B	8.5000	B	261.000
82		155.000	A	755.00	N	3.80000	A	8.5302	E	327.000
83		508.000	A	828.60	E	2.90000	A	9.2000	A	227.000
84	A	193.000	A	730.00	E	2.80000	A	7.9000	A	264.000
85	A	193.000	A	730.00	E	2.80000	A	7.9000	A	264.000
86	A	343.000	A	730.00	E	2.50000	A	7.1000	A	160.000
87	A	372.000	A	837.00	A	3.60000	A	6.7000	A	205.000
88	A	387.000	A	730.00	E	2.70000	A	8.0000	A	181.000
89	A	339.000	A	730.00	E	2.40000	A	6.4000	A	187.000
90	A	135.000	B	730.00	E	2.60000	B	7.2000	B	292.000

OBS	GFTAK	GFV	GFVAK	FT90ABK	FT90ABKA	E90ABK	E90ABKAK	TAU	BETA
77	E	940.00	A	2.72	A	358	A	1.96491	0.66316
78	B	693.00	B	3.80	K	388	E	2.55750	0.66316
79	A	999.00	E	2.74	A	340	A	1.80897	0.66316
80	A	940.00	A	2.52	A	500	A	1.41910	0.66316
81	B	789.00	B	3.40	K	365	E	2.19883	0.66316
82	E	999.00	E	4.09	A	404	A	2.51072	0.66316
83	A	1291.00	A	3.29	A	538	A	1.82456	0.66316
84	A	864.00	A	2.90	A	438	A	1.07123	0.15897
85	A	864.00	A	2.90	A	438	A	1.20798	0.15897
86	A	570.00	A	2.28	A	351	A	0.94587	0.15897
87	A	1320.00	A	3.67	A	441	A	1.05983	0.15897
88	A	1068.00	A	3.35	A	435	A	0.78632	0.15897
89	A	769.00	A	2.35	A	417	A	0.84330	0.15897
90	B	717.55	E	2.33	A	182	A	1.01425	0.15897

1   The SAS System   7
                                                    15:41 Monday, October 7, 1991

OBS	TNR	ID	B	H	ALFA	THETA	INCLI	A	MOIST	DENSI	PMAX	AR	EO
91	86	62-1-V	45	195	0.50	90	0	31	14.5	417	10.2	R	16.3
92	87	68-2-V	45	195	0.50	90	0	31	13.8	397	7.7	R	9.4
93	88	64-1-V	45	195	0.50	90	0	31	13.8	404	9.8	R	13.0
94	89	68-1-V	45	195	0.50	90	0	31	13.7	389	10.0	R	11.4

```
 95   90 69-2-V   45 195 0.50   90    0   31  13.7  342   8.2 R  10.6
 96   91 63-1-V   45 195 0.75   90    0   31  14.2  397  16.9 S  10.8
 97   92 67-2-H   45 195 0.75   90    0   31  13.8  419  17.7 S  12.5
 98   93 60-2-H   45 195 0.75   90    0   31  13.9  379  21.9 S  14.6
 99   94 64-1-H   45 195 0.75   90    0   31  13.6  394  20.4 S  14.5
100   95 60-1-V   45 195 0.75   90    0   31  14.2  389  22.4 S  13.6
101   96 65-1-V   45 195 0.75   90    0   31  13.8  369  21.0 S  15.1
102   97 66-2-H   45 195 0.75   90    0   31  14.4  447  22.6 R  16.5
103   98 66-1-H   45 195 0.75   90    0   31  14.4  448  18.7 R  16.4
104   99 62-1-H   45 195 0.75   90    0   31  14.5  416  21.4 R  16.3
```

OBS	EOAK	E90	E90AK	G	GAK	FT90	FT90AK	FV	FVAK	GFT
91	A	193.000	A	730.00	E	2.80000	A	7.9000	A	264.000
92	A	245.000	A	730.00	E	3.50000	A	9.7000	A	295.000
93	A	211.000	A	730.00	E	3.20000	A	8.1000	A	316.000
94	A	192.000	A	730.00	E	3.30000	A	8.0000	A	306.000
95	A	119.000	A	546.00	A	2.30000	A	7.2000	A	236.000
96	A	237.000	E	730.00	E	3.12176	E	7.9022	E	242.153
97	A	447.000	B	936.00	N	3.40000	B	8.7000	B	206.000
98	A	117.000	A	837.00	N	3.40000	A	8.2000	A	349.000
99	A	211.000	B	730.00	E	3.20000	B	8.1000	B	316.000
100	A	309.000	B	837.00	N	3.40000	B	7.3000	B	215.000
101	A	387.000	B	730.00	E	2.70000	B	8.0000	B	181.000
102	A	155.000	A	742.00	N	4.10000	A	8.0000	A	296.000
103	A	236.000	A	742.00	A	3.63584	E	9.2000	B	429.000
104	A	193.000	B	730.00	E	2.80000	B	7.9000	B	264.000

OBS	GFTAK	GFV	GFVAK	FT90ABK	FT90ABKA	E90ABK	E90ABKAK	TAU	BETA
91	A	864.00	A	3.83	A	315	A	1.16239	0.15897
92	A	794.00	A	3.59	A	474	A	0.87749	0.15897
93	A	1043.00	A	3.12	A	602	A	1.11681	0.15897
94	A	879.00	A	2.67	A	196	A	1.13960	0.15897
95	A	876.00	A	4.87	A	558	A	0.93447	0.15897
96	E	877.57	E	2.80	A	321	A	1.28395	0.15897
97	B	680.00	B	2.78	A	302	A	1.34473	0.15897
98	A	867.49	E	2.75	A	405	A	1.66382	0.15897
99	B	1043.00	B	2.22	A	280	A	1.54986	0.15897
100	B	1084.00	B	2.78	A	295	A	1.70180	0.15897
101	B	1068.00	B	3.35	A	435	A	1.59544	0.15897
102	A	1029.07	E	2.41	A	318	A	1.71700	0.15897
103	B	1266.00	B	3.62	A	639	A	1.42070	0.15897
104	B	864.00	B	3.05	A	328	A	1.62583	0.15897

```
1                              The SAS System                               8
                                       15:41 Monday, October 7, 1991
```

OBS	TNR	ID	B	H	ALFA	THETA	INCLI	A	MOIST	DENSI	PMAX	AR	EO
105	100	68-2-H	45	195	0.75	90	0	31	14.2	367	22.8	R	10.3
106	101	69-2-H	45	195	0.75	90	0	31	13.7	338	16.2	R	11.2
107	102	69-1-V	45	195	0.75	90	0	31	13.8	344	13.2	R	10.6
108	103	104-1-H	85	185	0.50	90	0	31	14.9	386	16.8	R	10.8
109	104	121-1-V	85	185	0.50	90	0	31	15.4	432	23.2	R	13.0
110	105	103-1-V	85	185	0.50	90	0	31	17.8	349	21.5	R	8.7

FILE: SASPRINT TEMP   A1   VM/SP Conversational Monitor System

111	106	118-1-V	85	185	0.50	90	0	31	14.9	398	21.5	R	12.9
112	107	116-1-H	85	185	0.50	90	0	31	14.8	404	20.6	R	18.0
113	108	115-1-V	85	185	0.50	90	0	31	15.0	355	20.8	R	11.1
114	109	120-1-H	85	185	0.50	162	3	31	14.8	397	23.0	R	14.4
115	110	121-1-H	85	185	0.50	162	3	31	15.1	447	35.5	R	12.8
116	111	103-1-H	85	185	0.50	162	3	31	19.0	380	23.9	R	7.8
117	112	118-1-H	85	185	0.50	162	3	31	14.8	381	38.7	R	14.2
118	113	109-1-V	85	185	0.50	162	3	31	14.6	370	42.4	R	11.9

OBS	EOAK	E90	E90AK	G	GAK	FT90	FT90AK	FV	FVAK	GFT
105	N	245.000	B	730.00	E	3.50000	B	9.7000	B	295.000
106	N	119.000	B	546.00	N	2.30000	B	7.2000	B	236.000
107	N	103.000	A	546.00	N	2.70000	A	7.3000	A	243.000
108	A	133.035	E	708.96	E	3.65430	E	6.7000	E	307.000
109	A	128.000	A	1033.72	A	2.40000	A	8.3000	A	348.000
110	A	230.000	A	1131.29	E	2.70000	A	6.6000	A	322.000
111	A	141.000	A	693.00	A	3.40000	A	5.8000	A	286.000
112	N	96.000	C	774.84	E	3.90000	B	5.7000	B	286.000
113	A	160.875	E	472.00	N	3.62500	E	6.7000	A	271.000
114	A	121.695	E	741.17	E	3.68360	E	6.7000	E	307.000
115	A	87.240	E	1043.77	E	3.59570	E	6.7000	E	307.000
116	A	230.000	A	1528.80	E	2.70000	A	6.6000	A	322.000
117	A	141.000	A	693.00	N	3.40000	A	5.8000	A	286.000
118	A	139.440	E	569.90	E	3.74220	E	6.7000	E	307.000

OBS	GFTAK	GFV	GFVAK	FT90ABK	FT90ABKA	E90ABK	E90ABKAK	TAU	BETA
105	B	794.00	B	3.35	A	306	A	1.73219	0.15897
106	B	876.00	B	1.78	A	243	A	1.23077	0.15897
107	A	614.00	A	1.17	A	258	A	1.00285	0.15897
108	E	949.78	E	1.24	A	209	A	1.06836	0.16757
109	A	1064.00	A	2.41	A	317	A	1.47536	0.16757
110	A	1590.00	A	2.24	A	380	A	1.36725	0.16757
111	A	843.00	A	4.32	A	539	A	1.36725	0.16757
112	B	913.32	E	2.53	A	330	A	1.31002	0.16757
113	A	1000.15	E	2.50	A	246	A	1.32273	0.16757
114	E	920.81	E	2.45	A	310	A	1.46264	0.16757
115	E	918.91	E	2.41	A	317	A	2.25755	0.16757
116	A	1590.00	A	2.24	A	380	A	1.51987	0.16757
117	A	843.00	A	4.32	A	539	A	2.46105	0.16757
118	E	915.30	E	2.84	A	288	A	2.69634	0.16757

1   The SAS System   9

15:41 Monday, October 7, 1991

OBS	TNR	ID	B	H	ALFA	THETA	INCLI	A	MOIST	DENSI	PMAX	AR	EO
119	114	115-1-H	85	185	0.50	162	3	31	14.3	364	29.2	R	11.9
120	115	117-1-V	85	185	0.75	90	0	31	14.7	393	63.4	R	11.1
121	116	104-1-V	85	185	0.75	90	0	31	14.4	374	70.7	R	10.4
122	1117	105-1-V	85	185	0.75	90	0	31	15.3	376	65.9	R	11.0
123	117	PILOT118	85	185	0.75	90	0	31	14.9	368	37.5	R	14.2
124	118	108-1-H	85	185	0.75	90	0	31	14.1	429	37.4	R	9.2
125	119	116-1-V	85	185	0.75	90	0	31	14.6	403	47.1	R	13.8
126	120	110-1-V	85	185	0.75	90	0	31	14.7	396	68.3	R	10.9

```
127  121 117-2-H  85 185 0.75  162   3    31  15.3  391  39.5 R  10.0
128  122 120-1-V  85 185 0.75  162   3·   31  15.1  395  45.7 R  15.1
129  123 105-2-H  85 185 0.75  162   3    31  14.5  356  46.1 R   9.3
130  124 108-1-V  85 185 0.75  162   3    31  14.6  416  51.8 R  13.7
131  125 109-2-H  85 185 0.75  162   3    31  14.2  362  35.5 R  12.9
132  126 110-2-V  85 185 0.75  162   3    31  14.9  386  65.8 R  11.9
```

OBS	EOAK	E90	E90AK	G	GAK	FT90	FT90AK	FV	FVAK	GFT
119	A	137.595	E	474.00	A	3.83010	E	6.7000	A	271.000
120	A	119.000	A	701.23	E	3.20000	A	6.6000	A	269.000
121	A	131.610	E	547.74	E	3.80080	E	6.7000	E	307.000
122	A	150.345	E	743.66	E	3.53710	E	6.7000	E	307.000
123	A	147.885	E	693.00	N	3.65430	E	6.7000	E	307.000
124	A	79.440	E	743.00	N	3.88870	E	6.7000	E	307.000
125	A	96.000	A	728.63	E	3.90000	A	5.7000	A	286.000
126	A	127.000	A	801.00	N	5.00000	A	7.4000	A	346.000
127	A	119.000	A	815.81	E	3.20000	A	6.6000	A	269.000
128	A	130.140	E	793.65	E	3.59570	E	6.7000	E	307.000
129	A	164.000	A	481.86	E	3.20000	A	7.2000	A	363.000
130	A	101.490	E	735.00	A	3.74220	E	6.7000	E	307.000
131	A	136.980	E	448.62	E	3.85940	E	6.7000	E	307.000
132	A	127.000	A	801.00	A	5.00000	A	7.4000	A	346.000

OBS	GFTAK	GFV	GFVAK	FT90ABK	FT90ABKA	E90ABK	E90ABKAK	TAU	BETA
119	A	870.12	E	2.50	A	246	A	1.85692	0.16757
120	A	851.00	A	2.74	A	379	A	2.68786	0.16757
121	E	876.62	E	3.82	A	388	A	2.99735	0.16757
122	E	1029.28	E	2.56	N	499	N	2.79385	0.16757
123	E	969.04	E	.		.		1.58983	0.16757
124	E	766.17	E	3.80	A	732	A	1.58559	0.16757
125	A	879.99	E	2.70	A	394	A	1.99682	0.16757
126	A	1060.00	A	2.82	A	523	A	2.89560	0.16757
127	A	851.00	A	2.98	A	522	A	1.67462	0.16757
128	E	974.55	E	.		.		1.93747	0.16757
129	A	913.08	E	1.86	A	379	A	1.95443	0.16757
130	E	866.08	E	3.80	A	732	A	2.19608	0.16757
131	E	855.06	E	2.24	A	299	A	1.50503	0.16757
132	A	1060.00	A	2.95	A	483	A	2.78961	0.16757

GLULAM

1   The SAS System   1
                                         15:07 Monday, October 7, 1991

OBS	TNR	ID	B	H	ALFA	THETA	INCLI	A	DENSN	EOL	MOIST	DENSBEAM	E90NL	E90NLAK	G
1	127	L3-2-V	90	300	0.500	90	0	45	504	19.4	11.2	458	357	A	886
2	128	L6-1-V	90	300	0.500	90	0	45	418	16.1	11.5	429	406	A	555
3	129	L5-2-V	90	300	0.500	90	0	45	424	12.7	12.1	441	650	A	733
4	130	L6-2-V	90	300	0.500	90	0	45	364	11.9	12.1	445	620	A	733
5	131	L2-1-V	90	300	0.500	135	1	45	496	16.0	12.2	445	539	A	733
6	132	L6-1-H	90	300	0.500	135	1	45	418	16.1	12.4	429	406	A	733
7	133	L4-2-H	90	300	0.500	135	1	45	439	11.6	11.7	425	756	A	713
8	134	L5-1-V	90	300	0.500	135	1	45	407	14.9	12.5	449	470	A	733
9	135	L2-1-H	90	300	0.500	153	2	45	496	16.0	12.7	449	539	A	733
10	136	L3-1-V	90	300	0.500	153	2	45	450	8.8	12.4	472	663	A	671
11	137	L1-2-V	90	300	0.500	153	2	45	432	15.5	11.5	453	560	A	733
12	138	L3-2-H	90	300	0.500	153	2	45	407	14.9	12.6	445	470	E	596
13	139	L4-2-V	90	300	0.500	169	5	45	485	16.2	11.9	445	457	A	733
14	140	L3-1-H	90	300	0.500	169	5	45	451	8.8	11.8	466	663	A	733
15	141	L1-2-H	90	300	0.500	169	5	45	432	15.5	12.0	451	560	A	733
16	142	L9-1-V	90	300	0.500	169	5	45	399	10.0	11.5	439	474	A	733

OBS	GAK	FT90	FT90AK	FV	FVAK	GF	GFAK	GV	GVAK	PMAX	TAU	EOBEAM
1	A	3.54	A	11.3000	A	324.000	A	1120	A	36.7	1.35926	14.4578
2	A	2.29	A	6.8000	A	221.000	A	730	A	35.1	1.30000	13.4723
3	E	3.19	A	8.6256	E	293.261	E	932	E	44.5	1.64815	13.7903
4	E	4.78	A	7.4000	A	328.000	A	1210	A	39.2	1.45185	13.9211
5	E	3.16	A	9.6000	A	350.000	A	950	A	37.2	1.37778	13.9087
6	E	2.29	A	6.8000	A	221.000	A	730	A	35.3	1.30741	13.3607
7	A	5.34	A	8.6000	A	396.000	A	790	A	59.2	2.19259	13.3167
8	E	3.41	A	10.2000	A	277.000	A	932	E	48.1	1.78148	14.0023
9	E	3.16	A	9.6000	A	350.000	A	950	A	49.4	1.82963	13.9775
10	A	5.03	A	5.2000	A	329.000	A	932	E	48.5	1.79630	14.7668
11	E	3.53	A	6.5000	A	253.000	A	820	A	45.5	1.68519	14.2571
12	A	3.41	E	10.2000	E	277.000	E	932	E	55.4	2.05185	13.8591
13	E	3.61	A	9.9000	A	373.000	A	1020	A	93.4	3.45926	13.9459
14	E	5.03	A	5.2000	A	329.000	A	932	E	65.4	2.42222	14.6450
15	E	3.53	A	6.5000	A	253.000	A	820	A	75.6	2.80000	14.1297
16	E	3.52	A	8.1000	A	304.000	A	630	A	65.1	2.41111	13.7993

1   The SAS System   2

GLULAM

15:07 Monday, October 7, 1991

OBS	TNR	ID	B	H	ALFA	THETA	INCLI	A	DENSNL	EONL	MOIST	DENSBEAM	E90NL	E90NAK	G
17	143	L1-1-V	90	300	0.500	173	8	45	480	16.6	13.0	451	232	A	733
18	144	L9-2-V	90	300	0.500	173	8	45	463	16.8	11.4	461	342	A	733
19	145	L2-2-V	90	300	0.500	173	8	45	420	11.4	11.2	447	517	A	733
20	146	L9-2-H	90	300	0.500	173	8	45	405	14.3	12.4	439	625	A	733
21	147	L8-1-V	90	300	0.722	90	0	45	459	13.3	11.3	435	541	A	708
22	148	L8-1-H	90	300	0.722	90	0	45	459	13.3	11.8	438	541	A	733
23	149	L8-2-V	90	300	0.722	90	0	45	427	9.3	12.5	446	576	E	733
24	150	L8-2-H	90	300	0.722	90	0	45	461	15.0	12.8	448	588	E	733
25	151	L7-1-V	90	300	0.833	90	0	45	461	15.0	12.4	449	602	A	733
26	152	L7-1-H	90	300	0.833	90	0	45	415	11.8	12.2	438	471	A	733
27	153	L7-2-V	90	300	0.833	90	0	45	434	14.8	12.5	441	578	E	733
28	154	L7-2-H	90	300	0.833	90	0	45	434	14.8	12.0	444	578	E	667
29	155	L1-1-H	90	300	0.500	90	0	90	480	16.6	12.1	463	232	A	733
30	156	L4-1-V	90	300	0.500	90	0	90	479	8.5	11.4	434	950	A	713
31	157	L2-2-H	90	300	0.500	90	0	90	420	11.4	13.1	435	517	A	784
32	158	L6-2-H	90	300	0.500	90	0	90	364	11.9	12.8	435	620	A	733

OBS	GAK	FT90	AK	FV	AK	GFT	AK	GV	FAK	PMAX	TAU	EOBEAM
17	E	3.70	A	9.9000	A	344.000	A	880	A	78.4	2.90370	14.0057
18	E	3.45	A	12.0000	A	592.000	K	1370	A	75.5	2.79630	14.5311
19	E	3.30	A	6.1000	A	249.000	A	932	E	71.5	2.64815	14.0981
20	E	4.24	A	9.2000	A	338.000	A	760	A	76.0	2.81481	13.6877
21	A	2.97	A	10.4000	A	291.000	A	932	E	78.3	2.00831	13.6933
22	E	2.97	A	10.4000	A	291.000	A	932	E	63.8	1.63640	13.7294
23	E	3.63	E	9.5000	A	286.000	A	680	A	63.8	1.63640	13.9042
24	E	3.59	E	10.5000	A	232.000	A	940	A	48.9	1.25423	13.9324
25	E	3.71	A	6.4000	A	232.000	E	830	A	73.4	1.63176	14.0147
26	E	3.53	A	10.7000	A	305.000	A	840	A	99.1	2.20310	13.6798
27	E	3.62	E	10.8000	A	248.000	A	1240	A	89.1	1.98079	13.7407
28	A	3.62	E	10.8000	A	248.000	A	1240	A	109.4	2.43208	13.9008
29	E	3.79	A	9.9000	A	344.000	A	880	A	29.9	1.10741	14.5097
30	A	4.18	A	9.5000	A	330.000	A	1040	A	37.8	1.40000	13.6482
31	A	3.30	A	6.1000	A	249.000	E	932	A	39.8	1.47407	13.4701
32	E	4.78	A	7.4000	A	328.000	A	1210	A	29.7	1.10000	13.5073

1   The SAS System   3

15:07 Monday, October 7, 1991

FILE: SASPRINT TEMP   A1   VM/SP Conversational Monitor System

OBS	TNR	ID	B	H	ALFA	THETA	INCLI	DENSL	ENSNL	ENL	MOIST	DENSBAM	E9900NL	E9900NLK	G
33	159	L5-2-H	90	300	0.500	153	2	90	480	16.6	11.9	445	825	A	733
34	160	L4-1-H	90	300	0.500	153	2	90	479	8.5	11.3	452	950	A	734
35	161	L9-1-H	90	300	0.500	153	2	90	399	10.0	12.5	449	474	A	733
36	162	L5-1-H	90	300	0.500	153	2	90	407	14.9	12.4	457	470	A	733
37	163	L11-1-V	90	200	0.500	90	0	35	434	14.8	11.8	404	572	A	733
38	164	L11-1-H	90	200	0.500	90	0	35	434	14.8	12.7	406	572	A	733
39	165	L11-2-V	90	200	0.500	90	0	35	424	10.3	11.8	405	789	A	1142
40	166	L11-2-H	90	200	0.500	90	0	35	410	14.8	11.7	398	747	A	733
41	167	L10-1-V	90	200	0.750	90	0	35	410	14.8	10.4	424	771	A	631
42	168	L10-1-H	90	200	0.750	90	0	35	485	17.6	10.4	447	693	E	733
43	169	L10-2-V	90	200	0.750	90	0	35	485	17.6	12.0	461	693	A	733
44	170	L10-2-H	90	200	0.750	90	0	35	485	17.6	11.9	437	693	A	733
45	171	L13-1-V	160	567	0.500	90	0	70	422	11.2	12.6	419	772	A	733
46	172	L12-1-H	160	567	0.500	90	0	70	348	9.9	13.6	416	495	E	733
47	173	L13-1-H	160	567	0.500	90	0	70	425	12.5	13.6	415	529	A	733
48	174	L12-1-V	160	567	0.500	90	0	70	428	11.3	12.5	422	427	A	733

OBS	GAK	FT900	FT900AK	FV	FVAK	GFT	GFTAK	GFV	GFVAK	PMAX	TAU	EOBEAM
33	E	3.40	A	7.5000	A	343.000	A	840	A	34.7	1.28519	13.9459
34	A	4.18	A	9.5000	A	330.000	A	1040	A	59.5	2.20370	14.2492
35	E	3.52	A	8.1000	A	304.000	A	630	A	56.3	2.08519	14.0023
36	E	3.41	A	10.2000	A	277.000	A	932	E	54.2	2.00741	14.2763
37	E	2.31	A	9.2000	A	264.000	A	1040	A	28.7	1.59444	12.6176
38	E	2.31	A	9.2000	A	264.000	A	1040	A	22.0	1.22222	12.5714
39	A	3.39	A	9.9000	A	440.000	K	932	E	30.0	1.66667	12.6503
40	E	3.68	A	8.0000	A	324.000	A	932	E	33.6	1.86667	12.4338
41	A	2.89	A	11.7000	A	229.000	A	1000	A	83.9	3.10741	13.4452
42	E	3.67	E	11.7000	A	414.000	E	1000	A	70.8	2.62222	14.1973
43	E	3.67	A	8.3000	A	414.000	A	780	A	66.7	2.47037	14.4567
44	E	3.67	A	8.3000	A	414.000	A	780	A	55.1	2.04074	13.6843
45	E	1.89	A	7.8000	A	301.000	A	1010	A	107.9	1.18937	13.0089
46	E	1.66	E	5.2528	E	288.309	E	1077	E	77.3	0.85207	12.7868
47	E	1.44	A	8.7000	A	296.000	A	1050	A	90.0	0.99206	12.7541
48	E	1.52	A	10.3000	A	306.000	A	1170	A	77.3	0.85207	13.1194

GLULAM

```
                                         D
                                         E            E
                                 D       N            9
                         T   I   E               M   S    E   0
                     A   H   N   N       E       O   B    9   N
 O   T               L   E   C   S       0       I   E    0   L
 B   N    I      B   H   F   T   L       N   N   S   A    N   A
 S   R    D          A   A   I   A       L   L   T   M    L   K   G

49  175  L15-1-H  160  567  0.500  153  2  70  368  11.5  12.6  400  749  A  733
50  176  L15-1-V  160  567  0.500  153  2  70  368  11.5  12.8  423  749  A  733
51  177  L14-1-V  160  567  0.500  153  2  70  364  11.4  12.3  432  412  A  733
52  178  L14-1-H  160  567  0.500  153  2  70  364  11.4  12.5  419  412  A  733
```

```
                F
                T
          F     9                              G           G                         E
          F     9                      G       F     G      F     P                   O
   O  G   T     0           F          V       T     G      V     M         T         B
   B  A   9     0    F      A    G     A       F     A      A     A         A         A
   S  K   0     K    V      K    T     K       V     K      X     U                   M

49  E  1.69  A  7.2000  A  289.000  A  1077  E   93.9  1.03505  12.3876
50  E  1.69  A  7.2000  A  289.000  A  1077  E  112.6  1.24118  13.1149
51  E  1.80  A  5.2000  A  322.000  A  1077  E  106.2  1.17063  13.4712
52  E  1.80  A  5.2000  A  322.000  A  1077  E   87.3  0.96230  13.0213
```

This annex contains the mean values and the standard deviations for each type of notched beam. The upper number is the mean value, the lower the standard deviation.

The annex gives the geometry, the material properties and the shear capacity of the notched beam cross section. The last mentioned is expressed by the average shear stress at failure and as the shear force at catastrophic failure at which the crack propagated rapidly.

In case of that the material property has not been measured for a notched beam specimen, this property has been estimated from the regression equation, if determined, otherwise has the material property been set equal to the mean value of timber/glulam of the relevant cross section.

Mean and standard deviation. GLULAM specimens.

No	α	θ	a mm	Density, kg/m^3 notch	lam.	Beam	Moist. %	E_0 GPa	E_{90} MPa ABK	AfB	G MPa	$f_{t,90}$ MPa ABK	AfB	f_v MPa	G_{ft} Nm/m^2	G_{fv} Nm/m^2	τ_{max} N/mm^2	V_{max} kN
Cross section 90 x 300 mm																		
1	0.5	90	45	428	443	11.7	13.9	508		727	3.5		8.5	292	998	1.44	19.4
				58	12	0.5	0.4	148		135	1.0		2.0	50	213	0.15	
2		135		440	437	12.2	13.6	543		728	3.6		8.8	311	851	1.66	22.4
		(1:1)		40	12	0.4	0.4	152		10	1.3		1.5	77	108	0.41	
3		153		446	455	12.3	14.2	558		683	3.8		7.9	303	909	1.84	24.8
		(1:2)		38	12	0.5	0.4	80		65	0.8		2.4	45	60	0.15	
4		169		442	450	11.8	14.1	539		733	3.9		7.4	315	851	2.77	37.4
		(1:5)		36	12	0.2	0.4	94		–	0.7		2.0	50	168	0.49	
5		173		442	450	12.0	14.1	429		733	3.7		9.3	381	986	2.79	37.7
		(1:8)		35	9	0.8	0.3	176		–	0.4		1.4	147	266	0.11	
6	0.722	90	45	452	442	12.1	13.8	562		727	3.3		10.2	275	871	1.63	22.0
				16	6	0.2	0.1	24		13	0.4		0.5	29	127	0.31	
7	0.833			436	443	12.3	13.8	557		717	3.6		9.7	258	1038	2.06	27.8
				19	5	0.2	0.2	59		33	0.1		2.2	32	234	0.34	
8	0.5	90	90	436	442	12.4	13.8	580		741	4.0		8.2	313	1016	1.27	17.1
				55	14	0.8	0.5	296		30	0.6		1.8	43	146	0.19	
9	0.5	153		441	451	12.0	14.1	680		733	3.6		8.8	314	861	1.90	25.7
		(1:2)		44	5	0.6	0.2	245		–	0.4		1.2	29	174	0.41	
Cross section 90 x 200 mm																		
10	0.5	90	35	426	403	12.0	12.6	670		835	2.9		9.1	323	986	1.59	14.3
				11	4	0.5	0.1	114		205	0.7		0.8	83	62	0.27	
11	0.75			466	442	11.2	13.9	713		708	3.5		10.0	368	890	2.56	23.0
				38	16	0.9	0.5	39		51	0.4		2.0	93	127	0.44	
Cross section 160 x 567 mm																		
12	0.5	90	70	406	418	13.1	12.9	556		733	1.6		8.0	298	1077	0.97	44.0
				39	3	0.6	0.2	150		–	0.2		2.1	7	68	0.16	
13		153		366	419	12.6	13.0	581		733	1.7		6.2	306	1077	1.10	49.9
		(1:2)		2	13	0.2	0.5	195		–	0.1		1.2	29	–	0.13	

Mean and standard deviation   Structural timber

No	α	θ	a mm	Density kg/m^3	Moist %	E_0 GPa	E_{90} MPa		G MPa	$f_{t,90}$ MPa		f_v MPa	G_{ft} Nm/m^2	G_{fv} Nm/m^2	τ_{max} N/mm^2	V_{max} kN
							ABK	AfB		ABK	AfB					
Cross section 45 x 195 mm																
21	0.50S*	90	31	385	13.9	13.5	420	305	748	2.9	2.8	7.3	210	909	0.99	4.34
				30	0.2	1.3	35	88	44	0.5	0.4	0.7	44	258	0.16	
21	0.50R*			384	14.0	12.0	388	183	699	3.4	3.0	8.0	285	862	1.04	4.56
				29	0.3	2.4	183	47	75	0.9	0.5	0.9	30	108	0.11	
22	0.75S*			392	13.9	13.5	340	285	800	2.8	3.2	8.0	252	937	1.52	10.00
				27	0.2	1.6	64	121	85	0.4	0.3	0.5	67	158	0.17	
22	0.75R*			393	14.2	13.6	349	175	672	2.6	3.2	8.2	294	907	1.45	9.54
				50	0.3	3.1	146	59	98	1.0	0.7	1.0	71	221	0.29	

* Signifies Standing or Round annual rings.

No	α	θ	a mm	Density kg/m^3	Moist %	E_0 GPa	E_{90} MPa		G MPa	$f_{t,90}$ MPa		f_v MPa	G_{ft} Nm/m^2	G_{fv} Nm/m^2	τ_{max} N/mm^2	V_{max} kN
							ABK	AfB		ABK	AfB					
Cross section 85 x 185 mm																
31	0.5	90	31	387	15.4	12.4	337	148	801	2.5	3.3	6.6	303	1060	1.32	10.4
				31	1.2	3.2	116	45	242	1.0	0.6	0.9	28	270	0.14	
32		162 (1:3)		390	15.4	12.2	347	143	842	2.8	3.5	6.5	300	1010	2.04	16.0
				30	1.8	2.4	104	47	388	0.8	0.4	0.4	18	286	0.51	
33	0.75	90	31	394	14.6	11.6	483	117	702	3.2	3.9	6.6	304	900	2.29	27.0
				22	0.3	2.0	151	25	85	0.6	0.6	0.5	26	102	0.65	
34		162 (1:3)		384	14.8	12.1	483	130	679	2.8	3.8	6.9	317	920	2.01	23.7
				22	0.4	2.2	164	21	168	0.7	0.7	0.3	33	83	0.45	

3

Mean and standard deviation. GLULAM specimens.

No	α	θ	a mm	Density, kg/m³ notch	lam.	Beam	Moist. %	E_0 GPa	E_{90} (MPa) ABK	AfB	G MPa	$f_{t,90}$ (MPa) ABK	AfB	f_v MPa	G_{ft} Nm/m²	G_{fv} Nm/m²	τ_{max} N/mm²	V_{max} kN
Cross section 90 x 300 mm																		
1	0.5	90	45	428	443		11.7	13.9	508		727	3.5		8.5	292	998	1.44	19.4
				58	12		0.5	0.4	148		135	1.0		2.0	50	213	0.15	
2		135 (1:1)		440	437		12.2	13.6	543		728	3.6		8.8	311	851	1.66	22.4
				40	12		0.4	0.4	152		10	1.3		1.5	77	108	0.41	
3		153 (1:2)		446	455		12.3	14.2	558		683	3.8		7.9	303	909	1.84	24.8
				38	12		0.5	0.4	80		65	0.8		2.4	45	60	0.15	
4		169 (1:5)		442	450		11.8	14.1	539		733	3.9		7.4	315	851	2.77	37.4
				36	12		0.2	0.4	94		-	0.7		2.0	50	168	0.49	
5		173 (1:8)		442	450		12.0	14.1	429		733	3.7		9.3	381	986	2.79	37.7
				35	9		0.8	0.3	176		-	0.4		1.4	147	266	0.11	
6	0.722	90	45	452	442		12.1	13.8	562		727	3.3		10.2	275	871	1.63	22.0
				16	6		0.2	0.1	24		13	0.4		0.5	29	127	0.31	
7	0.833			436	443		12.3	13.8	557		717	3.6		9.7	258	1038	2.06	27.8
				19	5		0.2	0.2	59		33	0.1		2.2	32	234	0.34	
8	0.5	90	90	436	442		12.4	13.8	580		741	4.0		8.2	313	1016	1.27	17.1
				55	14		0.8	0.5	296		30	0.6		1.8	43	146	0.19	
9	0.5	153 (1:2)		441	451		12.0	14.1	680		733	3.6		8.8	314	861	1.90	25.7
				44	5		0.6	0.2	245		-	0.4		1.2	29	174	0.41	
Cross section 90 x 200 mm																		
10	0.5	90	35	426	403		12.0	12.6	670		835	2.9		9.1	323	986	1.59	14.3
				11	4		0.5	0.1	114		205	0.7		0.8	83	62	0.27	
11	0.75			466	442		11.2	13.9	713		708	3.5		10.0	368	890	2.56	23.0
				38	16		0.9	0.5	39		51	0.4		2.0	93	127	0.44	
Cross section 160 x 567 mm																		
12	0.5	90	70	406	418		13.1	12.9	556		733	1.6		8.0	298	1077	0.97	44.0
				39	3		0.6	0.2	150		-	0.2		2.1	7	68	0.16	
13		153 (1:2)		366	419		12.6	13.0	581		733	1.7		6.2	306	1077	1.10	49.9
				2	13		0.2	0.5	195		-	0.1		1.2	29	-	0.13	